NTNU
Norwegian University of
Science and Technology

Investigating the excitation spectrum of a spin-orbit coupled Bose-Einstein condensate

Sigve Solli

Master of Science in Physics and Mathematics
Submission date: June 2017
Supervisor: Asle Sudbø, IFY

Norwegian University of Science and Technology
Department of Physics

Investigating the excitation spectrum of a spin-orbit coupled Bose-Einstein condensate

Master's Thesis

Author: **Sigve Solli**

Supervisor: **Prof. Asle Sudbø**

Summary

The excitation spectrum of a spin-orbit coupled Bose-Einstein condensate is investigated by the use of the Bose-Hubbard model and a mean-field approach. The undiagonalized Hamiltonian matrix for a general inversion-symmetric Bravais lattice is found. Analytical expressions for the excitation spectrum is then found in the limiting case of on-site interactions and nearest-neighbor hopping on a one-dimensional chain and a two-dimensional quadratic lattice. The densities of particles in the ground state acting as mean-field parameters are found self-consistently by minimization of the free energy, and they are seen to be in agreement with published literature.

Sammendrag

Eksitasjonsspekteret for et spinbanekoblet Bose-Einstein-kondensat undersøkes ved hjelp av Bose-Hubbard-modellen og en middelfelttilnærming. Det blir funnet en ikke-diagonalisert Hamilton-operator for et generelt inversjonssymmetrisk Bravais-gitter. Deretter finnes analytiske uttrykk for eksitasjonsspekteret i grensetilfellet med kun lokale vekselvirkninger og hopping til nærmeste nabo på en kjede i én dimensjon og et kvadratisk gitter i to dimensjoner. Middelfeltparametrene tetthet av partikler i grunntilstand bestemmes selvkonsistent ved minimering av fri energi, noe som resulterer i verdier som stemmer overens med litteraturen.

Preface

This Master's thesis is the conclusion of a five-year Master's degree program in Mathematics and Physics at the Norwegian University of Science and Technology. The topic is theoretical condensed matter physics.

The project was supervised by professor Asle Sudbø. I would like to thank my supervisor for helpful guidance and discussions. I also wish to thank professor Jacob Linder and fellow student Even Thingstad for many interesting discussions during the semester. My gratitude is also extended to the extensive and enthusiastic lunch and dinner group, providing my everyday life with laughter and, of course, food.

Sigve Solli
Trondheim, Norway
June, 2017

Contents

1. Introduction

Most people should be familiar with the three phases of matter that surround us in everyday life: gas, liquid, and solid. Under extreme conditions there exist several other phases as well. One such phase is the **Bose-Einstein condensate** (BEC). Condensation to this phase occurs when bosons are cooled down to just above absolute zero, i.e. $-273.15\,^{\circ}\mathrm{C}$. In this phase, a macroscopic number of particles are occupying the quantum mechanical ground state of the system. A BEC is thus a macroscopic manifestation of quantum mechanical phenomena. This is impossible in higher-temperature many-body systems where the thermal energy excites the particles into a number of excited states. The study of BECs makes it possible to develop theories that are experimentally verifiable in many-body quantum mechanics.

The existence of BECs was predicted theoretically by Satyendra Nath Bose and Albert Einstein in the 1920's. Helium superfluids were subsequently produced by Pyotr Kapitza [1], John F. Allen, and Don Misener [2] in 1937. However, as the name "fluid" signals, the strong interatomic interactions of helium atoms easily lift the system out of the ground state, making it unfitting to consider the weak-coupling limit. Only in the last couple of decades have BECs with weak interactions been created experimentally, by sufficient cooling of atomic gases: In 1995 this was achieved with rubidium [3] and sodium [4] atoms. Novel advancements in cooling methods made sufficient cooling possible [5]. There has been an intensification in both theoretical and experimental research on BECs made from ultracold gases ever since.

Research on BECs has revolved around the case of a continuous uniform condensate, and on the case of ultracold atoms being confined to a lattice. The latter case can be obtained through the optical lattice: Periodic potentials produced by the interference of two or more lasers acting as a lattice for the atoms. Periodic confinement of atoms allows for the mathematically less

involved discrete Fourier transform, as well as application of the physically intuitive Bose-Hubbard model. Moreover, investigations into BECs on a lattice may provide insight into the physics of solids, since the optical lattice structurally mimic a crystal. The optical lattice, however, has the advantage of having tunable lattice parameters such as the degree of binding to lattice points and lattice constants, in addition to being devoid of complicating interactions such as those of the phonon.

While the investigation into BECs is concerned with bosons, the study of crystals typically involves electrons. One complicating interaction arising in a material is the **spin-orbit coupling** (SOC) experienced by the spin-1/2 fermions. In quantum mechanics, SOC is an interaction that couples the particle's spin to its movement that arises naturally from the relativistic Dirac equation [6]. It contributes to the fine structure of the energy levels of an electron bound to an atom. It also affects electrons moving in spatially inhomogeneous electric fields in matter. Creating an environment for the isolated study of SOC on electrons experimentally, however, would require electric fields that are much stronger than what is typically available in a laboratory [7].

SOC experienced naturally by bosons is of the integer-spin type, instead of the spin-1/2 version for electrons. Its experimental fabrication would also require strong fields because of its weak nature. However, extensive research has been done on creating systems of **synthetic SOC**. All needed is a two-state system with a transition that both impacts and is influenced by the atom's momentum, and the result is essentially spin-1/2 SOC. For example, by using a two-component BEC containing two hyperfine states of an atom, such as rubidium, that interacts with an external electric field, an observable and highly tunable synthetic SOC is created [8]. In addition to being used in the understanding of SOC in electrons, the unique situation of a spin-1/2 coupling of integer-spin particles allows for some new and fascinating phenomena [9].

In recent years there has been intensive research in the area of synthetic SOC in BECs. A comprehensive review of experimental and theoretical studies of synthetic spin systems can be found in Ref. [10]. More recently, particles in such a system were shown to display properties of having negative mass [11], triggering mainstream interest in popular science [12]. Phase diagrams and density distributions of a spin-orbit coupled BEC on a two-dimensional lattice was done in Ref. [13], making use of the Bose-Hubbard model and the so-called Rashba-type SOC both of the weak and strong type. Phase

transitions and real-space density distributions have been the focus for this and many other papers through finding the wave function of the condensate.

Finding the excitation spectrum of the BEC does not necessarily include working with wave functions. In this thesis the aim is to investigate the excitation spectrum of a weakly interacting BEC, bypassing wave functions altogether, and instead focusing on operator formalism. Starting from the treatment of a two-component weakly interacting BEC in Ref. [14], the two components may be interpreted as spin states, and boson operators may be expressed in terms of the helicity basis that diagonalizes the spin-orbit coupled single-particle Hamiltonian. This procedure includes mean field theory in momentum space where ground state bosons interacting with both helicity bands are included. The result of this treatment is two-fold: an expression for the Hamiltonian matrix with a high degree of generality, and explicit expressions for the energy spectrum in limiting cases. The limiting cases discussed will be the case of nearest-neighbor hopping and on-site interactions, applied on a one-dimensional chain and a two-dimensional quadratic lattice. The highly general excitation matrix could be of use by others in investigations into further limiting cases.

A similar treatment with an erroneous and excessively simplifying assumption was made in the author's specialization project [15]. This lead to results that did not agree with literature. Because the underlying concepts mostly overlap, parts of this thesis will be based on sections of Ref. [15], and these parts will be marked with an **asterisk (*)**.

First some preliminary concepts are presented. The Bose-Hubbard model and SOC models are then described and cast in a form used in this paper. The general case of an inversion symmetric Bravais lattice is then considered. Explicit results for the excitation spectrum is then found for the limiting case of nearest-neighbor hopping, and on-site interactions in the one- and two-dimensional cases. A discussion of the results follows, before we conclude.

2. Preliminaries

2.1 Mathematical conventions*

We write variable vectors in italic boldface, as in the wave vector $\boldsymbol{k}$; Cartesian unit vectors are denoted $\hat{x}$, $\hat{y}$ and $\hat{z}$; while basis vectors are denoted by Φ, ξ, Ψ, and χ. Complex conjugation of scalars is denoted with an asterisk, as in s^*; Hermitian conjugation is denoted by a dagger, as in $\Phi^\dagger$; transpose is denoted T, as in $\Phi_{\boldsymbol{k}} = \begin{pmatrix} b_{\boldsymbol{k}\uparrow} & b_{\boldsymbol{k}\downarrow} \end{pmatrix}^T$. Vectors and matrices are enclosed by parentheses. We do not use any specific notation for operators, but we use hats on field operators $\hat{\psi}$ to emphasize that they are not wavefunctions. The commutator between operators A and B is $[A, B] = AB - BA$. The Kronecker delta is written δ_{ij}. Greek letters α and β refer to either components, spin states, or helicity bands depending on the context. Spin states are written $\uparrow$ and $\downarrow$; helicity bands are written $+$ and $-$. a ($a^\dagger$) and b ($b^\dagger$) are used for annihilation (creation) operators. Multiple subscripts are in general not separated by commas, as in $b_{\boldsymbol{k}\uparrow}$. The Pauli spin matrices are

$$\sigma_x = \begin{pmatrix} 0 & 1 \\ 1 & 0 \end{pmatrix},$$
$$\sigma_y = \begin{pmatrix} 0 & -i \\ i & 0 \end{pmatrix}, \tag{2.1}$$
$$\sigma_z = \begin{pmatrix} 1 & 0 \\ 0 & -1 \end{pmatrix}.$$

The notation $\sigma_i^{\alpha\beta}$ means the element of σ_i where $\alpha = \uparrow, \downarrow$ picks out the first or second row, respectively, and $\beta = \uparrow, \downarrow$ picks out the first or second column, respectively.

2.2 Second quantization*

Describing a many-body system by the use of wavefunctions can be awkward due to the complexity of the resulting functions. Also, one is not necessarily interested in the exact probability density for the location of each particle. In the second quantization scheme one has therefore introduced the number state, in bra-ket notation:

$$|A\rangle = |n_{\nu_1}, n_{\nu_2}, ...\rangle\,, \tag{2.2}$$

where n_{ν_i} denotes the number of particles in state ν_i. We also introduce the annihilation and creation operators, a_{ν_i} and $a^\dagger_{\nu_i}$, which reduce and increase the number n_{ν_i} by one, respectively:

$$a_{\nu_i}\,|n_{\nu_1}, n_{\nu_2}, ..., n_{\nu_i}, ...\rangle = \sqrt{n_{\nu_i} - 1}\,|n_{\nu_1}, n_{\nu_2}, ..., n_{\nu_i} - 1, ...\rangle\,, \tag{2.3}$$

$$a^\dagger_{\nu_i}\,|n_{\nu_1}, n_{\nu_2}, ..., n_{\nu_i}, ...\rangle = \sqrt{n_{\nu_i}}\,|n_{\nu_1}, n_{\nu_2}, ..., n_{\nu_i} + 1, ...\rangle\,. \tag{2.4}$$

For a many-particle system of bosons, considered in this thesis, the numbers n_{ν_i} can have any non-negative integer value, whereas in fermionic systems they can only be 0 or 1 by the Pauli exclusion principle. By the symmetry properties of bosons it can be shown [16] that the bosonic creation and annihilation operators obey the commutation relations

$$\begin{aligned} [a_{\nu_i}, a_{\nu_j}] &= 0, \\ [a^\dagger_{\nu_i}, a^\dagger_{\nu_j}] &= 0, \\ [a_{\nu_i}, a^\dagger_{\nu_j}] &= \delta_{\nu_i\nu_j}. \end{aligned} \tag{2.5}$$

Whenever the basis ν is the position $\boldsymbol{r}$ the annihilation and creation operators are called field operators, $\hat{\psi}$ and $\hat{\psi}^\dagger$, respectively, by convention. When working with number states, operators can be expressed in terms of annihilation and creation operators. For single-particle operators H_1 and two-particle operators H_2 this is done by the following scheme [17], in terms of field operators:

$$\begin{aligned} H_1 &= \sum_i h(\boldsymbol{r}_i) \rightarrow \int d\boldsymbol{r}\hat{\psi}^\dagger(\boldsymbol{r})h(\boldsymbol{r})\hat{\psi}(\boldsymbol{r}), \\ H_2 &= \frac{1}{2}\sum_{i\neq j} v(\boldsymbol{r}_i, \boldsymbol{r}_j) \rightarrow \int d\boldsymbol{r} \int d\boldsymbol{r}'\hat{\psi}^\dagger(\boldsymbol{r})\hat{\psi}^\dagger(\boldsymbol{r}')v(\boldsymbol{r}, \boldsymbol{r}')\hat{\psi}(\boldsymbol{r}')\hat{\psi}(\boldsymbol{r}), \end{aligned} \tag{2.6}$$

where $h(\boldsymbol{r})$ is the single-particle Hamiltonian of a single particle located at $\boldsymbol{r}$, $v(\boldsymbol{r}, \boldsymbol{r}')$ is the two-particle interaction of two particles located at $\boldsymbol{r}$ and $\boldsymbol{r}'$. Here we have igored a possible spin-dependency of the operators, which would result in sums over spin states as well. We note that single-particle operators are quadratic in creation and annihilation operators, while two-particle operators are biquadratic.

In a system of bosons residing on lattice points it is convenient to choose the basis ν to be lattice points i. Thus a_i ($a_i^\dagger$) annihilates (creates) a boson at lattice site i. The periodic nature of the lattice allows the creation and annihilation operators to be expressed as a descrete Fourier transform of creation and annihilation operators for $\boldsymbol{k}$-states:

$$a_i = \frac{1}{\sqrt{N_s}} \sum_{\boldsymbol{k}} b_{\boldsymbol{k}} e^{-i\boldsymbol{k}\cdot\boldsymbol{r}_i}, \tag{2.7}$$

where N_s is the number of lattice sites, $\boldsymbol{r}_i$ is the location of lattice site i, and the sum is over all $\boldsymbol{k}$-vectors of the first Brillouin zone.

In addition we mention that we have the following relation on lattice, where the sum is over all lattice points:

$$\frac{1}{N_s} \sum_j e^{-i(\boldsymbol{k}-\boldsymbol{k}')\cdot\boldsymbol{r}_j} = \delta_{\boldsymbol{k},\boldsymbol{k}'}. \tag{2.8}$$

This relation is shown in Ref. [18].

2.3 Bose-Einstein condensate

A gas of bosons will condense into a Bose-Einstein condensate under some critical conditions. This is a quantum mechanical effect that could never occur in a classical gas. According to statistical mechanics, such a boson gas will obey Bose-Einstein statistics, i.e. the number of particles in an energy state i of energy ϵ_i and degeneracy g_i is given by

$$n_i(\epsilon_i) = \frac{g_i}{e^{(\epsilon_i-\mu)/kT} - 1}, \tag{2.9}$$

where μ is the chemical potential, k is Boltzmann constant og T is the temperature. The total number of particles is

$$N = \sum_i n_i = \int_0^\infty \frac{g(\epsilon)}{e^{(\epsilon_i-\mu)/kT} - 1} \, \mathrm{d}\epsilon, \tag{2.10}$$

where $g(\epsilon)$ is the density of states.

From this it is seen that the density $\rho = N/V$ is an increasing function of μ. From statistical mechanics it is known that we must have $\mu < \epsilon_i$ for the partition function of state i to exist. Specifically, this means that $\mu < \epsilon_0$, where ϵ_0 is the ground state energy. When N is sufficiently large, the zero-point energy may be ignored by setting $\epsilon_0 = 0$ [19], leading to $\mu < 0$. Combined with the known result $g(\epsilon) = CV\epsilon^{1/2}$ for a non-interacting Bose gas in three dimensions [19], and defining the integration variable $x = \epsilon/kT$, we find the maximum possible density to be

$$\rho = C(kT)^{3/2} \int_0^\infty \frac{x^{1/2}}{e^x - 1} \, \mathrm{d}x = \rho_c, \tag{2.11}$$

i.e. a finite value.

This result is paradoxical since higher densities can indeed be obtained. The solution is that the integral approximation in (2.10) fails for the lowest energy levels. Singling out the ground state (assuming $g_0 = 1$),

$$\rho = \frac{1}{V} \frac{1}{e^{-\mu/kT} - 1} + C \int_0^\infty \frac{\epsilon^{1/2}}{e^{(\epsilon_i - \mu)/kT} - 1} \, \mathrm{d}\epsilon = \rho_0 + \rho_c. \tag{2.12}$$

Thus we see that increases in density only occur in the ground state density ρ_0. By surpassing ρ_c, or equivalently going below a critical temperature T_c, the system undergoes a continuous phase transition, where one possible order parameter could be ρ_0. As seen from (2.11), ρ_c is a function of T and thus for $T > T_c$, ρ_0 vanishes when ρ_c is made arbitrarily large. At the transition ρ_0 would be close to zero, but by moving further into the ordered state this number is made finite and therefore macroscopic, in a process called condensation. We can thus speak of BECs having a macroscopic number of particles in the ground state.

For a system to exhibit Bose-Einstein condensation it is required that ρ_c be finite for a given T, as in (2.11). In a three-dimensional system the form of $g(\epsilon)$ makes the integral converge. The same is true for a two-dimensional system at $T = 0$ or if the particles are confined by a harmonic-oscillator potential [19]. Bose-Einstein condensation in one-dimensional free Bose gases is not possible. However, one-dimensional BECs may nevertheless be obtained experimentally given that either the confining potential or the lattice point potentials are sufficiently strong [20].

3. Theoretical models

3.1 Bose-Hubbard model for two-component system*

We consider a many-body system of particles of two distinct species, labeled $\alpha, \beta = A, B$. Each particle of species α has the single-particle Hamiltonian $h_\alpha(\boldsymbol{r})$. Two particles of species α and β located at position $\boldsymbol{r}$ and $\boldsymbol{r}'$, respectively, have the two-particle interaction $v_{\alpha\beta}(\boldsymbol{r}, \boldsymbol{r}')$; note that we consider both intra- and interspecies interactions. The general second-quantized Hamiltonian for the system is then, by (2.6):

$$\begin{aligned} H &= H_1 + H_2 \\ &= \sum_\alpha \int d\boldsymbol{r} \hat{\psi}_\alpha^\dagger(\boldsymbol{r}) h_\alpha(\boldsymbol{r}) \hat{\psi}_\alpha(\boldsymbol{r}) \\ &\quad + \frac{1}{2} \sum_{\alpha\beta} \int d\boldsymbol{r} \int d\boldsymbol{r}' \hat{\psi}_\alpha^\dagger(\boldsymbol{r}) \hat{\psi}_\alpha^\dagger(\boldsymbol{r}') v_{\alpha\beta}(\boldsymbol{r}, \boldsymbol{r}') \hat{\psi}_\alpha(\boldsymbol{r}') \hat{\psi}_\alpha(\boldsymbol{r}), \end{aligned} \tag{3.1}$$

where $\hat{\psi}_\alpha(\boldsymbol{r})$ and $\hat{\psi}_\alpha^\dagger(\boldsymbol{r})$ are the annihilation and creation field operators, respectively. Suppressing the species index α, the annihilation field operator can be written as

$$\hat{\psi}(\boldsymbol{r}) = \sum_\nu \phi_\nu(\boldsymbol{r}) b_\nu, \tag{3.2}$$

and correspondingly for the creation field operator $\hat{\psi}^\dagger(\boldsymbol{r})$. ν is the quantum number of a member of any basis set, $\phi_\nu(\boldsymbol{r})$ and b_ν are the basis wavefunction and annihilation operator, respectively, for any specific ν.

We now consider the system to be on a lattice. We do not specify the dimensionality. This means that there are periodic potential wells in $h_\alpha(\boldsymbol{r})$,

common for both species, that make the particles attracted to periodic lattice points. We do not consider interactions between the particles and the lattice points[1]. We assume that the space between the lattice points are much larger than the reach of the potential wells (called the "atomic limit"), meaning that the particles tend to be located at specific lattice sites. This situation is called the tight-binding model [21].

The tight-binding model motivates choosing the basis in (3.2) to be the lattice sites, $\nu = \boldsymbol{r}_i$. The wavefunctions $\phi_{\boldsymbol{r}_i}$ then becomes Wannier functions $W_{\alpha\boldsymbol{r}_i}(\boldsymbol{r}) \equiv W_\alpha(\boldsymbol{r} - \boldsymbol{r}_i)$[2]. The field operator then becomes

$$\hat{\psi}_\alpha(\boldsymbol{r}) = \sum_i W_\alpha(\boldsymbol{r} - \boldsymbol{r}_i) b_{i\alpha}, \tag{3.3}$$

where the sum is over all lattice sites $\boldsymbol{r}_i$. Inserting (3.3) into (3.1) and collecting single-particle terms into sums where $i = j$ and $i \neq j$ produces the first expression for the Bose-Hubbard model:

$$H = -\sum_\alpha \sum_{i \neq j} t_{ij\alpha} b^\dagger_{i\alpha} b_{j\alpha} + \sum_{i\alpha} \epsilon_{i\alpha} b^\dagger_{i\alpha} b_{i\alpha} + \frac{1}{2} \sum_{\alpha\beta} \sum_{ijkl} U_{ijkl\alpha\beta} b^\dagger_{i\alpha} b^\dagger_{j\beta} b_{k\beta} b_{l\alpha}, \tag{3.4}$$

where we have introduced the parameters

$$t_{ij\alpha} = -\int d\boldsymbol{r} W^*_\alpha(\boldsymbol{r} - \boldsymbol{r}_i) h_\alpha W_\alpha(\boldsymbol{r} - \boldsymbol{r}_j), \tag{3.5}$$

$$\varepsilon_{i\alpha} = \int d\boldsymbol{r} W^*_\alpha(\boldsymbol{r} - \boldsymbol{r}_i) h_\alpha W_\alpha(\boldsymbol{r} - \boldsymbol{r}_i), \tag{3.6}$$

$$U_{ijkl\alpha\beta} = \int d\boldsymbol{r} \int d\boldsymbol{r}' W^*_\alpha(\boldsymbol{r} - \boldsymbol{r}_i) W^*_\beta(\boldsymbol{r} - \boldsymbol{r}_j) v_{\alpha\beta}(\boldsymbol{r}, \boldsymbol{r}') W_\beta(\boldsymbol{r} - \boldsymbol{r}_k) W_\alpha(\boldsymbol{r} - \boldsymbol{r}_l). \tag{3.7}$$

Physically, $t_{ij\alpha}$ is the hopping amplitude from site i to site j, $\epsilon_{i\alpha}$ is the energy offset at site i, and $U_{ijkl\alpha\beta}$ is the interaction amplitude. (3.4) represents the version of the Bose-Hubbard model used in this thesis.

[1] I.e. the lattice point potentials are unaffected by the particles. In a material this means we neglect phonons

[2] We use the Wannier basis of the lowest energy band.

It is clear that the parameters (3.5), (3.6), and (3.7) are calculated by integrating the overlap of Wannier functions. However, since Wannier functions are highly localized around their respective lattice points the overlap of different sites quickly vanish with increasing distance between the points. The convenient consequence of choosing the Wannier basis is thus that most parameters vanish. It is therefore common to only include lowest-order contributions in the sums in (3.4), thus obtaining the most common form of the Bose-Hubbard model:

$$H = -\sum_{\alpha} t_{\alpha} \sum_{<i,j>} b_{i\alpha}^{\dagger} b_{j\alpha} + \sum_{i\alpha} \epsilon_{i\alpha} b_{i\alpha}^{\dagger} b_{i\alpha} + \frac{1}{2} \sum_{\alpha\beta} U_{\alpha\beta} \sum_{i} b_{i\alpha}^{\dagger} b_{i\beta}^{\dagger} b_{i\beta} b_{i\alpha}, \quad (3.8)$$

where $< i, j >$ denotes the sum over nearest-neighbor sites i and j, t_{α} is the corresponding hopping amplitude, and $U_{\alpha\beta}$ is the onsite interaction amplitude.

The following expressions were used for $h_{\alpha}(\boldsymbol{r})$ and $v_{\alpha\beta}(\boldsymbol{r}, \boldsymbol{r}')$ in Ref. [14] and serve as examples for concreteness:

$$h_{\alpha}(\boldsymbol{r}) = -\frac{\nabla^2}{2m_{\alpha}} - \mu_{\alpha} + V_0(\boldsymbol{r}) + V_{T,\alpha}(\boldsymbol{r}), \quad (3.9)$$

$$v_{\alpha\beta}(\boldsymbol{r}, \boldsymbol{r}') = \gamma_{\alpha\beta} \delta(\boldsymbol{r} - \boldsymbol{r}'), \quad (3.10)$$

where m_{α} and μ_{α} are the mass and chemical potential, respectively, of component α; $V_0(\boldsymbol{r})$ is the optical lattice potential; $V_{T,\alpha}(\boldsymbol{r})$ is the trapping potential of component α; and $\gamma_{\alpha\beta}$ is the onsite interaction strenght between species α and β.

The Bose-Hubbard model is in this thesis applied on a boson gas residing on an optical lattice. To obtain this the bosons are trapped by a trapping potential $V_{T,\alpha}(\boldsymbol{r})$; this slowly varying electric field confines the bosons to a certain volume of space. The optical lattice is made by a periodic potential $V_0(\boldsymbol{r})$ made possible by two interfering lasers making an interference pattern that influences the bosons such as to mimic a lattice. See e.g. Ref. [14] for details.

In the following we interpret the two species A and B to be so-called synthetic spin states, explained in Section 3.2.2. We thus have the designation $\alpha, \beta = \uparrow, \downarrow$.

3.1.1 Fourier transform

We want to express H in terms of the momentum of the particles, rather than the position. The real space boson operators can be defined in terms of the Fourier-transformed boson operators:

$$b_{i\alpha} = \frac{1}{\sqrt{N_s}} \sum_{\boldsymbol{k}} b_{\boldsymbol{k}\alpha} e^{-i\boldsymbol{k}\cdot\boldsymbol{r}_i}, \tag{3.11}$$

where N_s is the number of lattice sites. We assume that the energy offset at each lattice point is constant for each spin, $\varepsilon_{i\alpha} = T_\alpha$. Inserting (3.11) into the single-particle part of (3.4) gives

$$\begin{aligned} H_1 = &- \sum_\alpha \sum_{i \neq j} t_{ij\alpha} \frac{1}{N_s} \sum_{\boldsymbol{k}\boldsymbol{k}'} b^\dagger_{\boldsymbol{k}\alpha} b_{\boldsymbol{k}'\alpha} e^{-i\boldsymbol{k}'\cdot\boldsymbol{r}_j} e^{i\boldsymbol{k}\cdot\boldsymbol{r}_i} \\ &+ \sum_{i\alpha} T_\alpha \frac{1}{N_s} \sum_{\boldsymbol{k}\boldsymbol{k}'} b^\dagger_{\boldsymbol{k}\alpha} b_{\boldsymbol{k}'\alpha} e^{-i\boldsymbol{k}'\cdot\boldsymbol{r}_i} e^{i\boldsymbol{k}\cdot\boldsymbol{r}_i}. \end{aligned} \tag{3.12}$$

We let $\boldsymbol{r}_j = \boldsymbol{r}_i + \boldsymbol{\delta}$ so that the sum over j is replaced by a sum over all vectors $\boldsymbol{\delta}$ between point i and all other neighboring points. We do not restrict ourselves to nearest-neighbor hopping. We assume that the hopping amplitude is only dependent on the vector $\boldsymbol{\delta}$ between the two lattice points, so that $t_{ij\alpha} = t_\alpha(\boldsymbol{\delta})$. Using this, and eliminating the sum over $\boldsymbol{k}'$ by the relation (2.8), yield

$$\begin{aligned} H_1 &= - \sum_\alpha \sum_{\boldsymbol{\delta}} t_\alpha(\boldsymbol{\delta}) e^{-i\boldsymbol{k}'\cdot\boldsymbol{\delta}} \sum_{\boldsymbol{k}\boldsymbol{k}'} b^\dagger_{\boldsymbol{k}\alpha} b_{\boldsymbol{k}'\alpha} \frac{1}{N_s} \sum_i e^{-i(\boldsymbol{k}'-\boldsymbol{k})\cdot\boldsymbol{r}_i} \\ &\quad + \sum_\alpha T_\alpha \sum_{\boldsymbol{k}\boldsymbol{k}'} b^\dagger_{\boldsymbol{k}\alpha} b_{\boldsymbol{k}'\alpha} \frac{1}{N_s} \sum_i e^{-i(\boldsymbol{k}'-\boldsymbol{k})\cdot\boldsymbol{r}_i} \\ &= \sum_{\boldsymbol{k}\alpha} \left(\varepsilon_{\boldsymbol{k}\alpha} + T_\alpha\right) b^\dagger_{\boldsymbol{k}\alpha} b_{\boldsymbol{k}\alpha}, \end{aligned} \tag{3.13}$$

where

$$\varepsilon_{\boldsymbol{k}\alpha} = - \sum_{\boldsymbol{\delta}} t_\alpha(\boldsymbol{\delta}) e^{-i\boldsymbol{k}\cdot\boldsymbol{\delta}}. \tag{3.14}$$

The Fourier transform of the interaction Hamiltonian becomes

$$
\begin{aligned}
H_2 &= \frac{1}{2}\sum_{\alpha\beta}\sum_{\{\boldsymbol{k}_i\}}\sum_{ijkl} U_{ijkl\alpha\beta}\frac{1}{N_s^2} b^\dagger_{\boldsymbol{k}_1\alpha} e^{i\boldsymbol{k}_1\cdot\boldsymbol{r}_i} b^\dagger_{\boldsymbol{k}_2\beta} e^{i\boldsymbol{k}_2\cdot\boldsymbol{r}_j} b_{\boldsymbol{k}_3\beta} e^{i\boldsymbol{k}_3\cdot\boldsymbol{r}_k} b_{\boldsymbol{k}_4\alpha} e^{i\boldsymbol{k}_4\cdot\boldsymbol{r}_l} \\
&= H_2^{\uparrow\downarrow} + \sum_\alpha H_2^\alpha,
\end{aligned}
\tag{3.15}
$$

where $\{\boldsymbol{k}_i\}$ indicates a sum over $\boldsymbol{k}_1, \boldsymbol{k}_2, \boldsymbol{k}_3, \boldsymbol{k}_4$, and H_2^α includes the terms for which $\alpha = \beta$ and $H_2^{\uparrow\downarrow}$ includes the terms for which $\alpha \neq \beta$. We now let $\boldsymbol{r}_j = \boldsymbol{r}_i + \boldsymbol{\delta}_1$, $\boldsymbol{r}_k = \boldsymbol{r}_i + \boldsymbol{\delta}_2$, and $\boldsymbol{r}_l = \boldsymbol{r}_i + \boldsymbol{\delta}_3$. We assume that the scattering potential is independent of the lattice points involved, only their relative positions, so that $U_{ijkl\alpha\beta} = U_{\alpha\beta}(\boldsymbol{\delta}_1, \boldsymbol{\delta}_2, \boldsymbol{\delta}_3)$. When $\alpha = \beta$ we let $U_{\alpha\beta}(\boldsymbol{\delta}_1, \boldsymbol{\delta}_2, \boldsymbol{\delta}_3) \equiv U_\alpha(\boldsymbol{\delta}_1, \boldsymbol{\delta}_2, \boldsymbol{\delta}_3)$ and obtain

$$
\begin{aligned}
H_2^\alpha &= \frac{1}{2N_s}\sum_\alpha\sum_{\{\boldsymbol{k}_i\}}\left(U_\alpha(0,0,0) + \sum_{\{\boldsymbol{\delta}_i\}} U_\alpha(\boldsymbol{\delta}_1,\boldsymbol{\delta}_2,\boldsymbol{\delta}_3) e^{i(\boldsymbol{k}_2\cdot\boldsymbol{\delta}_1 - \boldsymbol{k}_3\cdot\boldsymbol{\delta}_2 - \boldsymbol{k}_4\cdot\boldsymbol{\delta}_3)}\right) \\
&\quad b^\dagger_{\boldsymbol{k}_1\alpha} b^\dagger_{\boldsymbol{k}_2\alpha} b_{\boldsymbol{k}_3\alpha} b_{\boldsymbol{k}_4\alpha} \frac{1}{N_s}\sum_i e^{-i(\boldsymbol{k}_3+\boldsymbol{k}_4-\boldsymbol{k}_1-\boldsymbol{k}_2)\cdot\boldsymbol{r}_i} \\
&= \frac{1}{2N_s}\sum_\alpha\sum_{\{\boldsymbol{k}_i\}} \tilde{U}_\alpha(\boldsymbol{k}_2,\boldsymbol{k}_3,\boldsymbol{k}_4) b^\dagger_{\boldsymbol{k}_1\alpha} b^\dagger_{\boldsymbol{k}_2\alpha} b_{\boldsymbol{k}_3\alpha} b_{\boldsymbol{k}_4\alpha} \delta_{\boldsymbol{k}_1+\boldsymbol{k}_2,\boldsymbol{k}_3+\boldsymbol{k}_4},
\end{aligned}
\tag{3.16}
$$

where $\{\boldsymbol{\delta}_i\}$ indicates a sum over all $\boldsymbol{\delta}_1, \boldsymbol{\delta}_2, \boldsymbol{\delta}_3$, except for $(\boldsymbol{\delta}_1, \boldsymbol{\delta}_2, \boldsymbol{\delta}_3) = (0,0,0)$. In the last equality we have again used (2.8), and introduced the Fourier transform of the intra-spin scattering potential,

$$
\tilde{U}_\alpha(\boldsymbol{k}_2,\boldsymbol{k}_3,\boldsymbol{k}_4) = U_\alpha(0,0,0) + \sum_{\{\boldsymbol{\delta}_i\}} U_\alpha(\boldsymbol{\delta}_1,\boldsymbol{\delta}_2,\boldsymbol{\delta}_3) e^{i(\boldsymbol{k}_2\cdot\boldsymbol{\delta}_1 - \boldsymbol{k}_3\cdot\boldsymbol{\delta}_2 - \boldsymbol{k}_4\cdot\boldsymbol{\delta}_3)}. \tag{3.17}
$$

When $\alpha \neq \beta$ we obtain

$$
\begin{aligned}
H_2^{\uparrow\downarrow} &= \frac{1}{2N_s}\sum_{\{\boldsymbol{k}_i\}}\sum_{\alpha\neq\beta}\sum_{\{\boldsymbol{\delta}_i\}}^{0} U_{\alpha\beta}(\boldsymbol{\delta}_1,\boldsymbol{\delta}_2,\boldsymbol{\delta}_3) b^\dagger_{\boldsymbol{k}_1\alpha} b^\dagger_{\boldsymbol{k}_2\beta} b_{\boldsymbol{k}_3\beta} b_{\boldsymbol{k}_4\alpha} e^{i(\boldsymbol{k}_2\cdot\boldsymbol{\delta}_1-\boldsymbol{k}_3\cdot\boldsymbol{\delta}_2-\boldsymbol{k}_4\cdot\boldsymbol{\delta}_3)} \\
&\quad\cdot\frac{1}{N_s}\sum_i e^{-i(\boldsymbol{k}_3+\boldsymbol{k}_4-\boldsymbol{k}_1-\boldsymbol{k}_2)\cdot\boldsymbol{r}_i} \\
&= \frac{1}{2N_s}\sum_{\{\boldsymbol{k}_i\}}\sum_{\{\boldsymbol{\delta}_i\}}^{0}\Big[U_{\uparrow\downarrow}(\boldsymbol{\delta}_1,\boldsymbol{\delta}_2,\boldsymbol{\delta}_3) b^\dagger_{\boldsymbol{k}_1\uparrow} b^\dagger_{\boldsymbol{k}_2\downarrow} b_{\boldsymbol{k}_3\downarrow} b_{\boldsymbol{k}_4\uparrow} e^{i(\boldsymbol{k}_2\cdot\boldsymbol{\delta}_1-\boldsymbol{k}_3\cdot\boldsymbol{\delta}_2-\boldsymbol{k}_4\cdot\boldsymbol{\delta}_3)} \\
&\qquad + U_{\downarrow\uparrow}(\boldsymbol{\delta}_1,\boldsymbol{\delta}_2,\boldsymbol{\delta}_3) b^\dagger_{\boldsymbol{k}_1\downarrow} b^\dagger_{\boldsymbol{k}_2\uparrow} b_{\boldsymbol{k}_3\uparrow} b_{\boldsymbol{k}_4\downarrow} e^{i(\boldsymbol{k}_2\cdot\boldsymbol{\delta}_1-\boldsymbol{k}_3\cdot\boldsymbol{\delta}_2-\boldsymbol{k}_4\cdot\boldsymbol{\delta}_3)}\Big]\delta_{\boldsymbol{k}_1+\boldsymbol{k}_2,\boldsymbol{k}_3+\boldsymbol{k}_4},
\end{aligned}
\tag{3.18}
$$

where 0 above the sum indicates that the sum includes $(\boldsymbol{\delta}_1,\boldsymbol{\delta}_2,\boldsymbol{\delta}_3)=(0,0,0)$, and where we used (2.8) in the last equality. We now assume that $U_{\uparrow\downarrow}=U_{\downarrow\uparrow}$. In the first term in the parathesis we change the names of the $\boldsymbol{k}$ variables so that $\boldsymbol{k}_2\to\boldsymbol{k}_3$, $\boldsymbol{k}_3\to\boldsymbol{k}_4$, and $\boldsymbol{k}_4\to\boldsymbol{k}_2$; in the second term we do the assignment $\boldsymbol{k}_2\to\boldsymbol{k}_1$, $\boldsymbol{k}_3\to\boldsymbol{k}_2$, and $\boldsymbol{k}_1\to\boldsymbol{k}_3$. Thus we obtain

$$
\begin{aligned}
&H_2^{\uparrow\downarrow} \\
&= \frac{1}{2N_s}\sum_{\{\boldsymbol{k}_i\}}\sum_{\{\boldsymbol{\delta}_i\}}^{0} U_{\uparrow\downarrow}(\boldsymbol{\delta}_1,\boldsymbol{\delta}_2,\boldsymbol{\delta}_3)\Big[b^\dagger_{\boldsymbol{k}_1\uparrow} b^\dagger_{\boldsymbol{k}_3\downarrow} b_{\boldsymbol{k}_4\downarrow} b_{\boldsymbol{k}_2\uparrow} e^{i(\boldsymbol{k}_3\cdot\boldsymbol{\delta}_1-\boldsymbol{k}_4\cdot\boldsymbol{\delta}_2-\boldsymbol{k}_2\cdot\boldsymbol{\delta}_3)}\delta_{\boldsymbol{k}_4+\boldsymbol{k}_2,\boldsymbol{k}_1+\boldsymbol{k}_3} \\
&\qquad + b^\dagger_{\boldsymbol{k}_3\downarrow} b^\dagger_{\boldsymbol{k}_1\uparrow} b_{\boldsymbol{k}_2\uparrow} b_{\boldsymbol{k}_4\downarrow} e^{i(\boldsymbol{k}_1\cdot\boldsymbol{\delta}_1-\boldsymbol{k}_2\cdot\boldsymbol{\delta}_2-\boldsymbol{k}_4\cdot\boldsymbol{\delta}_3)}\delta_{\boldsymbol{k}_2+\boldsymbol{k}_4,\boldsymbol{k}_3+\boldsymbol{k}_1}\Big] \\
&= \frac{1}{2N_s}\sum_{\{\boldsymbol{k}_i\}}\Bigg[2U_{\uparrow\downarrow}(0,0,0)+\sum_{\{\boldsymbol{\delta}_i\}} U_{\uparrow\downarrow}(\boldsymbol{\delta}_1,\boldsymbol{\delta}_2,\boldsymbol{\delta}_3)\left(e^{i(\boldsymbol{k}_1\cdot\boldsymbol{\delta}_1-\boldsymbol{k}_2\cdot\boldsymbol{\delta}_2-\boldsymbol{k}_4\cdot\boldsymbol{\delta}_3)}\right. \\
&\qquad \left.+\, e^{i(\boldsymbol{k}_3\cdot\boldsymbol{\delta}_1-\boldsymbol{k}_4\cdot\boldsymbol{\delta}_2-\boldsymbol{k}_2\cdot\boldsymbol{\delta}_3)}\right)\Bigg] b^\dagger_{\boldsymbol{k}_1\uparrow} b_{\boldsymbol{k}_2\uparrow} b^\dagger_{\boldsymbol{k}_3\downarrow} b_{\boldsymbol{k}_4\downarrow}\delta_{\boldsymbol{k}_1+\boldsymbol{k}_3,\boldsymbol{k}_2+\boldsymbol{k}_4} \\
&= \frac{1}{N_s}\sum_{\{\boldsymbol{k}_i\}}\tilde{U}_{\uparrow\downarrow}(\boldsymbol{k}_1,\boldsymbol{k}_2,\boldsymbol{k}_3,\boldsymbol{k}_4) b^\dagger_{\boldsymbol{k}_1\uparrow} b_{\boldsymbol{k}_2\uparrow} b^\dagger_{\boldsymbol{k}_3\downarrow} b_{\boldsymbol{k}_4\downarrow}\delta_{\boldsymbol{k}_1+\boldsymbol{k}_3,\boldsymbol{k}_2+\boldsymbol{k}_4},
\end{aligned}
\tag{3.19}
$$

where we in the penultimate equality commuted the boson operators according to the commutation relation (2.5), and then introduced the Fourier transform of the inter-spin scattering potential,

$$\tilde{U}_{\uparrow\downarrow}(\boldsymbol{k}_1,\boldsymbol{k}_2,\boldsymbol{k}_3,\boldsymbol{k}_4) = U_{\uparrow\downarrow}(0,0,0) + \frac{1}{2}\sum_{\{\boldsymbol{\delta}_i\}} U_{\uparrow\downarrow}(\boldsymbol{\delta}_1,\boldsymbol{\delta}_2,\boldsymbol{\delta}_3)\left(e^{i(\boldsymbol{k}_1\cdot\boldsymbol{\delta}_1-\boldsymbol{k}_2\cdot\boldsymbol{\delta}_2-\boldsymbol{k}_4\cdot\boldsymbol{\delta}_3)} + e^{i(\boldsymbol{k}_3\cdot\boldsymbol{\delta}_1-\boldsymbol{k}_4\cdot\boldsymbol{\delta}_2-\boldsymbol{k}_2\cdot\boldsymbol{\delta}_3)}\right). \tag{3.20}$$

In total we now have the following Fourier transformed Hamiltonian:

$$\begin{aligned} H &= \sum_{\boldsymbol{k}\alpha}\left(\varepsilon_{\boldsymbol{k}\alpha}+T_\alpha\right) b^\dagger_{\boldsymbol{k}\alpha} b_{\boldsymbol{k}\alpha} \\ &\quad + \frac{1}{N_s}\sum_{\{\boldsymbol{k}_i\}}\left[\frac{1}{2}\sum_\alpha \tilde{U}_\alpha(\boldsymbol{k}_2,\boldsymbol{k}_3,\boldsymbol{k}_4) b^\dagger_{\boldsymbol{k}_1\alpha} b^\dagger_{\boldsymbol{k}_2\alpha} b_{\boldsymbol{k}_3\alpha} b_{\boldsymbol{k}_4\alpha}\delta_{\boldsymbol{k}_1+\boldsymbol{k}_2,\boldsymbol{k}_3+\boldsymbol{k}_4}\right. \\ &\qquad \left. + \tilde{U}_{\uparrow\downarrow}(\boldsymbol{k}_1,\boldsymbol{k}_2,\boldsymbol{k}_3,\boldsymbol{k}_4) b^\dagger_{\boldsymbol{k}_1\uparrow} b_{\boldsymbol{k}_2\uparrow} b^\dagger_{\boldsymbol{k}_3\downarrow} b_{\boldsymbol{k}_4\downarrow}\delta_{\boldsymbol{k}_1+\boldsymbol{k}_3,\boldsymbol{k}_2+\boldsymbol{k}_4}\right] \\ &\equiv H_1 + \frac{1}{N_s}\left[\frac{1}{2}\sum_\alpha H_2^\alpha + H_2^{\uparrow\downarrow}\right]. \end{aligned} \tag{3.21}$$

This result is the same as in Ref. [14] except for a factor of 1/2 supposedly missing in the Fourier-transformed inter-spin potential.

3.2 Spin-orbit coupling*

Spin-orbit coupling (abbreviated SOC throughout this thesis) is a coupling between a particle's spin and movement appearing in the Hamiltonian. We will here consider spin-1/2 SOC, typically affecting electrons. SOC appears as a consequence of the movement of electrons in electric fields. This movement causes a magnetic field in the electron's frame of reference. When considering electrons bound to hydrogen-like atoms the spin-orbit coupling can either be derived through a non-relativistic qualitative argument, or through an exact relativistic argument. The non-relativistic argument finds an expression for the magnetic field in the electron's frame of reference by a non-relativistic transformation between frames of reference, and thereby finds this field's coupling to the electron's spin; see Chapter 4 in Ref. [22] for the complete argument.

The relativistic argument obtains the SOC as a consequence of treating the system relativistically through the Dirac equation. Taking the non-relativistic limit produces explicitly a term in the Hamiltonian proportional to $\boldsymbol{L} \cdot \boldsymbol{S}$, representing SOC. See Chapter 15 of Ref. [23] for a thorough derivation.

3.2.1 Rashba SOC

In materials, electrons experience electric fields e.g. caused by broken spatial symmetry, giving rise to SOC. The review article referenced in Ref. [7] offers an insightful discussion on this phenomena. Rashba spin-orbit coupling is a special case of SOC where the electric field experienced by the electrons is perpendicular to the two-dimensional plane on which the electrons are confined [7]. Introducing the electric field $\boldsymbol{E} = E\hat{\boldsymbol{z}}$ into the SOC term in the Dirac equation yields

$$\begin{aligned} H_{SOC} &= -\frac{e\hbar}{4m_e^2c^2}\boldsymbol{\sigma} \cdot (\boldsymbol{E} \times \boldsymbol{p}) \\ &= -\frac{e\hbar}{4m_e^2c^2}E\boldsymbol{\sigma} \cdot (\hat{\boldsymbol{z}} \times \boldsymbol{p}) \\ &= \frac{e\hbar}{4m_e^2c^2}E(\sigma_x p_y - \sigma_y p_x) \\ &= \frac{e\hbar^2}{4m_e^2c^2}E(\sigma_x p_y - \sigma_y p_x) \\ &= \lambda_R(\sigma_x p_y - \sigma_y p_x), \end{aligned} \tag{3.22}$$

which is the familiar form of the Rashba SOC, where we have used the operator identity $\boldsymbol{p} = \hbar\boldsymbol{k}$ and defined $\lambda_R = \frac{e\hbar^2 E}{4m_e^2c^2}$.

The second-quantized version of (3.22) for a general two-dimensional inversion-symmetric Bravais lattice is provided in Ref. [24], but only the one-dimensional version is derived in the same reference. We thus seek to make a heuristic justification for this expression using the same procedure as in Ref. [24], but generalized from the case of a one-dimensional chain.

The k_i operator in the i-direction is $k_i = -i\partial_i$, by definition. Let $\hat{\boldsymbol{a}}_j$ be a unit vector in the direction of a nearest-neighbor lattice site j. The inversion symmetry of the lattice implies a nearest neighbor site in the $-\hat{\boldsymbol{a}}_j$-direction as well. The derivative in the $\hat{\boldsymbol{a}}_j$-direction can then be expressed in a second quantized form, and we write

$$k_{\hat{\boldsymbol{a}}_j} = -i \sum_{\boldsymbol{r}_i} \left(b^\dagger_{\boldsymbol{r}_i} b_{\boldsymbol{r}_i + \hat{\boldsymbol{a}}_j} - b^\dagger_{\boldsymbol{r}_i} b_{\boldsymbol{r}_i - \hat{\boldsymbol{a}}_j} \right). \tag{3.23}$$

The y-component of this operator is

$$\begin{aligned} k_{\hat{\boldsymbol{a}}_j, y} &= (k_{\hat{\boldsymbol{a}}_j} \hat{\boldsymbol{a}}_j) \cdot \hat{\boldsymbol{y}} \\ &= -i \sum_{\boldsymbol{r}_i} \left(b^\dagger_{\boldsymbol{r}_i} b_{\boldsymbol{r}_i + \hat{\boldsymbol{a}}_j} - b^\dagger_{\boldsymbol{r}_i} b_{\boldsymbol{r}_i - \hat{\boldsymbol{a}}_j} \right) \hat{\boldsymbol{a}}_j \cdot \hat{\boldsymbol{y}}. \end{aligned} \tag{3.24}$$

The total k_y is found from summing over all non-parallel nearest-neighbor unit vectors, $k_y = \sum_{\hat{\boldsymbol{a}}_j} k_{\hat{\boldsymbol{a}}_j, y}$. We thus obtain

$$\begin{aligned} \sigma_x k_y &= \sum_{\hat{\boldsymbol{a}}_j} \sigma_x k_{\hat{\boldsymbol{a}}_j, y} \\ &= \sum_{\boldsymbol{r}_i, \hat{\boldsymbol{a}}_j} \sum_{\alpha,\beta} \left[b^\dagger_{\boldsymbol{r}_i,\alpha} \sigma_x^{\alpha\beta} (-i \hat{\boldsymbol{a}}_j \cdot \hat{\boldsymbol{y}}) b_{\boldsymbol{r}_i + \hat{\boldsymbol{a}}_j, \beta} + b^\dagger_{\boldsymbol{r}_i,\alpha} \sigma_x^{\alpha\beta} (i \hat{\boldsymbol{a}}_j \cdot \hat{\boldsymbol{y}}) b_{\boldsymbol{r}_i - \hat{\boldsymbol{a}}_j, \beta} \right]. \end{aligned} \tag{3.25}$$

By the same arguments we obtain

$$\sigma_y k_x = \sum_{\boldsymbol{r}_i, \hat{\boldsymbol{a}}_j} \sum_{\alpha,\beta} \left[b^\dagger_{\boldsymbol{r}_i,\alpha} \sigma_y^{\alpha\beta} (-i \hat{\boldsymbol{a}}_j \cdot \hat{\boldsymbol{x}}) b_{\boldsymbol{r}_i + \hat{\boldsymbol{a}}_j, \beta} + b^\dagger_{\boldsymbol{r}_i,\alpha} \sigma_y^{\alpha\beta} (i \hat{\boldsymbol{a}}_j \cdot \hat{\boldsymbol{x}}) b_{\boldsymbol{r}_i - \hat{\boldsymbol{a}}_j, \beta} \right]. \tag{3.26}$$

Using periodic boundary conditions we can change the summation variable $\boldsymbol{r}_i \to \boldsymbol{r}_i + \hat{\boldsymbol{a}}_j$ in the second terms. Reordering, we finally obtain

$$\begin{aligned} H_{SOC} &= \lambda_R (\sigma_x p_y - \sigma_y p_x) \\ &= \lambda_R \sum_{\boldsymbol{r}_i, \hat{\boldsymbol{a}}_j} \sum_{\alpha,\beta} \Big[b^\dagger_{\boldsymbol{r}_i,\alpha} \left(\sigma_x^{\alpha\beta} (-i \boldsymbol{a}_j \cdot \hat{\boldsymbol{y}}) + \sigma_y^{\alpha\beta} (i \boldsymbol{a}_j \cdot \hat{\boldsymbol{x}}) \right) b_{\boldsymbol{r}_i + \boldsymbol{a}_j, \beta} \\ &\qquad + b^\dagger_{\boldsymbol{r}_i + \boldsymbol{a}_j, \alpha} \left(\sigma_x^{\alpha\beta} (i \boldsymbol{a}_j \cdot \hat{\boldsymbol{y}}) + \sigma_y^{\alpha\beta} (-i \boldsymbol{a}_j \cdot \hat{\boldsymbol{x}}) \right) b_{\boldsymbol{r}_i, \beta} \Big] \\ &= \lambda_R \sum_{\boldsymbol{r}_i, \hat{\boldsymbol{a}}_j} \sum_{\alpha,\beta} b^\dagger_{\boldsymbol{r}_i,\alpha} \left[-\sigma_x^{\alpha\beta} (i \boldsymbol{a}_j \cdot \hat{\boldsymbol{y}}) + \sigma_y^{\alpha\beta} (i \boldsymbol{a}_j \cdot \hat{\boldsymbol{x}}) \right] b_{\boldsymbol{r}_i + \boldsymbol{a}_j, \beta} + H.c. \end{aligned} \tag{3.27}$$

where $H.c.$ means Hermitian conjugate. This expression is the same as the one provided in Ref. [24]. Equation (3.27) is valid for an inversion-symmetric two-dimensional Bravais lattice. However, by only including one pair of oppositely positioned nearest neighbors, i.e. only one term $\boldsymbol{a}$ in the sum over $\boldsymbol{a}_j$, (3.27) represents spin-orbit coupling on a one-dimensional chain in the $\boldsymbol{a}$-direction.

3.2.2 Synthetic SOC

The SOC of spin-1/2 systems are of great importance in many interesting materials [7]. These effects, however, are difficult to study directly since they would require electric fields that are much stronger than what is typically produced in a laboratory. This thesis is concerned with a system that can simulate spin-1/2 SOC with the use of a ultracold boson gas. The bosons are typically spin-1 and would thus possess a real intrinsic SOC. However, this coupling is also very weak, just like the spin-1/2 type, and not as interesting as spin-1/2 since systems of electron gases are much more abundant.

Producing a synthetic SOC in a ultracold boson gas is accomplished through the introduction of so-called dressed spin states. These are boson states that in certain regards can simulate the spin property created through some laboratory introduced interaction. The dressed spin states can be created by the use of two-photon Raman transitions, which is the subject of this thesis. This mechanism was first proposed in Ref. [25]; we now briefly discuss synthetic SOC by the use of Raman transitions based on the arguments of this paper.

The transition between two atom states of different energy through an intermediate state by the absorption and emission of two photons is called a two-photon Raman transition. It is an example of inelastic photon scattering. The bosons being used in the boson gas possess two internal hyperfine ground states, $|a\rangle$ and $|b\rangle$, and an excited state $|e\rangle$. The energy levels of $|a\rangle$ and $|b\rangle$ are separated by $\hbar\omega_0$. Two lasers are directed at the gas with non-parallel wave vectors $\boldsymbol{k}_1$ and $\boldsymbol{k}_2$. The two lasers have angular frequencies ω_1 and ω_2 which couple $|a\rangle$ and $|b\rangle$ to an intermediate energy level which is lower than $|e\rangle$ by an angular frequency Δ. The deviation Δ ensures that the lasers do not couple $|a\rangle$ and $|b\rangle$ to $|e\rangle$ resonantly, which would lead to irrelevant one-photon elastic scattering, called Rayleigh scattering. The lasers will thus induce transitions from $|a\rangle$ to $|b\rangle$, and vice versa, via the intermediate state. When $\omega_2 - \omega_1 = \omega_0$ we say that we have Raman resonance, which is much weaker than the resonance of Rayleigh scattering, and the transition is called a Raman transition.

Raman transitions result in the absorption and emission of photons of different wave vectors, meaning that the atom is subject to a momentum transfer of $\pm\hbar(\boldsymbol{k}_2 - \boldsymbol{k}_1)$ by conservation of momentum. One of the lasers is detuned away from Raman resonance by a small angular frequency δ. However, the movement of the bosons causes them to experience slightly

different laser frequencies due to the Doppler shift. Thus, depending of the movement of the bosons, the frequencies can be shifted towards or away from Raman resonance. In other words, the movements of the bosons influence which state $|a\rangle$ or $|b\rangle$ they are in, while the transition between the states influence the movement via the momentum transfer $\pm\hbar(\boldsymbol{k}_2 - \boldsymbol{k}_1)$. Upon designating $|a\rangle$ or $|b\rangle$ "spin up" and "spin down" we now effectively have a synthetic spin-1/2 spin-orbit coupling. Unlike real SOC, this coupling is highly tunable. It also involves bosons that are not subject to the same fermionic constrictions, leading to many more exotic behaviors, not seen anywhere else in physics [7]. This form of SOC produces both Rashba and Dresselhaus type SOC of equal magnitude [7]; however, this thesis is only concerned with the former.

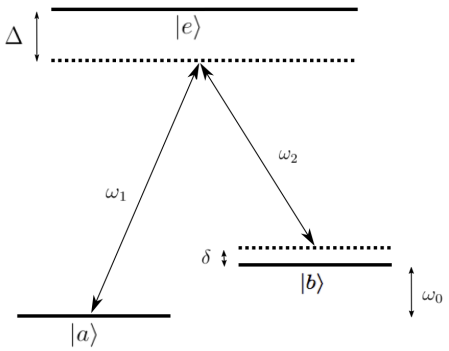

Figure 3.1: Two-photon Raman scattering. Ground state energy levels $|a\rangle$ and $|b\rangle$ are separated by ω_0. Transition between $|a\rangle$ and $|b\rangle$ can occur via an intermediate energy level which is Δ below the excited state $|e\rangle$. The transition occurs by the absorption and emission of photons of frequency ω_1 and ω_2 at Raman resonance $\omega_2 - \omega_1 = \omega_0$. δ is the small detuning from Raman resonance which is influenced by the boson's movement by the Doppler shift.

3.2.3 Spin-orbit coupling on a lattice

We now consider the Rashba spin-orbit coupling of spin particles residing on a two-dimensional Bravais lattice. Fourier transforming (3.27) in 3.2 and summing over spin indices yield

$$
\begin{aligned}
H_{SOC} &= \lambda_R \sum_{\boldsymbol{k},\hat{\boldsymbol{a}}_j,\alpha,\beta} \Big[b^\dagger_{\boldsymbol{k}\alpha} \left(-\sigma_x^{\alpha\beta}(i\hat{\boldsymbol{a}}_j \cdot \hat{\boldsymbol{y}}) + \sigma_y^{\alpha\beta}(i\hat{\boldsymbol{a}}_j \cdot \hat{\boldsymbol{x}}) \right) b_{\boldsymbol{k}\beta} e^{i\boldsymbol{k}\cdot\hat{\boldsymbol{a}}_j} \\
&\qquad - b^\dagger_{\boldsymbol{k}\beta} \left(-\sigma_x^{\beta\alpha}(i\hat{\boldsymbol{a}}_j \cdot \hat{\boldsymbol{y}}) + \sigma_y^{\beta\alpha}(i\hat{\boldsymbol{a}}_j \cdot \hat{\boldsymbol{x}}) \right) b_{\boldsymbol{k}\alpha} e^{-i\boldsymbol{k}\cdot\hat{\boldsymbol{a}}_j} \Big] \\
&= \lambda_R \sum_{\boldsymbol{k},\hat{\boldsymbol{a}}_j} \Big[b^\dagger_{\boldsymbol{k}\uparrow} b_{\boldsymbol{k}\downarrow} (-i\hat{\boldsymbol{a}}_j \cdot \hat{\boldsymbol{y}} + \hat{\boldsymbol{a}}_j \cdot \hat{\boldsymbol{x}})(e^{i\boldsymbol{k}\cdot\hat{\boldsymbol{a}}_j} - e^{-i\boldsymbol{k}\cdot\hat{\boldsymbol{a}}_j}) \\
&\qquad + b^\dagger_{\boldsymbol{k}\downarrow} b_{\boldsymbol{k}\uparrow} (-i\hat{\boldsymbol{a}}_j \cdot \hat{\boldsymbol{y}} - \hat{\boldsymbol{a}}_j \cdot \hat{\boldsymbol{x}})(e^{i\boldsymbol{k}\cdot\hat{\boldsymbol{a}}_j} - e^{-i\boldsymbol{k}\cdot\hat{\boldsymbol{a}}_j}) \Big] \\
&= 2i\lambda_R \sum_{\boldsymbol{k},\hat{\boldsymbol{a}}_j} \Big[b^\dagger_{\boldsymbol{k}\uparrow} b_{\boldsymbol{k}\downarrow} (-i\hat{\boldsymbol{a}}_j \cdot \hat{\boldsymbol{y}} + \hat{\boldsymbol{a}}_j \cdot \hat{\boldsymbol{x}}) \sin(\boldsymbol{k}\cdot\hat{\boldsymbol{a}}_j) \\
&\qquad + b^\dagger_{\boldsymbol{k}\downarrow} b_{\boldsymbol{k}\uparrow} (-i\hat{\boldsymbol{a}}_j \cdot \hat{\boldsymbol{y}} - \hat{\boldsymbol{a}}_j \cdot \hat{\boldsymbol{x}}) \sin(\boldsymbol{k}\cdot\hat{\boldsymbol{a}}_j) \Big] \\
&= \sum_{\boldsymbol{k}} \begin{pmatrix} b^\dagger_{\boldsymbol{k}\uparrow} & b^\dagger_{\boldsymbol{k}\downarrow} \end{pmatrix}^T \begin{pmatrix} 0 & s_{\boldsymbol{k}} \\ s^*_{\boldsymbol{k}} & 0 \end{pmatrix} \begin{pmatrix} b_{\boldsymbol{k}\uparrow} \\ b_{\boldsymbol{k}\downarrow} \end{pmatrix},
\end{aligned}
\tag{3.28}
$$

where $\hat{\boldsymbol{a}}_j$ are non-parallel nearest neighbor unit vectors, and we in the first equality made use of the relation (2.8), and where

$$
\begin{aligned}
s_{\boldsymbol{k}} &= 2i\lambda_R \sum_{\hat{\boldsymbol{a}}_j} (-i\hat{\boldsymbol{a}}_j \cdot \hat{\boldsymbol{y}} + \hat{\boldsymbol{a}}_j \cdot \hat{\boldsymbol{x}}) \sin(\boldsymbol{k}\cdot\hat{\boldsymbol{a}}_j) \\
&= 2i\lambda_R \sum_j e^{-i\theta_j} \sin(\boldsymbol{k}\cdot\hat{\boldsymbol{a}}_j),
\end{aligned}
\tag{3.29}
$$

θ_j being the angle between $\hat{\boldsymbol{a}}_j$ and the x-axis. The exponential follows from

$$
\begin{aligned}
\hat{\boldsymbol{a}}_j \cdot \hat{\boldsymbol{x}} - i\hat{\boldsymbol{a}}_j \cdot \hat{\boldsymbol{y}} &= \cos\theta_j - i\cos(\pi - \theta_j) \\
&= \cos\theta_j - i\sin\theta_j \\
&= e^{-i\theta_j}.
\end{aligned}
\tag{3.30}
$$

We now incorporate H_{SOC} into the H_1 found in (3.21) of Section 3.1.1. Furthermore, we assume the energy parameters $\varepsilon_{\boldsymbol{k}\alpha}$ and T_α to be independent of synthetic spin state. Assigning $\varepsilon_{\boldsymbol{k}\alpha} \equiv \varepsilon_{\boldsymbol{k}}$ and $T_\alpha \equiv T$, the total single-particle Hamiltonian is now identified, namely

$$
\begin{aligned}
H_1 &= \sum_{\boldsymbol{k}} \begin{pmatrix} b^\dagger_{\boldsymbol{k}\uparrow} & b^\dagger_{\boldsymbol{k}\downarrow} \end{pmatrix} \begin{pmatrix} \varepsilon_{\boldsymbol{k}} + T & s_{\boldsymbol{k}} \\ s^*_{\boldsymbol{k}} & \varepsilon_{\boldsymbol{k}} + T \end{pmatrix} \begin{pmatrix} b_{\boldsymbol{k}\uparrow} \\ b_{\boldsymbol{k}\downarrow} \end{pmatrix} \\
&= \sum_{\boldsymbol{k}} \xi^\dagger_{\boldsymbol{k}} \mathcal{A}_{\boldsymbol{k}} \xi_{\boldsymbol{k}}.
\end{aligned}
\tag{3.31}
$$

We now transform H_1 from the current spin basis $\xi_{\boldsymbol{k}} = \begin{pmatrix} b_{\boldsymbol{k}\uparrow} & b_{\boldsymbol{k}\downarrow} \end{pmatrix}^T$, to a new basis $\Psi_{\boldsymbol{k}}$, such that H_1 is diagonal:

$$H_1 = \sum_{\boldsymbol{k}} \Psi^\dagger_{\boldsymbol{k}} \mathcal{D}_{\boldsymbol{k}} \Psi_{\boldsymbol{k}}, \tag{3.32}$$

where $\mathcal{D}_{\boldsymbol{k}}$ is a diagonal matrix with the eigenvalues of $\mathcal{A}_{\boldsymbol{k}}$ on its diagonal. These eigenvalues are found to be

$$\mathcal{E}^{\pm}_{\boldsymbol{k}} = \varepsilon_{\boldsymbol{k}} + T \pm |s_{\boldsymbol{k}}| = -\sum_{\boldsymbol{\delta}} t(\boldsymbol{\delta}) e^{-i\boldsymbol{k}\cdot\boldsymbol{\delta}} + T \pm 2\lambda_R \Big| \sum_j e^{-i\theta_j} \sin(\boldsymbol{k}\cdot\hat{\boldsymbol{a}}_j) \Big|. \tag{3.33}$$

$\mathcal{E}^{\pm}_{\boldsymbol{k}}$ are the single-particle energy bands in the spin-orbit coupled Bose-Hubbard model. The energy offset T only represent a constant shift in the energy which is qualitatively uninteresting in this treatment. In what remains we will set this offset T to zero.

With the new basis labeled $\Psi_{\boldsymbol{k}} = \begin{pmatrix} a_{\boldsymbol{k}+} & a_{\boldsymbol{k}-} \end{pmatrix}^T$ we arrive at the single-particle Hamiltonian

$$\begin{aligned} H_1 &= \sum_{\boldsymbol{k}} \Psi^\dagger_{\boldsymbol{k}} \begin{pmatrix} \mathcal{E}^+_{\boldsymbol{k}} & 0 \\ 0 & \mathcal{E}^-_{\boldsymbol{k}} \end{pmatrix} \Psi_{\boldsymbol{k}} \\ &= \sum_{\boldsymbol{k}} \left(\mathcal{E}^+_{\boldsymbol{k}} a^\dagger_{\boldsymbol{k}+} a_{\boldsymbol{k}+} + \mathcal{E}^-_{\boldsymbol{k}} a^\dagger_{\boldsymbol{k}-} a_{\boldsymbol{k}-} \right). \end{aligned} \tag{3.34}$$

We will see that $a_{\boldsymbol{k}+}$ and $a_{\boldsymbol{k}-}$ are boson operators, where the $+$ $(-)$ subscript indicate the highest (lowest) energy band for the given $\boldsymbol{k}$; we call them helicity band operators.

We now consider some characteristics of the spin-orbit coupled single-particle energy. These characteristics will be made use of in the following treatment. Some assumptions concerning the lattice are needed. Firstly, we assume the hopping parameter to be symmetric in the hopping vector $\boldsymbol{\delta}$, $t(\boldsymbol{\delta}) = t(-\boldsymbol{\delta})$, due to the translational invariance of the system. This makes the single-particle energy real, since

$$\begin{aligned}(\mathcal{E}_{\boldsymbol{k}}^{\pm})^* &= \varepsilon_{\boldsymbol{k}}^* \pm |s_{\boldsymbol{k}}| \\ &= -\sum_{\boldsymbol{\delta}} t(\boldsymbol{\delta}) e^{i\boldsymbol{k}\cdot\boldsymbol{\delta}} \pm |s_{\boldsymbol{k}}| \\ &= -\sum_{\boldsymbol{\delta}} t(-\boldsymbol{\delta}) e^{-i\boldsymbol{k}\cdot\boldsymbol{\delta}} \pm |s_{\boldsymbol{k}}| \\ &= -\sum_{\boldsymbol{\delta}} t(\boldsymbol{\delta}) e^{-i\boldsymbol{k}\cdot\boldsymbol{\delta}} \pm |s_{\boldsymbol{k}}| \\ &= \mathcal{E}_{\boldsymbol{k}}^{\pm},\end{aligned} \tag{3.35}$$

making, in fact, the symmetric nature of the hopping parameter a physical demand in our model.

Secondly, since the lattice is inversion symmetric, all neighbors of a lattice site are situated in pairs opposite of each other with respect to the lattice site, i.e. they all appear in pairs $(\boldsymbol{\delta_i}, \boldsymbol{\delta_j})$ such that $\boldsymbol{\delta_i} = -\boldsymbol{\delta_j}$. We can then write

$$\mathcal{E}_{\boldsymbol{k}}^{\pm} = -2\sum_{\boldsymbol{\delta}} t(\boldsymbol{\delta}) \cos(\boldsymbol{k}\cdot\boldsymbol{\delta}) \pm 2\lambda_R \Big|\sum_j e^{-i\theta_j} \sin(\boldsymbol{k}\cdot\hat{\boldsymbol{a}}_j)\Big|, \tag{3.36}$$

where now the sum over $\boldsymbol{\delta}$ is only over one of each such pair. We observe from this expression that $\mathcal{E}_{\boldsymbol{k}}^{\pm}$ is symmetric in $\boldsymbol{k}$, $\mathcal{E}_{-\boldsymbol{k}}^{\pm} = \mathcal{E}_{\boldsymbol{k}}^{\pm}$. We also note that the ground state of H_1 cannot be $\boldsymbol{k} = 0$. To realize this we look at the Maclaurin expansion of $\mathcal{E}_{\boldsymbol{k}}^{-}$, for $\boldsymbol{k}$ in the $x \geq 0$ half plane:

$$\begin{aligned}\mathcal{E}_{\boldsymbol{k}}^{\pm} &= -2\sum_{\boldsymbol{\delta}} t(\boldsymbol{\delta}) \cos(\boldsymbol{k}\cdot\boldsymbol{\delta}) - 2\lambda_R \sum_j e^{-i\theta_j} \sin(\boldsymbol{k}\cdot\hat{\boldsymbol{a}}_j) \\ &\approx -2\sum_{\boldsymbol{\delta}} t(\boldsymbol{\delta}) \left(1 - \frac{(\boldsymbol{k}\cdot\boldsymbol{\delta})^2}{2}\right) - 2\lambda_R \sum_j e^{-i\theta_j} \boldsymbol{k}\cdot\hat{\boldsymbol{a}}_j,\end{aligned} \tag{3.37}$$

which clearly decreases with increasing $\boldsymbol{k}$ close to $\boldsymbol{k} = 0$. We thus conclude that the ground state vectors, named $\boldsymbol{k}^i$, are non-zero and pairwise negatives of each other.

With $a^{\dagger}_{\boldsymbol{k}^i\_} a_{\boldsymbol{k}^i\_} \equiv N_i$ being the number of particles in ground state i, we rewrite H_1 in the form

$$\begin{aligned} H_1 &= \sum_{\boldsymbol{k}} \left(\mathcal{E}^+_{\boldsymbol{k}} a^\dagger_{\boldsymbol{k}+} a_{\boldsymbol{k}+} + \mathcal{E}^-_{\boldsymbol{k}} a^\dagger_{\boldsymbol{k}-} a_{\boldsymbol{k}-} \right) \\ &= \sum_i \mathcal{E}^-_{\boldsymbol{k}^i} N_i + \sum_{\boldsymbol{k}}{}' \left(\mathcal{E}^+_{\boldsymbol{k}} a^\dagger_{\boldsymbol{k}+} a_{\boldsymbol{k}+} + \mathcal{E}^-_{\boldsymbol{k}} a^\dagger_{\boldsymbol{k}-} a_{\boldsymbol{k}-} \right) \\ &= \mathcal{E}^0 N_0 + \sum_{\boldsymbol{k}}{}' \left(\mathcal{E}^+_{\boldsymbol{k}} a^\dagger_{\boldsymbol{k}+} a_{\boldsymbol{k}+} + \mathcal{E}^-_{\boldsymbol{k}} a^\dagger_{\boldsymbol{k}-} a_{\boldsymbol{k}-} \right), \end{aligned} \tag{3.38}$$

where $\mathcal{E}^0 \equiv \mathcal{E}^-_{\boldsymbol{k}^i}$ is the degenerate single-particle ground state energy, $N_0 \equiv \sum_i N_i$ is the total number of ground state particles, and $\sum'_{\boldsymbol{k}}$ indicates that the sum is taken over only non-ground-state $\boldsymbol{k}$-vectors. Using the fact that

$$N_0 = N - \sum_{\boldsymbol{k}}{}' \left(a^\dagger_{\boldsymbol{k}+} a_{\boldsymbol{k}+} + a^\dagger_{\boldsymbol{k}-} a_{\boldsymbol{k}-} \right), \tag{3.39}$$

where N is the total number of particles, we obtain

$$\begin{aligned} H_1 &= \mathcal{E}^0 N + \sum_{\boldsymbol{k}}{}' \left[(\mathcal{E}^+_{\boldsymbol{k}} - \mathcal{E}^0) a^\dagger_{\boldsymbol{k}+} a_{\boldsymbol{k}+} + (\mathcal{E}^-_{\boldsymbol{k}} - \mathcal{E}^0) a^\dagger_{\boldsymbol{k}-} a_{\boldsymbol{k}-} \right] \\ &\equiv \mathcal{E}^0 N + \sum_{\boldsymbol{k}}{}' \left[\Delta\mathcal{E}^+_{\boldsymbol{k}} a^\dagger_{\boldsymbol{k}+} a_{\boldsymbol{k}+} + \Delta\mathcal{E}^-_{\boldsymbol{k}} a^\dagger_{\boldsymbol{k}-} a_{\boldsymbol{k}-} \right], \end{aligned} \tag{3.40}$$

where we have defined the single-particle excitation energies $\Delta\mathcal{E}^\pm_{\boldsymbol{k}}$ for the two helicity bands.

Since $\mathcal{A}_{\boldsymbol{k}}$ is Hermitian by inspection, there exist a unitary transformation matrix $\mathcal{U}_{\boldsymbol{k}}$ composed of orthonormal eigenvectors of $\mathcal{A}_{\boldsymbol{k}}$ such that $\mathcal{A}_{\boldsymbol{k}} = \mathcal{U}_{\boldsymbol{k}} \mathcal{D}_{\boldsymbol{k}} \mathcal{U}^\dagger_{\boldsymbol{k}}$. We want

$$\begin{aligned} \xi^\dagger_{\boldsymbol{k}} \mathcal{A}_{\boldsymbol{k}} \xi_{\boldsymbol{k}} &= \xi^\dagger_{\boldsymbol{k}} \mathcal{U}_{\boldsymbol{k}} \mathcal{D}_{\boldsymbol{k}} \mathcal{U}^\dagger_{\boldsymbol{k}} \xi_{\boldsymbol{k}} \\ &= \Psi^\dagger_{\boldsymbol{k}} \mathcal{D}_{\boldsymbol{k}} \Psi_{\boldsymbol{k}}, \end{aligned} \tag{3.41}$$

meaning that $\Psi_{\boldsymbol{k}} = \mathcal{U}^\dagger_{\boldsymbol{k}} \xi_{\boldsymbol{k}}$.

$\mathcal{A}_{\boldsymbol{k}}$ has the orthonormal eigenvectors

$$\chi^\pm = \frac{1}{\sqrt{2}} \begin{pmatrix} \pm s_{\boldsymbol{k}}/|s_{\boldsymbol{k}}| \\ 1 \end{pmatrix}. \tag{3.42}$$

The quantity $s_{\boldsymbol{k}}/|s_{\boldsymbol{k}}|$ is a complex number with modulus 1, and thus we write

$$e^{i\gamma_{\boldsymbol{k}}} \equiv s_{\boldsymbol{k}}/|s_{\boldsymbol{k}}|, \tag{3.43}$$

for some real phase factor $\gamma_{\boldsymbol{k}}$, and we obtain

$$\begin{aligned}
\xi_{\boldsymbol{k}} &= \begin{pmatrix} b_{\boldsymbol{k}\uparrow} \\ b_{\boldsymbol{k}\downarrow} \end{pmatrix} \\
&= \mathcal{U}_{\boldsymbol{k}} \Psi_{\boldsymbol{k}} \\
&= \frac{1}{\sqrt{2}} \begin{pmatrix} e^{i\gamma_{\boldsymbol{k}}} & -e^{i\gamma_{\boldsymbol{k}}} \\ 1 & 1 \end{pmatrix} \begin{pmatrix} a_{\boldsymbol{k}+} \\ a_{\boldsymbol{k}-} \end{pmatrix} \\
&= \frac{1}{\sqrt{2}} \begin{pmatrix} e^{i\gamma_{\boldsymbol{k}}} a_{\boldsymbol{k}+} - e^{i\gamma_{\boldsymbol{k}}} a_{\boldsymbol{k}-} \\ a_{\boldsymbol{k}+} + a_{\boldsymbol{k}-} \end{pmatrix},
\end{aligned} \tag{3.44}$$

meaning that the transformation from the spin basis to the helicity band basis is given by

$$\begin{aligned}
b_{\boldsymbol{k}\uparrow} &= \frac{e^{i\gamma_{\boldsymbol{k}}}}{\sqrt{2}} \left(a_{\boldsymbol{k}+} - a_{\boldsymbol{k}-} \right), \\
b_{\boldsymbol{k}\downarrow} &= \frac{1}{\sqrt{2}} (a_{\boldsymbol{k}+} + a_{\boldsymbol{k}-}), \\
b^\dagger_{\boldsymbol{k}\uparrow} &= \frac{e^{-i\gamma_{\boldsymbol{k}}}}{\sqrt{2}} \left(a^\dagger_{\boldsymbol{k}+} - a^\dagger_{\boldsymbol{k}-} \right), \\
b^\dagger_{\boldsymbol{k}\downarrow} &= \frac{1}{\sqrt{2}} (a^\dagger_{\boldsymbol{k}+} + a^\dagger_{\boldsymbol{k}-}).
\end{aligned} \tag{3.45}$$

It is shown in Appendix A by the inverse transformation that the helicity band operators obey the boson commutation relations, i.e.

$$[a_{\boldsymbol{k}\alpha}, a_{\boldsymbol{k}'\beta}] = 0, \quad \left[a^\dagger_{\boldsymbol{k}\alpha}, a^\dagger_{\boldsymbol{k}'\beta} \right] = 0, \quad \left[a_{\boldsymbol{k}\alpha}, a^\dagger_{\boldsymbol{k}'\beta} \right] = \delta_{\boldsymbol{k},\boldsymbol{k}'} \delta_{\alpha,\beta}, \tag{3.46}$$

where $\alpha, \beta = +, -$.

We now consider some properties of $e^{i\gamma_{\boldsymbol{k}}}$ and $\gamma_{\boldsymbol{k}}$. We note that $e^{i\gamma_{\boldsymbol{k}}}$ is antisymmetric in $\boldsymbol{k}$:

$$\begin{aligned}
e^{i\gamma_{-\boldsymbol{k}}} &= \frac{s_{-\boldsymbol{k}}}{|s_{-\boldsymbol{k}}|} = i \frac{\sum_j a_j e^{-i\theta_j} \sin(-\boldsymbol{k} \cdot \hat{\boldsymbol{a}}_j)}{|\sum_j a_j e^{-i\theta_j} \sin(-\boldsymbol{k} \cdot \hat{\boldsymbol{a}}_j)|} \\
&= -i \frac{\sum_j a_j e^{-i\theta_j} \sin(\boldsymbol{k} \cdot \hat{\boldsymbol{a}}_j)}{|\sum_j a_j e^{-i\theta_j} \sin(\boldsymbol{k} \cdot \hat{\boldsymbol{a}}_j)|} = -\frac{s_{\boldsymbol{k}}}{|s_{\boldsymbol{k}}|} = -e^{i\gamma_{\boldsymbol{k}}}.
\end{aligned} \tag{3.47}$$

This implies that

$$e^{i\gamma_{-\boldsymbol{k}}} = e^{i(\gamma_{\boldsymbol{k}}+\pi)}, \tag{3.48}$$

in other words that

$$\gamma_{-\boldsymbol{k}} = \gamma_{\boldsymbol{k}} + \pi. \tag{3.49}$$

We observe that $\gamma_{\boldsymbol{k}}$ can be viewed as the angle of $\boldsymbol{k}$ relative to some axis in $\boldsymbol{k}$-space.

4. Analytical results

The Fourier transformed Bose-Hubbard model is applied for a system of a weakly interacting spin-orbit coupled Bose-Einstein condensate. In order to allow for a high degree of generality, the system is in Section 4.1 considered on a general inversion-symmetric Bravais lattice. Inversion symmetry is required for the form of second quantized Rashba SOC Hamiltonian found in equation (3.27). However, the complicated form of the resulting Hamiltonian matrix occluded the formulation of comprehensible eigenvalues, and thereby of the excitation spectrum.

The excitation spectrum is, however, found in the following Section 4.2: The limiting case only allowing for nearest-neighbor hopping and on-site interactions. The cases of the one-dimensional chain and two-dimensional square lattice are investigated in particular.

4.1 Inversion symmetric Bravais lattice

The general case of bosons of two synthetic spin states residing on a Bravais lattice are considered firstly. The discussion is valid for both one- and two-dimensional lattices. The bosons are bound to the lattice points sufficiently strongly, so that localized Wannier functions can be used to describe their wave functions. This is the tight binding model, leading to the Bose-Hubbard model.

4.1.1 Transformation of the two-particle interaction from spin basis to helicity basis*

It was shown in section 3.1.1 that the Fourier transformed two-particle interaction can be written:

$$\begin{aligned} H_2 &= \frac{1}{N_s}\sum_{\{\boldsymbol{k}^i\}}\left[\frac{1}{2}\sum_{\alpha}\tilde{U}_{\alpha}b^{\dagger}_{\boldsymbol{k}_1\alpha}b^{\dagger}_{\boldsymbol{k}_2\alpha}b_{\boldsymbol{k}_3\alpha}b_{\boldsymbol{k}_4\alpha}+\tilde{U}_{\uparrow\downarrow}b^{\dagger}_{\boldsymbol{k}_1\uparrow}b_{\boldsymbol{k}_2\uparrow}b^{\dagger}_{\boldsymbol{k}_3\downarrow}b_{\boldsymbol{k}_4\downarrow}\right] \\ &\equiv \frac{1}{N_s}\sum_{\{\boldsymbol{k}^i\}}\left[\frac{1}{2}H_{intra}+H_{inter}\right] \end{aligned} \tag{4.1}$$

$$\alpha = \uparrow,\downarrow \tag{4.2}$$

where

$$\begin{aligned} \tilde{U}_{\alpha}(\boldsymbol{k}_2,\boldsymbol{k}_3,\boldsymbol{k}_4) =& U_{\alpha}(0,0,0)+\sum_{\{\boldsymbol{\delta}_i\}}U_{\alpha}(\boldsymbol{\delta}_1,\boldsymbol{\delta}_2,\boldsymbol{\delta}_3)e^{i(\boldsymbol{k}_2\cdot\boldsymbol{\delta}_1-\boldsymbol{k}_3\cdot\boldsymbol{\delta}_2-\boldsymbol{k}_4\cdot\boldsymbol{\delta}_3)}, \\ \tilde{U}_{\uparrow\downarrow}(\boldsymbol{k}_1,\boldsymbol{k}_2,\boldsymbol{k}_3,\boldsymbol{k}_4) =& U_{\uparrow\downarrow}(0,0,0)+\frac{1}{2}\sum_{\{\boldsymbol{\delta}_i\}}U_{\uparrow\downarrow}(\boldsymbol{\delta}_1,\boldsymbol{\delta}_2,\boldsymbol{\delta}_3) \\ & \cdot\left(e^{i(\boldsymbol{k}_1\cdot\boldsymbol{\delta}_1-\boldsymbol{k}_2\cdot\boldsymbol{\delta}_2-\boldsymbol{k}_4\cdot\boldsymbol{\delta}_3)}+e^{i(\boldsymbol{k}_3\cdot\boldsymbol{\delta}_1-\boldsymbol{k}_4\cdot\boldsymbol{\delta}_2-\boldsymbol{k}_2\cdot\boldsymbol{\delta}_3)}\right). \end{aligned} \tag{4.3}$$

The sum over $\{\boldsymbol{\delta}_i\} = (\boldsymbol{\delta}_1,\boldsymbol{\delta}_2,\boldsymbol{\delta}_3)$ is over all possible combinations of lattice vectors except for pure on-site scattering $\{\boldsymbol{\delta}_i\} = \{\boldsymbol{0}\}$. The tilde on the potentials U signal a Fourier transformed potential.

The fundamental idea in this treatment is to transform the spin-basis boson operators into the helicity-basis boson operators found in 3.2.3. Inserting (3.45) into the intra-spin part H_{intra} of (4.1) gives

$$
\begin{aligned}
H_{intra} =& \sum_{\alpha} \tilde{U}_{\alpha} b^{\dagger}_{\boldsymbol{k}_1\alpha} b^{\dagger}_{\boldsymbol{k}_2\alpha} b_{\boldsymbol{k}_3\alpha} b_{\boldsymbol{k}_4\alpha} \delta_{\boldsymbol{k}_1+\boldsymbol{k}_2,\boldsymbol{k}_3+\boldsymbol{k}_4} \\
=& \left(\frac{1}{\sqrt{2}}\right)^4 \tilde{U}_{\uparrow} e^{i(\gamma_{\boldsymbol{k}_3}+\gamma_{\boldsymbol{k}_4}-\gamma_{\boldsymbol{k}_1}-\gamma_{\boldsymbol{k}_2})} (a^{\dagger}_{\boldsymbol{k}_1+} - a^{\dagger}_{\boldsymbol{k}_1-})(a^{\dagger}_{\boldsymbol{k}_2+} - a^{\dagger}_{\boldsymbol{k}_2-}) \\
& \cdot (a_{\boldsymbol{k}_3+} - a_{\boldsymbol{k}_3-})(a_{\boldsymbol{k}_4+} - a_{\boldsymbol{k}_4-}) \delta_{\boldsymbol{k}_1+\boldsymbol{k}_2,\boldsymbol{k}_3+\boldsymbol{k}_4} \\
& + \left(\frac{1}{\sqrt{2}}\right)^4 \tilde{U}_{\downarrow} (a^{\dagger}_{\boldsymbol{k}_1+} + a^{\dagger}_{\boldsymbol{k}_1-})(a^{\dagger}_{\boldsymbol{k}_2+} + a^{\dagger}_{\boldsymbol{k}_2-})(a_{\boldsymbol{k}_3+} + a_{\boldsymbol{k}_3-})(a_{\boldsymbol{k}_4+} + a_{\boldsymbol{k}_4-}) \delta_{\boldsymbol{k}_1+\boldsymbol{k}_2,\boldsymbol{k}_3+\boldsymbol{k}_4} \\
=& \frac{1}{4} \delta_{\boldsymbol{k}_1+\boldsymbol{k}_2,\boldsymbol{k}_3+\boldsymbol{k}_4} \begin{pmatrix} a^{\dagger}_{\boldsymbol{k}_1+} a^{\dagger}_{\boldsymbol{k}_2+} \\ a^{\dagger}_{\boldsymbol{k}_1+} a^{\dagger}_{\boldsymbol{k}_2-} \\ a^{\dagger}_{\boldsymbol{k}_1-} a^{\dagger}_{\boldsymbol{k}_2+} \\ a^{\dagger}_{\boldsymbol{k}_1-} a^{\dagger}_{\boldsymbol{k}_2-} \end{pmatrix}^T \begin{pmatrix} \tilde{U}^+ & \tilde{U}^- & \tilde{U}^- & \tilde{U}^+ \\ \tilde{U}^- & \tilde{U}^+ & \tilde{U}^+ & \tilde{U}^- \\ \tilde{U}^- & \tilde{U}^+ & \tilde{U}^+ & \tilde{U}^- \\ \tilde{U}^+ & \tilde{U}^- & \tilde{U}^- & \tilde{U}^+ \end{pmatrix} \begin{pmatrix} a_{\boldsymbol{k}_3+} a_{\boldsymbol{k}_4+} \\ a_{\boldsymbol{k}_3+} a_{\boldsymbol{k}_4-} \\ a_{\boldsymbol{k}_3-} a_{\boldsymbol{k}_4+} \\ a_{\boldsymbol{k}_3-} a_{\boldsymbol{k}_4-} \end{pmatrix},
\end{aligned} \tag{4.4}
$$

where

$$
\tilde{U}^{\pm}(\boldsymbol{k}_1, \boldsymbol{k}_2, \boldsymbol{k}_3, \boldsymbol{k}_4) = \tilde{U}_{\downarrow}(\boldsymbol{k}_2, \boldsymbol{k}_3, \boldsymbol{k}_4) \pm \tilde{U}_{\uparrow}(\boldsymbol{k}_2, \boldsymbol{k}_3, \boldsymbol{k}_4) e^{i(\gamma_{\boldsymbol{k}_3}+\gamma_{\boldsymbol{k}_4}-\gamma_{\boldsymbol{k}_1}-\gamma_{\boldsymbol{k}_2})}. \tag{4.5}
$$

Inserting (3.45) into the inter-spin part H_{inter} of (4.1) gives

$$
\begin{aligned}
H_{inter} =& \tilde{U}_{\uparrow\downarrow} b^{\dagger}_{\boldsymbol{k}_1\uparrow} b_{\boldsymbol{k}_2\uparrow} b^{\dagger}_{\boldsymbol{k}_3\downarrow} b_{\boldsymbol{k}_4\downarrow} \delta_{\boldsymbol{k}_1+\boldsymbol{k}_3,\boldsymbol{k}_2+\boldsymbol{k}_4} \\
=& \left(\frac{1}{\sqrt{2}}\right)^4 \tilde{U}_{\uparrow\downarrow} e^{i(\gamma_{\boldsymbol{k}_2}-\gamma_{\boldsymbol{k}_1})} (a^{\dagger}_{\boldsymbol{k}_1+} - a^{\dagger}_{\boldsymbol{k}_1-})(a_{\boldsymbol{k}_2+} - a_{\boldsymbol{k}_2-}) \\
& \cdot (a^{\dagger}_{\boldsymbol{k}_3+} + a^{\dagger}_{\boldsymbol{k}_3-})(a_{\boldsymbol{k}_4+} + a_{\boldsymbol{k}_4-}) \delta_{\boldsymbol{k}_1+\boldsymbol{k}_3,\boldsymbol{k}_2+\boldsymbol{k}_4} \\
=& \frac{1}{4} \tilde{U}_{\uparrow\downarrow} e^{i(\gamma_{\boldsymbol{k}_2}-\gamma_{\boldsymbol{k}_1})} \delta_{\boldsymbol{k}_1+\boldsymbol{k}_3,\boldsymbol{k}_2+\boldsymbol{k}_4} \\
& \cdot \begin{pmatrix} a^{\dagger}_{\boldsymbol{k}_1+} a_{\boldsymbol{k}_2+} \\ a^{\dagger}_{\boldsymbol{k}_1+} a_{\boldsymbol{k}_2-} \\ a^{\dagger}_{\boldsymbol{k}_1-} a_{\boldsymbol{k}_2+} \\ a^{\dagger}_{\boldsymbol{k}_1-} a_{\boldsymbol{k}_2-} \end{pmatrix}^T \begin{pmatrix} 1 & 1 & 1 & 1 \\ -1 & -1 & -1 & -1 \\ -1 & -1 & -1 & -1 \\ 1 & 1 & 1 & 1 \end{pmatrix} \begin{pmatrix} a^{\dagger}_{\boldsymbol{k}_3+} a_{\boldsymbol{k}_4+} \\ a^{\dagger}_{\boldsymbol{k}_3+} a_{\boldsymbol{k}_4-} \\ a^{\dagger}_{\boldsymbol{k}_3-} a_{\boldsymbol{k}_4+} \\ a^{\dagger}_{\boldsymbol{k}_3-} a_{\boldsymbol{k}_4-} \end{pmatrix}
\end{aligned} \tag{4.6}
$$

Matrix notation has been used in (4.4) and (4.6) in order to simplify notation. Performing the matrix multiplication shows that H_2 now consists of

32 terms that are biquadratic in helicity band operators, with every combination of operators being represented twice, once from (4.4) and once from (4.6).

4.1.2 Mean field approximation

The single-particle spin-orbit coupled energy spectrum was found to contain an even number of ground state $\boldsymbol{k}$ vectors, as shown in 3.2.3. Transitioning to a many-particle system of interacting bosons could alter these energy minima. In the weak-coupling limit, however, the ground state $\boldsymbol{k}$ vectors are considered to be unchanged. Hence, in the BEC there is condensation to the degenerate ground state $\boldsymbol{k}$ vectors. The number of bosons in ground state $\boldsymbol{k}_0^i$ is denoted N_0^i. In order to simplify notation, we introduce

$$\boldsymbol{k}_0^i \equiv \boldsymbol{k}^i, \quad a_{\boldsymbol{k}_0^i -} \equiv a_i, \quad N_0^i \equiv N_i, \tag{4.7}$$

where i takes an even number of integers.

The condensed phase is characterized by having most particles in the ground state, so that it is safe to assume that

$$a_i^\dagger a_i = N_i >> 1, \tag{4.8}$$

which means that we can write $a_i^\dagger = a_i = \sqrt{N_i}$. From 3.2.3 it is known that the $\boldsymbol{k}^i$'s are pairwise negatives of each other, so that the occupation number of $-\boldsymbol{k}^i$, which we write N_{-i}, also satisfy (4.8). Since the $(\boldsymbol{k}^i, -)$ states dominate in the Bose-Einstein condensate, we only consider terms in H_2 where at least one of the interacting particles has $\boldsymbol{k} = \boldsymbol{k}^i$ and $\alpha = -$. This mean field approach reduces H_2 to a sum over terms which are at most quadratic in boson operators. Ground state bosons interacting with non-ground state bosons from both helicity bands are considered.

We can now find the contributions from (4.4) and (4.6), taking into account the delta functions and the mean field approach. In (4.4) we get the following contributions from the sum over the four independent $\boldsymbol{k}$'s:

$$\begin{aligned}
\boldsymbol{k}_1 = \boldsymbol{k}_2 = \boldsymbol{k}_3 = \boldsymbol{k}_4 = \boldsymbol{k}^i &\to \sum_i N_i^2 \tilde{U}^+(\boldsymbol{k}^i, \boldsymbol{k}^i, \boldsymbol{k}^i, \boldsymbol{k}^i) \\
\boldsymbol{k}_1 = \boldsymbol{k}_3 = \boldsymbol{k}^i \neq \boldsymbol{k}_2 = \boldsymbol{k}_4 = \boldsymbol{k}^j &\to \sum_{i \neq j} N_i N_j \tilde{U}^+(\boldsymbol{k}^i, \boldsymbol{k}^j, \boldsymbol{k}^i, \boldsymbol{k}^j) \\
\boldsymbol{k}_1 = \boldsymbol{k}_4 = \boldsymbol{k}^i \neq \boldsymbol{k}_2 = \boldsymbol{k}_3 = \boldsymbol{k}^j &\to \sum_{i \neq j} N_i N_j \tilde{U}^+(\boldsymbol{k}^i, \boldsymbol{k}^j, \boldsymbol{k}^j, \boldsymbol{k}^i)
\end{aligned} \tag{4.9}$$

$$
\begin{aligned}
&\boldsymbol{k}_1 = -\boldsymbol{k}_2 = \boldsymbol{k}^i \neq \boldsymbol{k}_3 = -\boldsymbol{k}_4 = \boldsymbol{k} \to \sum_i {\sum_{\boldsymbol{k}}}' \sqrt{N_i N_{-i}} \\
&\cdot \Big[\tilde{U}^+(\boldsymbol{k}^i, -\boldsymbol{k}^i, \boldsymbol{k}, -\boldsymbol{k})(a_{\boldsymbol{k}+}a_{-\boldsymbol{k}+} + a_{\boldsymbol{k}-}a_{-\boldsymbol{k}-}) + \tilde{U}^-(\boldsymbol{k}^i, -\boldsymbol{k}^i, \boldsymbol{k}, -\boldsymbol{k})(a_{\boldsymbol{k}+}a_{-\boldsymbol{k}-} + a_{\boldsymbol{k}-}a_{-\boldsymbol{k}+})\Big] \\
&\boldsymbol{k}_3 = -\boldsymbol{k}_4 = \boldsymbol{k}^i \neq \boldsymbol{k}_1 = -\boldsymbol{k}_2 = \boldsymbol{k} \to \sum_i {\sum_{\boldsymbol{k}}}' \sqrt{N_i N_{-i}} \\
&\cdot \Big[\tilde{U}^+(\boldsymbol{k}, -\boldsymbol{k}, \boldsymbol{k}^i, -\boldsymbol{k}^i)(a^\dagger_{\boldsymbol{k}+}a^\dagger_{-\boldsymbol{k}+} + a^\dagger_{\boldsymbol{k}-}a^\dagger_{-\boldsymbol{k}-}) + \tilde{U}^-(\boldsymbol{k}, -\boldsymbol{k}, \boldsymbol{k}^i, -\boldsymbol{k}^i)(a^\dagger_{\boldsymbol{k}+}a^\dagger_{-\boldsymbol{k}-} + a^\dagger_{\boldsymbol{k}-}a^\dagger_{-\boldsymbol{k}+})\Big] \\
&\boldsymbol{k}_1 = \boldsymbol{k}_3 = \boldsymbol{k}^i \neq \boldsymbol{k}_2 = \boldsymbol{k}_4 = \boldsymbol{k} \to \sum_i {\sum_{\boldsymbol{k}}}' N_i \\
&\cdot \Big[\tilde{U}^+(\boldsymbol{k}^i, \boldsymbol{k}, \boldsymbol{k}^i, \boldsymbol{k})(a^\dagger_{\boldsymbol{k}+}a_{\boldsymbol{k}+} + a^\dagger_{\boldsymbol{k}-}a_{\boldsymbol{k}-}) + \tilde{U}^-(\boldsymbol{k}^i, \boldsymbol{k}, \boldsymbol{k}^i, \boldsymbol{k})(a^\dagger_{\boldsymbol{k}+}a_{\boldsymbol{k}-} + a^\dagger_{\boldsymbol{k}-}a_{\boldsymbol{k}+})\Big] \\
&\boldsymbol{k}_1 = \boldsymbol{k}_4 = \boldsymbol{k}^i \neq \boldsymbol{k}_2 = \boldsymbol{k}_3 = \boldsymbol{k} \to \sum_i {\sum_{\boldsymbol{k}}}' N_i \\
&\cdot \Big[\tilde{U}^+(\boldsymbol{k}^i, \boldsymbol{k}, \boldsymbol{k}, \boldsymbol{k}^i)(a^\dagger_{\boldsymbol{k}+}a_{\boldsymbol{k}+} + a^\dagger_{\boldsymbol{k}-}a_{\boldsymbol{k}-}) + \tilde{U}^-(\boldsymbol{k}^i, \boldsymbol{k}, \boldsymbol{k}, \boldsymbol{k}^i)(a^\dagger_{\boldsymbol{k}+}a_{\boldsymbol{k}-} + a^\dagger_{\boldsymbol{k}-}a_{\boldsymbol{k}+})\Big] \\
&\boldsymbol{k}_2 = \boldsymbol{k}_3 = \boldsymbol{k}^i \neq \boldsymbol{k}_1 = \boldsymbol{k}_4 = \boldsymbol{k} \to \sum_i {\sum_{\boldsymbol{k}}}' N_i \\
&\cdot \Big[\tilde{U}^+(\boldsymbol{k}, \boldsymbol{k}^i, \boldsymbol{k}^i, \boldsymbol{k})(a^\dagger_{\boldsymbol{k}+}a_{\boldsymbol{k}+} + a^\dagger_{\boldsymbol{k}-}a_{\boldsymbol{k}-}) + \tilde{U}^-(\boldsymbol{k}, \boldsymbol{k}^i, \boldsymbol{k}^i, \boldsymbol{k})(a^\dagger_{\boldsymbol{k}+}a_{\boldsymbol{k}-} + a^\dagger_{\boldsymbol{k}-}a_{\boldsymbol{k}+})\Big] \\
&\boldsymbol{k}_2 = \boldsymbol{k}_4 = \boldsymbol{k}^i \neq \boldsymbol{k}_1 = \boldsymbol{k}_3 = \boldsymbol{k} \to \sum_i {\sum_{\boldsymbol{k}}}' N_i \\
&\cdot \Big[\tilde{U}^+(\boldsymbol{k}, \boldsymbol{k}^i, \boldsymbol{k}, \boldsymbol{k}^i)(a^\dagger_{\boldsymbol{k}+}a_{\boldsymbol{k}+} + a^\dagger_{\boldsymbol{k}-}a_{\boldsymbol{k}-}) + \tilde{U}^-(\boldsymbol{k}, \boldsymbol{k}^i, \boldsymbol{k}, \boldsymbol{k}^i)(a^\dagger_{\boldsymbol{k}+}a_{\boldsymbol{k}-} + a^\dagger_{\boldsymbol{k}-}a_{\boldsymbol{k}+})\Big]
\end{aligned}
\tag{4.10}
$$

where $\boldsymbol{k}$ can be any vector except the ground state vectors $\boldsymbol{k}^i$ and $\sum_{\boldsymbol{k}}'$ is the sum over such non-ground-state vectors. The last eight cases also contribute with terms where $\boldsymbol{k} \to -\boldsymbol{k}$.

The cases involving negative momenta are inelastic terms. Individually they do not conserve kinetic energy, which lead to them being wrongly omitted in Ref. [15]. This greatly simplified the situation, but made the result erroneous since the excitation energies did not reduce to known results, such as Ref. [26] for the no-SOC case, in the non-interacting limit. Conservation of kinetic energy should not be demanded in every term of the mean field approach, but would rather put constraints on the excitations of the system as a whole.

$\tilde{U}^\pm$ can be simplified by our choice of $\boldsymbol{k}$-vectors. In (4.9) and in the the four last cases of (4.10) we see that the exponential in (4.5) can be simplified

to

$$e^{i(\gamma_{\boldsymbol{k}_3}+\gamma_{\boldsymbol{k}_4}-\gamma_{\boldsymbol{k}_1}-\gamma_{\boldsymbol{k}_2})}=1, \tag{4.11}$$

while

$$\begin{aligned} e^{i(\gamma_{\boldsymbol{k}_3}+\gamma_{\boldsymbol{k}_4}-\gamma_{\boldsymbol{k}_1}-\gamma_{\boldsymbol{k}_2})} &= e^{2i(\gamma_{\boldsymbol{k}}-\gamma_{\boldsymbol{k}^i})}, \\ e^{i(\gamma_{\boldsymbol{k}_3}+\gamma_{\boldsymbol{k}_4}-\gamma_{\boldsymbol{k}_1}-\gamma_{\boldsymbol{k}_2})} &= e^{-2i(\gamma_{\boldsymbol{k}}-\gamma_{\boldsymbol{k}^i})}, \end{aligned} \tag{4.12}$$

in the first two cases of (4.10), respectively. In the following we will use (4.11) and (4.12) inserted into (4.5) and thereby exchange $\tilde{U}^{\pm}$ with the Fourier transformed parameters $\tilde{U}_{\downarrow}$ and $\tilde{U}_{\uparrow}$.

Similarly, we get the following contributions from (4.6):

$$\begin{aligned} \boldsymbol{k}_1=\boldsymbol{k}_2=\boldsymbol{k}_3=\boldsymbol{k}_4=\boldsymbol{k}^i &\to \sum_i N_i^2 \tilde{U}_{\uparrow\downarrow}(\boldsymbol{k}^i,\boldsymbol{k}^i,\boldsymbol{k}^i,\boldsymbol{k}^i) \\ \boldsymbol{k}_1=\boldsymbol{k}_2=\boldsymbol{k}^i\neq\boldsymbol{k}_3=\boldsymbol{k}_4=\boldsymbol{k}^j &\to \sum_{i\neq j} N_i N_j \tilde{U}_{\uparrow\downarrow}(\boldsymbol{k}^i,\boldsymbol{k}^i,\boldsymbol{k}^j,\boldsymbol{k}^j) \\ \boldsymbol{k}_1=\boldsymbol{k}_4=\boldsymbol{k}^i\neq\boldsymbol{k}_2=\boldsymbol{k}_3=\boldsymbol{k}^j &\to \sum_{i\neq j} N_i N_j \tilde{U}_{\uparrow\downarrow}(\boldsymbol{k}^i,\boldsymbol{k}^j,\boldsymbol{k}^j,\boldsymbol{k}^i) e^{i(\gamma_{\boldsymbol{k}^j}-\gamma_{\boldsymbol{k}^i})} \end{aligned}$$

$$
\begin{aligned}
&\boldsymbol{k}_1 = -\boldsymbol{k}_3 = \boldsymbol{k}^i \neq \boldsymbol{k}_2 = -\boldsymbol{k}_4 = \boldsymbol{k} \rightarrow \sum_i {\sum_{\boldsymbol{k}}}' \sqrt{N_i N_{-i}} \\
&\cdot \tilde{U}_{\uparrow\downarrow}(\boldsymbol{k}^i, \boldsymbol{k}, -\boldsymbol{k}^i, -\boldsymbol{k}) e^{i(\gamma_{\boldsymbol{k}} - \gamma_{\boldsymbol{k}^i})} (a_{\boldsymbol{k}-} a_{-\boldsymbol{k}+} + a_{\boldsymbol{k}-} a_{-\boldsymbol{k}-} - a_{\boldsymbol{k}+} a_{-\boldsymbol{k}+} - a_{\boldsymbol{k}+} a_{-\boldsymbol{k}-}) \\
&\boldsymbol{k}_2 = -\boldsymbol{k}_4 = \boldsymbol{k}^i \neq \boldsymbol{k}_1 = -\boldsymbol{k}_3 = \boldsymbol{k} \rightarrow \sum_i {\sum_{\boldsymbol{k}}}' \sqrt{N_i N_{-i}} \\
&\cdot \tilde{U}_{\uparrow\downarrow}(\boldsymbol{k}, \boldsymbol{k}^i, -\boldsymbol{k}, -\boldsymbol{k}^i) e^{-i(\gamma_{\boldsymbol{k}} - \gamma_{\boldsymbol{k}^i})} (a^\dagger_{\boldsymbol{k}-} a^\dagger_{-\boldsymbol{k}+} + a^\dagger_{\boldsymbol{k}-} a^\dagger_{-\boldsymbol{k}-} - a^\dagger_{\boldsymbol{k}+} a^\dagger_{-\boldsymbol{k}+} - a^\dagger_{\boldsymbol{k}+} a^\dagger_{-\boldsymbol{k}-}) \\
&\boldsymbol{k}_1 = \boldsymbol{k}_2 = \boldsymbol{k}^i \neq \boldsymbol{k}_3 = \boldsymbol{k}_4 = \boldsymbol{k} \rightarrow \sum_i {\sum_{\boldsymbol{k}}}' N_i \\
&\cdot \tilde{U}_{\uparrow\downarrow}(\boldsymbol{k}^i, \boldsymbol{k}^i, \boldsymbol{k}, \boldsymbol{k}) (a^\dagger_{\boldsymbol{k}+} a_{\boldsymbol{k}+} + a^\dagger_{\boldsymbol{k}-} a_{\boldsymbol{k}-} + a^\dagger_{\boldsymbol{k}+} a_{\boldsymbol{k}-} + a^\dagger_{\boldsymbol{k}-} a_{\boldsymbol{k}+}) \\
&\boldsymbol{k}_1 = \boldsymbol{k}_4 = \boldsymbol{k}^i \neq \boldsymbol{k}_2 = \boldsymbol{k}_3 = \boldsymbol{k} \rightarrow \sum_i {\sum_{\boldsymbol{k}}}' N_i \\
&\cdot \tilde{U}_{\uparrow\downarrow}(\boldsymbol{k}^i, \boldsymbol{k}, \boldsymbol{k}, \boldsymbol{k}^i) e^{i(\gamma_{\boldsymbol{k}} - \gamma_{\boldsymbol{k}^i})} (a_{\boldsymbol{k}-} a^\dagger_{\boldsymbol{k}-} + a_{\boldsymbol{k}-} a^\dagger_{\boldsymbol{k}+} - a_{\boldsymbol{k}+} a^\dagger_{\boldsymbol{k}+} - a_{\boldsymbol{k}+} a^\dagger_{\boldsymbol{k}-}) \\
&\boldsymbol{k}_2 = \boldsymbol{k}_3 = \boldsymbol{k}^i \neq \boldsymbol{k}_1 = \boldsymbol{k}_4 = \boldsymbol{k} \rightarrow \sum_i {\sum_{\boldsymbol{k}}}' N_i \\
&\cdot \tilde{U}_{\uparrow\downarrow}(\boldsymbol{k}, \boldsymbol{k}^i, \boldsymbol{k}^i, \boldsymbol{k}) e^{-i(\gamma_{\boldsymbol{k}} - \gamma_{\boldsymbol{k}^i})} (a^\dagger_{\boldsymbol{k}-} a_{\boldsymbol{k}-} + a^\dagger_{\boldsymbol{k}-} a_{\boldsymbol{k}+} - a^\dagger_{\boldsymbol{k}+} a_{\boldsymbol{k}+} - a^\dagger_{\boldsymbol{k}+} a_{\boldsymbol{k}-}) \\
&\boldsymbol{k}_3 = \boldsymbol{k}_4 = \boldsymbol{k}^i \neq \boldsymbol{k}_1 = \boldsymbol{k}_2 = \boldsymbol{k} \rightarrow \sum_i {\sum_{\boldsymbol{k}}}' N_i \\
&\cdot \tilde{U}_{\uparrow\downarrow}(\boldsymbol{k}, \boldsymbol{k}, \boldsymbol{k}^i, \boldsymbol{k}^i) (a^\dagger_{\boldsymbol{k}+} a_{\boldsymbol{k}+} + a^\dagger_{\boldsymbol{k}-} a_{\boldsymbol{k}-} - a^\dagger_{\boldsymbol{k}+} a_{\boldsymbol{k}-} - a^\dagger_{\boldsymbol{k}-} a_{\boldsymbol{k}+})
\end{aligned}
\tag{4.13}
$$

The Hamiltonian can now be rewritten in matrix form in the basis

$$
\phi_{\boldsymbol{k}} = \left[a_{\boldsymbol{k}+}, a_{-\boldsymbol{k}+}, a_{\boldsymbol{k}-}, a_{-\boldsymbol{k}-}, a^\dagger_{\boldsymbol{k}+}, a^\dagger_{-\boldsymbol{k}+}, a^\dagger_{\boldsymbol{k}-}, a^\dagger_{-\boldsymbol{k}-} \right]^T . \tag{4.14}
$$

Using the expression (3.40) for H_1 together with the results (4.10) and (4.13), including the factor $\frac{1}{4}$ from (4.4) and (4.6), and $\frac{1}{2N_s}$ from (4.1), we arrive at

$$
H = H_0^{'} + \frac{1}{2} {\sum_{\boldsymbol{k}}}' \phi^\dagger_{\boldsymbol{k}} \widetilde{\mathcal{M}}^u_{\boldsymbol{k}} \phi_{\boldsymbol{k}}, \tag{4.15}
$$

having defined the matrix

$$\widetilde{\mathcal{M}}^{u}_{\boldsymbol{k}} = \begin{pmatrix} V_1^-(\boldsymbol{k}) & 0 & V_2^-(\boldsymbol{k}) & 0 & 0 & W_1^-(\boldsymbol{k}) & 0 & W_2^-(\boldsymbol{k}) \\ 0 & V_1^-(-\boldsymbol{k}) & 0 & V_2^-(-\boldsymbol{k}) & W_1^-(-\boldsymbol{k}) & 0 & W_2^-(-\boldsymbol{k}) & 0 \\ V_2^+(\boldsymbol{k}) & 0 & V_1^+(\boldsymbol{k}) & 0 & 0 & W_2^+(\boldsymbol{k}) & 0 & W_1^+(\boldsymbol{k}) \\ 0 & V_2^+(-\boldsymbol{k}) & 0 & V_1^+(-\boldsymbol{k}) & W_2^+(-\boldsymbol{k}) & 0 & W_1^+(-\boldsymbol{k}) & 0 \\ 0 & P_1^-(\boldsymbol{k}) & 0 & P_2^-(\boldsymbol{k}) & -T(\boldsymbol{k}) & 0 & -T(\boldsymbol{k}) & 0 \\ P_1^-(-\boldsymbol{k}) & 0 & P_2^-(-\boldsymbol{k}) & 0 & 0 & -T(-\boldsymbol{k}) & 0 & -T(-\boldsymbol{k}) \\ 0 & P_2^+(\boldsymbol{k}) & 0 & P_1^+(\boldsymbol{k}) & T(\boldsymbol{k}) & 0 & T(\boldsymbol{k}) & 0 \\ P_2^+(-\boldsymbol{k}) & 0 & P_1^+(-\boldsymbol{k}) & 0 & 0 & T(-\boldsymbol{k}) & 0 & T(-\boldsymbol{k}) \end{pmatrix}, \tag{4.16}$$

where

$$\begin{aligned}
V_1^{\pm}(\boldsymbol{k}) &= \Delta\mathcal{E}_{\boldsymbol{k}}^{\mp} + \sum_i \frac{n_i}{4}\Big[\tilde{U}_{\downarrow}(\boldsymbol{k},\boldsymbol{k}^i,\boldsymbol{k}) + \tilde{U}_{\uparrow}(\boldsymbol{k},\boldsymbol{k}^i,\boldsymbol{k}) + \tilde{U}_{\downarrow}(\boldsymbol{k},\boldsymbol{k},\boldsymbol{k}^i) + \tilde{U}_{\uparrow}(\boldsymbol{k},\boldsymbol{k},\boldsymbol{k}^i) \\
&\qquad + 2\tilde{U}_{\uparrow\downarrow}(\boldsymbol{k}^i,\boldsymbol{k}^i,\boldsymbol{k},\boldsymbol{k}) \pm \tilde{U}_{\uparrow\downarrow}(\boldsymbol{k}^i,\boldsymbol{k},\boldsymbol{k},\boldsymbol{k}^i)e^{-i(\gamma_{\boldsymbol{k}}-\gamma_{\boldsymbol{k}^i})}\Big] \\
V_2^{\pm}(\boldsymbol{k}) &= \sum_i \frac{n_i}{4}\Big[\tilde{U}_{\downarrow}(\boldsymbol{k},\boldsymbol{k}^i,\boldsymbol{k}) - \tilde{U}_{\uparrow}(\boldsymbol{k},\boldsymbol{k}^i,\boldsymbol{k}) + \tilde{U}_{\downarrow}(\boldsymbol{k},\boldsymbol{k},\boldsymbol{k}^i) - \tilde{U}_{\uparrow}(\boldsymbol{k},\boldsymbol{k},\boldsymbol{k}^i) \\
&\qquad \pm \tilde{U}_{\uparrow\downarrow}(\boldsymbol{k}^i,\boldsymbol{k},\boldsymbol{k},\boldsymbol{k}^i)e^{-i(\gamma_{\boldsymbol{k}}-\gamma_{\boldsymbol{k}^i})}\Big] \\
W_1^{\pm}(\boldsymbol{k}) &= \sum_i \frac{\sqrt{n_i n_{-i}}}{8}\Big[\tilde{U}_{\downarrow}(-\boldsymbol{k},\boldsymbol{k}^i,-\boldsymbol{k}^i) + \tilde{U}_{\uparrow}(-\boldsymbol{k},\boldsymbol{k}^i,-\boldsymbol{k}^i)e^{-2i(\gamma_{\boldsymbol{k}}-\gamma_{\boldsymbol{k}^i})} \\
&\qquad \pm 2\tilde{U}_{\uparrow\downarrow}(\boldsymbol{k},\boldsymbol{k}^i,-\boldsymbol{k},-\boldsymbol{k}^i)e^{-i(\gamma_{\boldsymbol{k}}-\gamma_{\boldsymbol{k}^i})}\Big] \\
W_2^{\pm}(\boldsymbol{k}) &= \sum_i \frac{\sqrt{n_i n_{-i}}}{8}\Big[\tilde{U}_{\downarrow}(-\boldsymbol{k},\boldsymbol{k}^i,-\boldsymbol{k}^i) - \tilde{U}_{\uparrow}(-\boldsymbol{k},\boldsymbol{k}^i,-\boldsymbol{k}^i)e^{-2i(\gamma_{\boldsymbol{k}}-\gamma_{\boldsymbol{k}^i})} \\
&\qquad \pm 2\tilde{U}_{\uparrow\downarrow}(\boldsymbol{k},\boldsymbol{k}^i,-\boldsymbol{k},-\boldsymbol{k}^i)e^{-i(\gamma_{\boldsymbol{k}}-\gamma_{\boldsymbol{k}^i})}\Big] \\
P_1^{\pm}(\boldsymbol{k}) &= \sum_i \frac{\sqrt{n_i n_{-i}}}{8}\Big[\tilde{U}_{\downarrow}(-\boldsymbol{k}^i,\boldsymbol{k},-\boldsymbol{k}) + \tilde{U}_{\uparrow}(-\boldsymbol{k}^i,\boldsymbol{k},-\boldsymbol{k})e^{2i(\gamma_{\boldsymbol{k}}-\gamma_{\boldsymbol{k}^i})} \\
&\qquad \pm 2\tilde{U}_{\uparrow\downarrow}(\boldsymbol{k}^i,\boldsymbol{k},-\boldsymbol{k}^i,-\boldsymbol{k})e^{i(\gamma_{\boldsymbol{k}}-\gamma_{\boldsymbol{k}^i})}\Big] \\
P_2^{\pm}(\boldsymbol{k}) &= \sum_i \frac{\sqrt{n_i n_{-i}}}{8}\Big[\tilde{U}_{\downarrow}(-\boldsymbol{k}^i,\boldsymbol{k},-\boldsymbol{k}) - \tilde{U}_{\uparrow}(-\boldsymbol{k}^i,\boldsymbol{k},-\boldsymbol{k})e^{2i(\gamma_{\boldsymbol{k}}-\gamma_{\boldsymbol{k}^i})} \\
&\qquad \pm 2\tilde{U}_{\uparrow\downarrow}(\boldsymbol{k}^i,\boldsymbol{k},-\boldsymbol{k}^i,-\boldsymbol{k})e^{i(\gamma_{\boldsymbol{k}}-\gamma_{\boldsymbol{k}^i})}\Big] \\
T(\boldsymbol{k}) &= \sum_i \frac{n_i}{4}\tilde{U}_{\uparrow\downarrow}(\boldsymbol{k}^i,\boldsymbol{k},\boldsymbol{k},\boldsymbol{k}^i)e^{i(\gamma_{\boldsymbol{k}}-\gamma_{\boldsymbol{k}^i})}.
\end{aligned} \tag{4.17}$$

The Fourier transformed potentials are restated ($\alpha = \downarrow, \uparrow$):

$$\begin{aligned}
\tilde{U}_\alpha(\boldsymbol{k}_2, \boldsymbol{k}_3, \boldsymbol{k}_4) =& U_\alpha(0,0,0) + \sum_{\{\boldsymbol{\delta}_i\}} U_\alpha(\boldsymbol{\delta}_1, \boldsymbol{\delta}_2, \boldsymbol{\delta}_3) e^{i(\boldsymbol{k}_2\cdot\boldsymbol{\delta}_1 - \boldsymbol{k}_3\cdot\boldsymbol{\delta}_2 - \boldsymbol{k}_4\cdot\boldsymbol{\delta}_3)}, \\
\tilde{U}_{\uparrow\downarrow}(\boldsymbol{k}_1, \boldsymbol{k}_2, \boldsymbol{k}_3, \boldsymbol{k}_4) =& U_{\uparrow\downarrow}(0,0,0) + \frac{1}{2}\sum_{\{\boldsymbol{\delta}_i\}} U_{\uparrow\downarrow}(\boldsymbol{\delta}_1, \boldsymbol{\delta}_2, \boldsymbol{\delta}_3) \\
& \cdot \left(e^{i(\boldsymbol{k}_1\cdot\boldsymbol{\delta}_1 - \boldsymbol{k}_2\cdot\boldsymbol{\delta}_2 - \boldsymbol{k}_4\cdot\boldsymbol{\delta}_3)} + e^{i(\boldsymbol{k}_3\cdot\boldsymbol{\delta}_1 - \boldsymbol{k}_4\cdot\boldsymbol{\delta}_2 - \boldsymbol{k}_2\cdot\boldsymbol{\delta}_3)} \right).
\end{aligned} \tag{4.18}$$

We have introduced the density of particles in ground state i, $n_i = N_i/N_s$. The factor $1/2$ in front of the sum over $\boldsymbol{k}$ in (4.15) is accounting for the fact that all terms are also included with negative argument, thereby appearing twice. Moreover, we have used that $\tilde{U}_{\uparrow\downarrow}(\boldsymbol{k}, \boldsymbol{k}^i, \boldsymbol{k}^i, \boldsymbol{k}) = \tilde{U}_{\uparrow\downarrow}(\boldsymbol{k}^i, \boldsymbol{k}, \boldsymbol{k}, \boldsymbol{k}^i)$ and $\tilde{U}_{\uparrow\downarrow}(\boldsymbol{k}, \boldsymbol{k}, \boldsymbol{k}^i, \boldsymbol{k}^i) = \tilde{U}_{\uparrow\downarrow}(\boldsymbol{k}^i, \boldsymbol{k}^i, \boldsymbol{k}, \boldsymbol{k})$, which are special cases of

$$\tilde{U}_{\uparrow\downarrow}(\boldsymbol{k}_1, \boldsymbol{k}_2, \boldsymbol{k}_3, \boldsymbol{k}_4) = \tilde{U}_{\uparrow\downarrow}(\boldsymbol{k}_3, \boldsymbol{k}_4, \boldsymbol{k}_1, \boldsymbol{k}_2), \tag{4.19}$$

which follows from the definition (4.18).

We have also used that

$$\tilde{U}^{\pm}(\boldsymbol{k}_1, \boldsymbol{k}_2, \boldsymbol{k}_3, \boldsymbol{k}_4) = \tilde{U}^{\pm}(\boldsymbol{k}_2, \boldsymbol{k}_1, \boldsymbol{k}_4, \boldsymbol{k}_3). \tag{4.20}$$

This follows from the fact that the interaction between two particles in the same spin state in real space should be the same regardless of which particle is moving from lattice site l to i, and from k to j, see Figure 4.1. In other words $U_\alpha(\boldsymbol{\delta}_1, \boldsymbol{\delta}_2, \boldsymbol{\delta}_3) = U_\alpha(-\boldsymbol{\delta}_1, \boldsymbol{\delta}_3 - \boldsymbol{\delta}_1, \boldsymbol{\delta}_2 - \boldsymbol{\delta}_1)$, leading to

$$\begin{aligned}
\tilde{U}_\alpha(\boldsymbol{k}_2, \boldsymbol{k}_3, \boldsymbol{k}_4) &= U_\alpha(0,0,0) + \sum_{\{\boldsymbol{\delta}_i\}} U_\alpha(\boldsymbol{\delta}_1, \boldsymbol{\delta}_2, \boldsymbol{\delta}_3) e^{i(\boldsymbol{k}_2\cdot\boldsymbol{\delta}_1 - \boldsymbol{k}_3\cdot\boldsymbol{\delta}_2 - \boldsymbol{k}_4\cdot\boldsymbol{\delta}_3)} \\
&= U_\alpha(0,0,0) + \sum_{\{\boldsymbol{\delta}_i\}} U_\alpha(\boldsymbol{\delta}_1, \boldsymbol{\delta}_2, \boldsymbol{\delta}_3) e^{i(\boldsymbol{k}_2\cdot(-\boldsymbol{\delta}_1) - \boldsymbol{k}_3\cdot(\boldsymbol{\delta}_3 - \boldsymbol{\delta}_1) - \boldsymbol{k}_4\cdot(\boldsymbol{\delta}_2 - \boldsymbol{\delta}_1))} \\
&= U_\alpha(0,0,0) + \sum_{\{\boldsymbol{\delta}_i\}} U_\alpha(\boldsymbol{\delta}_1, \boldsymbol{\delta}_2, \boldsymbol{\delta}_3) e^{i((\boldsymbol{k}_3 + \boldsymbol{k}_4 - \boldsymbol{k}_2)\cdot\boldsymbol{\delta}_1 - \boldsymbol{k}_4\cdot\boldsymbol{\delta}_2 - \boldsymbol{k}_3\cdot\boldsymbol{\delta}_3)} \\
&= \tilde{U}_\alpha(\boldsymbol{k}_1, \boldsymbol{k}_4, \boldsymbol{k}_3),
\end{aligned} \tag{4.21}$$

using the delta function requirement in the last equation, which immediately leads to (4.20). For the sake of clarity, the derivation of $V_1^{\pm}(\boldsymbol{k})$ is shown:

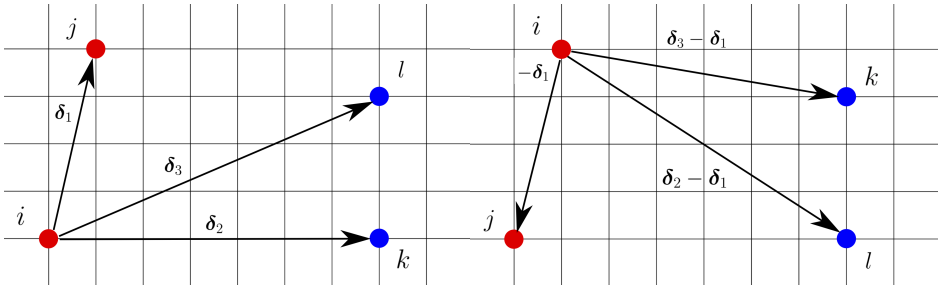

Figure 4.1: Illustration of $U_\alpha(\boldsymbol{\delta}_1, \boldsymbol{\delta}_2, \boldsymbol{\delta}_3) = U_\alpha(-\boldsymbol{\delta}_1, \boldsymbol{\delta}_3 - \boldsymbol{\delta}_1, \boldsymbol{\delta}_2 - \boldsymbol{\delta}_1)$. 4.1a represents $U_\alpha(\boldsymbol{\delta}_1, \boldsymbol{\delta}_2, \boldsymbol{\delta}_3)$, 4.1b represents $U_\alpha(-\boldsymbol{\delta}_1, \boldsymbol{\delta}_3 - \boldsymbol{\delta}_1, \boldsymbol{\delta}_2 - \boldsymbol{\delta}_1)$. A particle at lattice point k and l (both blue) interact and end up at i and j (both red). The two situations differ only by switching particles at i and j, and at k and l. Since the particles are indistinguishable bosons, the situations should be equivalent.

$$
\begin{aligned}
V_1^{\pm}(\boldsymbol{k}) = \Delta\mathcal{E}_{\boldsymbol{k}}^{\mp} &+ \frac{1}{N_s} \\
&\cdot \frac{1}{4} \sum_i N_i \left[\frac{1}{2} \Big(\tilde{U}^+(\boldsymbol{k}^i, \boldsymbol{k}, \boldsymbol{k}^i, \boldsymbol{k}) + \tilde{U}^+(\boldsymbol{k}^i, \boldsymbol{k}, \boldsymbol{k}, \boldsymbol{k}^i) + \tilde{U}^+(\boldsymbol{k}, \boldsymbol{k}^i, \boldsymbol{k}^i, \boldsymbol{k}) \right. \\
&\left. + \tilde{U}^+(\boldsymbol{k}, \boldsymbol{k}^i, \boldsymbol{k}, \boldsymbol{k}^i) \Big) + 2\tilde{U}_{\uparrow\downarrow}(\boldsymbol{k}^i, \boldsymbol{k}^i, \boldsymbol{k}, \boldsymbol{k}) \pm \tilde{U}_{\uparrow\downarrow}(\boldsymbol{k}^i, \boldsymbol{k}, \boldsymbol{k}, \boldsymbol{k}^i) e^{-i(\gamma_{\boldsymbol{k}} - \gamma_{\boldsymbol{k}^i})} \right] \\
= \Delta\mathcal{E}_{\boldsymbol{k}}^{\mp} &+ \sum_i \frac{n_i}{4} \left[\tilde{U}^+(\boldsymbol{k}^i, \boldsymbol{k}, \boldsymbol{k}^i, \boldsymbol{k}) + \tilde{U}^+(\boldsymbol{k}^i, \boldsymbol{k}, \boldsymbol{k}, \boldsymbol{k}^i) \right. \\
&\left. + 2\tilde{U}_{\uparrow\downarrow}(\boldsymbol{k}^i, \boldsymbol{k}^i, \boldsymbol{k}, \boldsymbol{k}) \pm \tilde{U}_{\uparrow\downarrow}(\boldsymbol{k}^i, \boldsymbol{k}, \boldsymbol{k}, \boldsymbol{k}^i) e^{-i(\gamma_{\boldsymbol{k}} - \gamma_{\boldsymbol{k}^i})} \right] \\
= \Delta\mathcal{E}_{\boldsymbol{k}}^{\mp} &+ \sum_i \frac{n_i}{4} \left[\tilde{U}_\downarrow(\boldsymbol{k}, \boldsymbol{k}^i, \boldsymbol{k}) + \tilde{U}_\uparrow(\boldsymbol{k}, \boldsymbol{k}^i, \boldsymbol{k}) + \tilde{U}_\downarrow(\boldsymbol{k}, \boldsymbol{k}, \boldsymbol{k}^i) \right. \\
&\left. + \tilde{U}_\uparrow(\boldsymbol{k}, \boldsymbol{k}, \boldsymbol{k}^i) + 2\tilde{U}_{\uparrow\downarrow}(\boldsymbol{k}^i, \boldsymbol{k}^i, \boldsymbol{k}, \boldsymbol{k}) \pm \tilde{U}_{\uparrow\downarrow}(\boldsymbol{k}^i, \boldsymbol{k}, \boldsymbol{k}, \boldsymbol{k}^i) e^{-i(\gamma_{\boldsymbol{k}} - \gamma_{\boldsymbol{k}^i})} \right]
\end{aligned}
$$

Furthermore, we will now show that $W_1^{\pm}$, $W_2^{\pm}$, $P_1^{\pm}$, and $P_2^{\pm}$ are all symmetric in $\boldsymbol{k}$. In a translationally invariant lattice it is reasonable to assume that

$$
U_\alpha(\boldsymbol{\delta}_1, \boldsymbol{\delta}_2, \boldsymbol{\delta}_3) = U_\alpha(-\boldsymbol{\delta}_1, -\boldsymbol{\delta}_2, -\boldsymbol{\delta}_3), \tag{4.22}
$$

which leads to

$$\begin{aligned}\tilde{U}_\alpha(-\boldsymbol{k}_2,-\boldsymbol{k}_3,-\boldsymbol{k}_4) &= U_\alpha(0,0,0)+\sum_{\{\boldsymbol{\delta}_i\}} U_\alpha(\boldsymbol{\delta}_1,\boldsymbol{\delta}_2,\boldsymbol{\delta}_3)e^{-i(\boldsymbol{k}_2\cdot\boldsymbol{\delta}_1-\boldsymbol{k}_3\cdot\boldsymbol{\delta}_2-\boldsymbol{k}_4\cdot\boldsymbol{\delta}_3)}\\ &= U_\alpha(0,0,0)+\sum_{\{\boldsymbol{\delta}_i\}} U_\alpha(-\boldsymbol{\delta}_1,-\boldsymbol{\delta}_2,-\boldsymbol{\delta}_3)e^{i(\boldsymbol{k}_2\cdot\boldsymbol{\delta}_1-\boldsymbol{k}_3\cdot\boldsymbol{\delta}_2-\boldsymbol{k}_4\cdot\boldsymbol{\delta}_3)}\\ &= \tilde{U}_\alpha(\boldsymbol{k}_2,\boldsymbol{k}_3,\boldsymbol{k}_4).\end{aligned} \tag{4.23}$$

Since the ground state vectors appear in pairs of $\boldsymbol{k}^i$ and $-\boldsymbol{k}^i$ they can be interchanged in a sum over all $\boldsymbol{k}^i$. Using this, (3.49), (4.19), and (4.23), we obtain

$$\begin{aligned}W_1^{\pm}(-\boldsymbol{k}) &= \sum_i \frac{\sqrt{n_i n_{-i}}}{8}\Big[\tilde{U}_\downarrow(\boldsymbol{k},\boldsymbol{k}^i,-\boldsymbol{k}^i)+\tilde{U}_\uparrow(\boldsymbol{k},\boldsymbol{k}^i,-\boldsymbol{k}^i)e^{-2i(\gamma_{-\boldsymbol{k}}-\gamma_{\boldsymbol{k}^i})}\\ &\qquad \pm 2\tilde{U}_{\uparrow\downarrow}(-\boldsymbol{k},\boldsymbol{k}^i,\boldsymbol{k},-\boldsymbol{k}^i)e^{-i(\gamma_{-\boldsymbol{k}}-\gamma_{\boldsymbol{k}^i})}\Big]\\ &= \sum_i \frac{\sqrt{n_{-i}n_i}}{8}\Big[\tilde{U}_\downarrow(\boldsymbol{k},-\boldsymbol{k}^i,\boldsymbol{k}^i)+\tilde{U}_\uparrow(\boldsymbol{k},-\boldsymbol{k}^i,\boldsymbol{k}^i)e^{-2i(\gamma_{-\boldsymbol{k}}-\gamma_{-\boldsymbol{k}^i})}\\ &\qquad \pm 2\tilde{U}_{\uparrow\downarrow}(-\boldsymbol{k},-\boldsymbol{k}^i,\boldsymbol{k},\boldsymbol{k}^i)e^{-i(\gamma_{-\boldsymbol{k}}-\gamma_{-\boldsymbol{k}^i})}\Big]\\ &= \sum_i \frac{\sqrt{n_{-i}n_i}}{8}\Big[\tilde{U}_\downarrow(\boldsymbol{k},-\boldsymbol{k}^i,\boldsymbol{k}^i)+\tilde{U}_\uparrow(\boldsymbol{k},-\boldsymbol{k}^i,\boldsymbol{k}^i)e^{-2i(\gamma_{\boldsymbol{k}}+\pi-\gamma_{\boldsymbol{k}^i}-\pi)}\\ &\qquad \pm 2\tilde{U}_{\uparrow\downarrow}(-\boldsymbol{k},-\boldsymbol{k}^i,\boldsymbol{k},\boldsymbol{k}^i)e^{-i(\gamma_{\boldsymbol{k}}+\pi-\gamma_{\boldsymbol{k}^i}-\pi)}\Big]\\ &= \sum_i \frac{\sqrt{n_{-i}n_i}}{8}\Big[\tilde{U}_\downarrow(-\boldsymbol{k},\boldsymbol{k}^i,-\boldsymbol{k}^i)+\tilde{U}_\uparrow(-\boldsymbol{k},\boldsymbol{k}^i,-\boldsymbol{k}^i)e^{-2i(\gamma_{\boldsymbol{k}}-\gamma_{\boldsymbol{k}^i})}\\ &\qquad \pm 2\tilde{U}_{\uparrow\downarrow}(\boldsymbol{k},\boldsymbol{k}^i,-\boldsymbol{k},-\boldsymbol{k}^i)e^{-i(\gamma_{\boldsymbol{k}}-\gamma_{\boldsymbol{k}^i})}\Big]\\ &= W_1^{\pm}(\boldsymbol{k}),\end{aligned} \tag{4.24}$$

and similarly we get

$$W_2^{\pm}(-\boldsymbol{k}) = W_2^{\pm}(\boldsymbol{k}), \quad P_1^{\pm}(-\boldsymbol{k}) = P_1^{\pm}(\boldsymbol{k}), \quad P_2^{\pm}(-\boldsymbol{k}) = P_2^{\pm}(\boldsymbol{k}). \tag{4.25}$$

We observe in addition that the symmetry demand on the intra-spin potential (4.22), together with the corresponding symmetry demand on the

inter-spin potential, make both $\tilde{U}_\alpha$ and $\tilde{U}_{\uparrow\downarrow}$ real, since the complex conjugation of the exponents in (4.18) can be countered by the change of summation variables $\{\boldsymbol{\delta}_i\} \to \{-\boldsymbol{\delta}_i\}$.

It is clear from (4.16) that $\widetilde{\mathcal{M}}^u_{\boldsymbol{k}}$ is not Hermitian: As an example the diagonal element $T(\boldsymbol{k})$ is clearly not real. The next section is concerned with creating a Hermitian matrix $\widetilde{\mathcal{M}}_{\boldsymbol{k}}$ by a process of symmetrization.

4.1.3 Symmetrization of excitation matrix

$\widetilde{\mathcal{M}}^u_{\boldsymbol{k}}$ will now be made Hermitian by commuting the boson operators by the use of the commutation relation (3.46), e.g.

$$a^\dagger_{\boldsymbol{k}+} a_{\boldsymbol{k}-} = \frac{1}{2}\left(a^\dagger_{\boldsymbol{k}+} a_{\boldsymbol{k}-} + a_{\boldsymbol{k}-} a^\dagger_{\boldsymbol{k}+}\right). \tag{4.26}$$

This process of symmetrization thus contributes with another factor 1/2. Diagonal non-commuting terms in $\widetilde{\mathcal{M}}^u_{\boldsymbol{k}}$ will also contribute with a term without boson operators, adding to the constant term H_0'. The treatment of the total constant term H_0 is found in Section 4.1.4.

The resulting symmetrized matrix is denoted in block form as follows:

$$\widetilde{\mathcal{M}}_{\boldsymbol{k}} = \begin{pmatrix} M_1 & M_2 \\ M_3 & M_4 \end{pmatrix} \tag{4.27}$$

where M_1 through M_4 are $\boldsymbol{k}$-dependent 4-by-4 matrices. We will now investigate the hermiticity of this matrix and which demands that follow.

If $\widetilde{\mathcal{M}}_{\boldsymbol{k}}$ can be written in the form

$$\breve{A} = \begin{pmatrix} A_1 & A_2 \\ A_2^* & A_1^* \end{pmatrix}, \tag{4.28}$$

where A_1 is Hermitian, $A_1^\dagger = A_1$, and A_2 is symmetric, $A_2^T = A_2$, then $\widetilde{\mathcal{M}}_{\boldsymbol{k}}$ is Hermitian. This follows from

$$\begin{aligned} \breve{A}^\dagger &= \begin{pmatrix} A_1 & A_2 \\ A_2^* & A_1^* \end{pmatrix}^\dagger = \begin{pmatrix} A_1^T & (A_2^*)^T \\ A_2^T & (A_1^*)^T \end{pmatrix}^* = \begin{pmatrix} A_1^\dagger & A_2^T \\ (A_2^T)^* & (A_1^\dagger)^* \end{pmatrix} \\ &= \begin{pmatrix} A_1 & A_2 \\ A_2^* & A_1^* \end{pmatrix} = \breve{A}. \end{aligned} \tag{4.29}$$

We first consider the diagonal matrices M_1 and M_4 in $\widetilde{\mathcal{M}}_{\boldsymbol{k}}$. We see from (4.29) that both must be Hermitian and that they must be the complex conjugate of each other. We have that

$$M_1 = \begin{pmatrix} V_1^-(\boldsymbol{k}) - T(\boldsymbol{k}) & 0 & V_2^-(\boldsymbol{k}) + T(\boldsymbol{k}) & 0 \\ 0 & V_1^-(-\boldsymbol{k}) - T(-\boldsymbol{k}) & 0 & V_2^-(-\boldsymbol{k}) + T(-\boldsymbol{k}) \\ V_2^+(\boldsymbol{k}) - T(\boldsymbol{k}) & 0 & V_1^+(\boldsymbol{k}) + T(\boldsymbol{k}) & 0 \\ 0 & V_2^+(-\boldsymbol{k}) - T(-\boldsymbol{k}) & 0 & V_1^+(-\boldsymbol{k}) + T(-\boldsymbol{k}) \end{pmatrix} \tag{4.30}$$

The diagonal must be real in a Hermitian matrix. One such term is

$$\begin{aligned} V_1^-(\boldsymbol{k}) - T(\boldsymbol{k}) &= \Delta\mathcal{E}_{\boldsymbol{k}}^{\mp} + \sum_i \frac{n_i}{4} \Big[\tilde{U}_\downarrow(\boldsymbol{k}, \boldsymbol{k}^i, \boldsymbol{k}) + \tilde{U}_\uparrow(\boldsymbol{k}, \boldsymbol{k}^i, \boldsymbol{k}) + \tilde{U}_\downarrow(\boldsymbol{k}, \boldsymbol{k}, \boldsymbol{k}^i) \\ &\qquad + \tilde{U}_\uparrow(\boldsymbol{k}, \boldsymbol{k}, \boldsymbol{k}^i) + 2\tilde{U}_{\uparrow\downarrow}(\boldsymbol{k}^i, \boldsymbol{k}^i, \boldsymbol{k}, \boldsymbol{k}) \\ &\qquad - \tilde{U}_{\uparrow\downarrow}(\boldsymbol{k}^i, \boldsymbol{k}, \boldsymbol{k}, \boldsymbol{k}^i) e^{-i(\gamma_{\boldsymbol{k}} - \gamma_{\boldsymbol{k}^i})} \Big] \\ &\quad - \sum_i \frac{n_i}{4} \tilde{U}_{\uparrow\downarrow}(\boldsymbol{k}^i, \boldsymbol{k}, \boldsymbol{k}, \boldsymbol{k}^i) e^{i(\gamma_{\boldsymbol{k}} - \gamma_{\boldsymbol{k}^i})} \\ &= \Delta\mathcal{E}_{\boldsymbol{k}}^{+} + \sum_i \frac{n_i}{4} \Big[\tilde{U}_\downarrow(\boldsymbol{k}, \boldsymbol{k}^i, \boldsymbol{k}) + \tilde{U}_\uparrow(\boldsymbol{k}, \boldsymbol{k}^i, \boldsymbol{k}) + \tilde{U}_\downarrow(\boldsymbol{k}, \boldsymbol{k}, \boldsymbol{k}^i) \\ &\qquad + \tilde{U}_\uparrow(\boldsymbol{k}, \boldsymbol{k}, \boldsymbol{k}^i) + 2\tilde{U}_{\uparrow\downarrow}(\boldsymbol{k}^i, \boldsymbol{k}^i, \boldsymbol{k}, \boldsymbol{k}) \\ &\qquad - 2\tilde{U}_{\uparrow\downarrow}(\boldsymbol{k}^i, \boldsymbol{k}, \boldsymbol{k}, \boldsymbol{k}^i) \cos(\gamma_{\boldsymbol{k}} - \gamma_{\boldsymbol{k}^i}) \Big] \end{aligned} \tag{4.31}$$

This term is real since $\Delta\mathcal{E}_{\boldsymbol{k}}^{+} = \mathcal{E}_{\boldsymbol{k}}^{+} - \mathcal{E}^0$, $\tilde{U}_\downarrow$, and $\tilde{U}_\uparrow$ are real from the discussions of Sections 3.2.3 and 4.1.2, respectively. The diagonal term (4.31) is therefore real by the sufficient and physically reasonable demands

$$\begin{aligned} t_\alpha(\boldsymbol{\delta}) &= t_\alpha(-\boldsymbol{\delta}), \\ U_\alpha(\boldsymbol{\delta}_1, \boldsymbol{\delta}_2, \boldsymbol{\delta}_3) &= U_\alpha(-\boldsymbol{\delta}_1, -\boldsymbol{\delta}_2, -\boldsymbol{\delta}_3), \\ U_{\uparrow\downarrow}(\boldsymbol{\delta}_1, \boldsymbol{\delta}_2, \boldsymbol{\delta}_3) &= U_{\uparrow\downarrow}(-\boldsymbol{\delta}_1, -\boldsymbol{\delta}_2, -\boldsymbol{\delta}_3). \end{aligned} \tag{4.32}$$

In fact, the same assumptions ensure that all diagonal terms are real, see (4.47) for the two expressions.

The demands (4.32) also make the off-diagonal terms in M_1 complex conjugate of each other, e.g.

$$
\begin{aligned}
V_2^+(\boldsymbol{k}) - T(\boldsymbol{k}) &= \sum_i \frac{n_i}{4} \Big[\tilde{U}_\downarrow(\boldsymbol{k},\boldsymbol{k}^i,\boldsymbol{k}) - \tilde{U}_\uparrow(\boldsymbol{k},\boldsymbol{k}^i,\boldsymbol{k}) + \tilde{U}_\downarrow(\boldsymbol{k},\boldsymbol{k},\boldsymbol{k}^i) \\
&\qquad - \tilde{U}_\uparrow(\boldsymbol{k},\boldsymbol{k},\boldsymbol{k}^i) + \tilde{U}_{\uparrow\downarrow}(\boldsymbol{k}^i,\boldsymbol{k},\boldsymbol{k},\boldsymbol{k}^i) e^{-i(\gamma_{\boldsymbol{k}} - \gamma_{\boldsymbol{k}^i})}\Big] \\
&\quad - \sum_i \frac{n_i}{4} \tilde{U}_{\uparrow\downarrow}(\boldsymbol{k}^i,\boldsymbol{k},\boldsymbol{k},\boldsymbol{k}^i) e^{i(\gamma_{\boldsymbol{k}} - \gamma_{\boldsymbol{k}^i})} \\
&= \sum_i \frac{n_i}{4} \Big[\tilde{U}_\downarrow(\boldsymbol{k},\boldsymbol{k}^i,\boldsymbol{k}) - \tilde{U}_\uparrow(\boldsymbol{k},\boldsymbol{k}^i,\boldsymbol{k}) + \tilde{U}_\downarrow(\boldsymbol{k},\boldsymbol{k},\boldsymbol{k}^i) \\
&\qquad - \tilde{U}_\uparrow(\boldsymbol{k},\boldsymbol{k},\boldsymbol{k}^i) - 2i\tilde{U}_{\uparrow\downarrow}(\boldsymbol{k}^i,\boldsymbol{k},\boldsymbol{k},\boldsymbol{k}^i) \sin(\gamma_{\boldsymbol{k}} - \gamma_{\boldsymbol{k}^i})\Big] \\
&= \left(\sum_i \frac{n_i}{4} \Big[\tilde{U}_\downarrow(\boldsymbol{k},\boldsymbol{k}^i,\boldsymbol{k}) - \tilde{U}_\uparrow(\boldsymbol{k},\boldsymbol{k}^i,\boldsymbol{k}) + \tilde{U}_\downarrow(\boldsymbol{k},\boldsymbol{k},\boldsymbol{k}^i) \right. \\
&\qquad \left. - \tilde{U}_\uparrow(\boldsymbol{k},\boldsymbol{k},\boldsymbol{k}^i) + 2i\tilde{U}_{\uparrow\downarrow}(\boldsymbol{k}^i,\boldsymbol{k},\boldsymbol{k},\boldsymbol{k}^i) \sin(\gamma_{\boldsymbol{k}} - \gamma_{\boldsymbol{k}^i})\Big] \right)^* \\
&= (V_2^-(\boldsymbol{k}) + T(\boldsymbol{k}))^*
\end{aligned}
\tag{4.33}
$$

For the other diagonal matrix M_4 we see that

$$
\begin{aligned}
M_4 &= \begin{pmatrix}
V_1^-(\boldsymbol{k}) - T(\boldsymbol{k}) & 0 & V_2^+(\boldsymbol{k}) - T(\boldsymbol{k}) & 0 \\
0 & V_1^-(-\boldsymbol{k}) - T(-\boldsymbol{k}) & 0 & V_2^+(-\boldsymbol{k}) - T(-\boldsymbol{k}) \\
V_2^-(\boldsymbol{k}) + T(\boldsymbol{k}) & 0 & V_1^+(\boldsymbol{k}) + T(\boldsymbol{k}) & 0 \\
0 & V_2^-(-\boldsymbol{k}) + T(-\boldsymbol{k}) & 0 & V_1^+(-\boldsymbol{k}) + T(-\boldsymbol{k})
\end{pmatrix} \\
&= M_1^*,
\end{aligned}
\tag{4.34}
$$

We define $E^\pm$ and V_1 such that

$$
M_1 = \begin{pmatrix}
E^+(\boldsymbol{k}) & 0 & V_1(\boldsymbol{k}) & 0 \\
0 & E^+(-\boldsymbol{k}) & 0 & V_1(-\boldsymbol{k}) \\
V_1^*(\boldsymbol{k}) & 0 & E^-(\boldsymbol{k}) & 0 \\
0 & V_1^*(-\boldsymbol{k}) & 0 & E^-(-\boldsymbol{k})
\end{pmatrix},
\tag{4.35}
$$

and we clearly see that both diagonal matrices M_1 and M_4 are Hermitian and complex conjugate of each other (see (4.47) and (4.47) for definitions of $E^\pm$ and V_1).

The symmetrization process, and using the symmetries (4.24) and (4.25), lead to the following inelastic off-diagonal block matrices in $\widetilde{\mathcal{M}}_{\boldsymbol{k}}$:

$$M_2 = \begin{pmatrix} 0 & 2W_1^-(\boldsymbol{k}) & 0 & W_2^-(\boldsymbol{k}) + W_2^+(\boldsymbol{k}) \\ 2W_1^-(\boldsymbol{k}) & 0 & W_2^-(\boldsymbol{k}) + W_2^+(\boldsymbol{k}) & 0 \\ 0 & W_2^+(\boldsymbol{k}) + W_2^-(\boldsymbol{k}) & 0 & 2W_1^+(\boldsymbol{k}) \\ W_2^+(\boldsymbol{k}) + W_2^-(\boldsymbol{k}) & 0 & 2W_1^+(\boldsymbol{k}) & 0 \end{pmatrix}, \tag{4.36}$$

$$M_3 = \begin{pmatrix} 0 & 2P_1^-(\boldsymbol{k}) & 0 & P_2^-(\boldsymbol{k}) + P_2^+(\boldsymbol{k}) \\ 2P_1^-(\boldsymbol{k}) & 0 & P_2^-(\boldsymbol{k}) + P_2^+(\boldsymbol{k}) & 0 \\ 0 & P_2^+(\boldsymbol{k}) + P_2^-(\boldsymbol{k}) & 0 & 2P_1^+(\boldsymbol{k}) \\ P_2^+(\boldsymbol{k}) + P_2^-(\boldsymbol{k}) & 0 & 2P_1^+(\boldsymbol{k}) & 0 \end{pmatrix}. \tag{4.37}$$

According to (4.29) M_2 and M_3 should be symmetric, which they are. We should also have that $M_2 = M_3^*$. To this end, we introduce two new demands on the Fourier transformed potentials:

$$\begin{aligned} \tilde{U}_\alpha(-\boldsymbol{k}, \boldsymbol{k}^i, -\boldsymbol{k}^i) &= \tilde{U}_\alpha(-\boldsymbol{k}^i, \boldsymbol{k}, -\boldsymbol{k}), \\ \tilde{U}_{\uparrow\downarrow}(\boldsymbol{k}, \boldsymbol{k}^i, -\boldsymbol{k}, -\boldsymbol{k}^i) &= \tilde{U}_{\uparrow\downarrow}(\boldsymbol{k}^i, \boldsymbol{k}, -\boldsymbol{k}^i, -\boldsymbol{k}). \end{aligned} \tag{4.38}$$

These demands are equivalent to demanding that the rate of particles entering the condensate be equal to that of particles exiting. While it remains to be shown explicitly to be the case from the definitions of the potentials (4.18), the demands (4.38) seem physically sound. The result is

$$P_1^\pm(\boldsymbol{k}) = (W_1^\pm(\boldsymbol{k}))^*, \tag{4.39}$$

$$P_2^\pm(\boldsymbol{k}) = (W_2^\pm(\boldsymbol{k}))^*, \tag{4.40}$$

and thus

$$\begin{aligned} M_2 &= \begin{pmatrix} 0 & V^-(\boldsymbol{k}) & 0 & V_2(\boldsymbol{k}) \\ V^-(\boldsymbol{k}) & 0 & V_2(-\boldsymbol{k}) & 0 \\ 0 & V_2(-\boldsymbol{k}) & 0 & V^+(\boldsymbol{k}) \\ V_2(\boldsymbol{k}) & 0 & V^+(\boldsymbol{k}) & 0 \end{pmatrix} \\ &= M_3^*, \end{aligned} \tag{4.41}$$

where we have defined

$$V^\pm(\boldsymbol{k}) = 2W_1^\pm(\boldsymbol{k}), \tag{4.42}$$

$$V_2(\boldsymbol{k}) = W_2^-(\boldsymbol{k}) + W_2^+(\boldsymbol{k}), \tag{4.43}$$

making M_2 and M_3 symmetric and complex conjugates of each other.

Everything considered we end up with the Hermitian block matrix

$$\breve{\mathcal{M}}_{\boldsymbol{k}} = \begin{pmatrix} M_1 & M_2 \\ M_2^* & M_1^* \end{pmatrix}, \tag{4.44}$$

where

$$M_1 = \begin{pmatrix} E^+(\boldsymbol{k}) & 0 & V_1(\boldsymbol{k}) & 0 \\ 0 & E^+(-\boldsymbol{k}) & 0 & V_1(-\boldsymbol{k}) \\ V_1^*(\boldsymbol{k}) & 0 & E^-(\boldsymbol{k}) & 0 \\ 0 & V_1^*(-\boldsymbol{k}) & 0 & E^-(-\boldsymbol{k}) \end{pmatrix}, \tag{4.45}$$

$$M_2 = \begin{pmatrix} 0 & V^-(\boldsymbol{k}) & 0 & V_2(\boldsymbol{k}) \\ V^-(\boldsymbol{k}) & 0 & V_2(\boldsymbol{k}) & 0 \\ 0 & V_2(\boldsymbol{k}) & 0 & V^+(\boldsymbol{k}) \\ V_2(\boldsymbol{k}) & 0 & V^+(\boldsymbol{k}) & 0 \end{pmatrix}, \tag{4.46}$$

and the matrix elements are defined as

$$\begin{aligned}
E^{\pm}(\boldsymbol{k}) &= V_1^{\mp}(\boldsymbol{k}) \mp T(\boldsymbol{k}) \\
&= \Delta\mathcal{E}_{\boldsymbol{k}}^{\pm} + \sum_i \frac{n_i}{4} \Big[\tilde{U}_{\downarrow}(\boldsymbol{k},\boldsymbol{k}^i,\boldsymbol{k}) + \tilde{U}_{\uparrow}(\boldsymbol{k},\boldsymbol{k}^i,\boldsymbol{k}) + \tilde{U}_{\downarrow}(\boldsymbol{k},\boldsymbol{k},\boldsymbol{k}^i) + \tilde{U}_{\uparrow}(\boldsymbol{k},\boldsymbol{k},\boldsymbol{k}^i) \\
&\qquad + 2\tilde{U}_{\uparrow\downarrow}(\boldsymbol{k}^i,\boldsymbol{k}^i,\boldsymbol{k},\boldsymbol{k}) \mp 2\tilde{U}_{\uparrow\downarrow}(\boldsymbol{k}^i,\boldsymbol{k},\boldsymbol{k},\boldsymbol{k}^i)\cos(\gamma_{\boldsymbol{k}} - \gamma_{\boldsymbol{k}^i})\Big], \\
V_1(\boldsymbol{k}) &= V_2^-(\boldsymbol{k}) + T(\boldsymbol{k}) \\
&= \sum_i \frac{n_i}{4} \Big[\tilde{U}_{\downarrow}(\boldsymbol{k},\boldsymbol{k}^i,\boldsymbol{k}) - \tilde{U}_{\uparrow}(\boldsymbol{k},\boldsymbol{k}^i,\boldsymbol{k}) + \tilde{U}_{\downarrow}(\boldsymbol{k},\boldsymbol{k},\boldsymbol{k}^i) - \tilde{U}_{\uparrow}(\boldsymbol{k},\boldsymbol{k},\boldsymbol{k}^i) \\
&\qquad + 2i\tilde{U}_{\uparrow\downarrow}(\boldsymbol{k}^i,\boldsymbol{k},\boldsymbol{k},\boldsymbol{k}^i)\sin(\gamma_{\boldsymbol{k}} - \gamma_{\boldsymbol{k}^i})\Big], \\
V^{\pm}(\boldsymbol{k}) &= 2W_1^{\pm}(\boldsymbol{k}) \\
&= \sum_i \frac{\sqrt{n_i n_{-i}}}{4} \Big[\tilde{U}_{\downarrow}(-\boldsymbol{k},\boldsymbol{k}^i,-\boldsymbol{k}^i) + \tilde{U}_{\uparrow}(-\boldsymbol{k},\boldsymbol{k}^i,-\boldsymbol{k}^i)e^{-2i(\gamma_{\boldsymbol{k}} - \gamma_{\boldsymbol{k}^i})} \\
&\qquad \pm 2\tilde{U}_{\uparrow\downarrow}(\boldsymbol{k},\boldsymbol{k}^i,-\boldsymbol{k},-\boldsymbol{k}^i)e^{-i(\gamma_{\boldsymbol{k}} - \gamma_{\boldsymbol{k}^i})}\Big], \\
V_2(\boldsymbol{k}) &= W_2^-(\boldsymbol{k}) + W_2^+(\boldsymbol{k}) \\
&= \sum_i \frac{\sqrt{n_i n_{-i}}}{4} \Big[\tilde{U}_{\downarrow}(-\boldsymbol{k},\boldsymbol{k}^i,-\boldsymbol{k}^i) - \tilde{U}_{\uparrow}(-\boldsymbol{k},\boldsymbol{k}^i,-\boldsymbol{k}^i)e^{-2i(\gamma_{\boldsymbol{k}} - \gamma_{\boldsymbol{k}^i})}\Big].
\end{aligned} \tag{4.47}$$

The method of diagonalizing a general bilinear bosonic Hamiltonian, where the basis consists of both creation and annihilation operators, is thoroughly investigated in Ref. [27]. The desired result is that H can be written

$$H = H_0 + \frac{1}{4}{\sum_{\boldsymbol{k}}}' \boldsymbol{\beta}_{\boldsymbol{k}}^T \breve{\mathcal{D}}_{\boldsymbol{k}} \boldsymbol{\beta}_{\boldsymbol{k}} \tag{4.48}$$

with the bosonic quasi-particle operators

$$\boldsymbol{\beta}_{\boldsymbol{k}} = \begin{pmatrix} \beta_{\boldsymbol{k},1} & \beta_{\boldsymbol{k},2} & \beta_{\boldsymbol{k},3} & \beta_{\boldsymbol{k},4} & \beta^{\dagger}_{\boldsymbol{k},1} & \beta^{\dagger}_{\boldsymbol{k},2} & \beta^{\dagger}_{\boldsymbol{k},3} & \beta^{\dagger}_{\boldsymbol{k},4} \end{pmatrix}^{T}, \tag{4.49}$$

and the diagonal matrix

$$\breve{\mathcal{D}}_{\boldsymbol{k}} = \begin{pmatrix} D & 0 \\ 0 & D \end{pmatrix}, \tag{4.50}$$

where D is the diagonal matrix containing the excitation energies $\mathscr{E}_{\boldsymbol{k},\sigma}$, $\sigma = 1,2,3,4$,

$$D = \begin{pmatrix} \mathscr{E}_{\boldsymbol{k},1} & 0 & 0 & 0 \\ 0 & \mathscr{E}_{\boldsymbol{k},2} & 0 & 0 \\ 0 & 0 & \mathscr{E}_{\boldsymbol{k},3} & 0 \\ 0 & 0 & 0 & \mathscr{E}_{\boldsymbol{k},4} \end{pmatrix}. \tag{4.51}$$

The commutation relation implies that

$$\boldsymbol{\beta}_{\boldsymbol{k}}\boldsymbol{\beta}^{\dagger}_{\boldsymbol{k}} - [\boldsymbol{\beta}^{*}_{\boldsymbol{k}}(\boldsymbol{\beta}^{*}_{\boldsymbol{k}})^{\dagger}]^{T} = \breve{\boldsymbol{\sigma}}, \tag{4.52}$$

where we have defined the diagonal matrix $\breve{\boldsymbol{\sigma}} = \mathrm{diag}(1,1,1,1,-1,-1,-1,-1)$.

By comparing commutators of H and $\boldsymbol{\beta}$, and H and the old basis $\phi_{\boldsymbol{k}}$ from (4.14), one realizes that the transition matrix from $\phi_{\boldsymbol{k}}$ to $\boldsymbol{\beta}$ diagonalizes $\widetilde{\mathcal{M}}_{\boldsymbol{k}}\breve{\boldsymbol{\sigma}}$ to produce the matrix $\breve{\mathcal{D}}_{\boldsymbol{k}}\breve{\boldsymbol{\sigma}}$. This is done explicitly in Ref. [27]. Hence, it is the eigenvalues of $\widetilde{\mathcal{M}}_{\boldsymbol{k}}\breve{\boldsymbol{\sigma}}$ that should be found, not $\widetilde{\mathcal{M}}_{\boldsymbol{k}}$, because of (4.52).

Writing out (4.48) explicitly yields

$$\begin{aligned} H &= H_0 + \frac{1}{4}\sum_{\sigma}{\sum_{\boldsymbol{k}}}' \mathscr{E}_{\boldsymbol{k}\sigma}\left(\beta^{\dagger}_{\boldsymbol{k}\sigma}\beta_{\boldsymbol{k}\sigma} + \beta_{\boldsymbol{k}\sigma}\beta^{\dagger}_{\boldsymbol{k}\sigma}\right) \\ &= H_0 + \frac{1}{2}\sum_{\sigma}{\sum_{\boldsymbol{k}}}' \mathscr{E}_{\boldsymbol{k}\sigma}\left(\beta^{\dagger}_{\boldsymbol{k}\sigma}\beta_{\boldsymbol{k}\sigma} + \frac{1}{2}\right) \\ &\equiv H_0 + \frac{1}{2}\sum_{\sigma}{\sum_{\boldsymbol{k}}}' \mathscr{E}_{\boldsymbol{k}\sigma}\left(n_{\boldsymbol{k}\sigma} + \frac{1}{2}\right), \end{aligned} \tag{4.53}$$

by the use of $[\beta_{\boldsymbol{k}\sigma}, \beta^{\dagger}_{\boldsymbol{k}\sigma}] = 1$, and where $n_{\boldsymbol{k}\sigma}$ is the number operator for a quasi particle of branch σ. Note that this is the general diagonalized form described by four branches – in many cases they reduce to only two unique ones, as in Ref. [14], which reduces the sum to over two unique branches and removes the factor $1/2$ in front of the sum.

Eigenvalues are in the thesis found by the use of the symbolic computing environment *Maple*. However, the large number of unique matrix elements in $\widetilde{\mathcal{M}}_{\boldsymbol{k}}\check{\boldsymbol{\sigma}}$ means that we in this very general situation are unable to find eigenvalues that are not unmanageably large.

4.1.4 Constant term

So far we have been concerned with the excitation spectrum, and in the process absorbing all other terms in H into the constant term H_0. This term is constant in the sense that it is not affected by excitations of the state. It does, however, depend on the ground state occupation numbers n_i.

H_0 consists of contributions from the transition from the sum over all $\boldsymbol{k}$ to the sum over non-ground state $\boldsymbol{k}$, $\sum \to \sum'$ in H_1 and in the mean field procedure, and from non-zero commutators in the symmetrization process. We write

$$H_0 = H_0^1 + H_0^{MFT} + H_0^{SYM} \tag{4.54}$$

for these three contributions, respectively. $H_0^1 = \mathcal{E}^0 N$ was shown in Section 3.2.3. H_0^{MFT} is composed of contributions from (4.9) and (4.1.2):

$$\begin{aligned} H_0^{MFT} &= \frac{1}{2N_s}\cdot\frac{1}{4}\sum_i N_i^2\left[\tilde{U}^+(\boldsymbol{k}^i,\boldsymbol{k}^i,\boldsymbol{k}^i,\boldsymbol{k}^i)+2\tilde{U}_{\uparrow\downarrow}(\boldsymbol{k}^i,\boldsymbol{k}^i,\boldsymbol{k}^i,\boldsymbol{k}^i)\right] \\ &\quad+\frac{1}{2N_s}\cdot\frac{1}{4}\sum_{i\neq j} N_iN_j\left[\tilde{U}^+(\boldsymbol{k}^i,\boldsymbol{k}^j,\boldsymbol{k}^i,\boldsymbol{k}^j)+\tilde{U}^+(\boldsymbol{k}^i,\boldsymbol{k}^j,\boldsymbol{k}^j,\boldsymbol{k}^i)\right. \\ &\qquad\left.+2\tilde{U}_{\uparrow\downarrow}(\boldsymbol{k}^i,\boldsymbol{k}^i,\boldsymbol{k}^j,\boldsymbol{k}^j)+2\tilde{U}_{\uparrow\downarrow}(\boldsymbol{k}^i,\boldsymbol{k}^j,\boldsymbol{k}^j,\boldsymbol{k}^i)e^{i(\gamma_{\boldsymbol{k}^j}-\gamma_{\boldsymbol{k}^i})}\right] \\ &= \frac{N_s}{8}\sum_i n_i^2\left[\tilde{U}^+(\boldsymbol{k}^i,\boldsymbol{k}^i,\boldsymbol{k}^i,\boldsymbol{k}^i)+2\tilde{U}_{\uparrow\downarrow}(\boldsymbol{k}^i,\boldsymbol{k}^i,\boldsymbol{k}^i,\boldsymbol{k}^i)\right] \\ &\quad+\frac{N_s}{8}\sum_{i\neq j} n_in_j\left[\tilde{U}^+(\boldsymbol{k}^i,\boldsymbol{k}^j,\boldsymbol{k}^i,\boldsymbol{k}^j)+\tilde{U}^+(\boldsymbol{k}^i,\boldsymbol{k}^j,\boldsymbol{k}^j,\boldsymbol{k}^i)\right. \\ &\qquad\left.+2\tilde{U}_{\uparrow\downarrow}(\boldsymbol{k}^i,\boldsymbol{k}^i,\boldsymbol{k}^j,\boldsymbol{k}^j)+2\tilde{U}_{\uparrow\downarrow}(\boldsymbol{k}^i,\boldsymbol{k}^j,\boldsymbol{k}^j,\boldsymbol{k}^i)e^{i(\gamma_{\boldsymbol{k}^j}-\gamma_{\boldsymbol{k}^i})}\right]. \end{aligned} \tag{4.55}$$

In the symmetrization process of Section 4.1.3 we used that, e.g.

$$\begin{aligned} a^\dagger_{\boldsymbol{k}+}a_{\boldsymbol{k}+}V_1^-(\boldsymbol{k}) &= \frac{1}{2}\left(a^\dagger_{\boldsymbol{k}+}a_{\boldsymbol{k}+}+a^\dagger_{\boldsymbol{k}+}a_{\boldsymbol{k}+}\right)V_1^-(\boldsymbol{k}) \\ &= \frac{1}{2}a^\dagger_{\boldsymbol{k}+}a_{\boldsymbol{k}+}V_1^-(\boldsymbol{k})+\frac{1}{2}a_{\boldsymbol{k}+}a^\dagger_{\boldsymbol{k}+}V_1^-(\boldsymbol{k})-\frac{1}{2}V_1^-(\boldsymbol{k}). \end{aligned} \tag{4.56}$$

Every diagonal matrix element of (4.16) contribute similarly to produce

$$\begin{aligned}
H_0^{SYM} &= -\frac{1}{4}{\sum_{\boldsymbol{k}}}' \big[V_1^-(\boldsymbol{k}) + V_1^-(-\boldsymbol{k}) + V_1^+(\boldsymbol{k}) + V_1^+(-\boldsymbol{k}) + T(\boldsymbol{k}) + T(-\boldsymbol{k}) \\
&\qquad\qquad - T(\boldsymbol{k}) - T(-\boldsymbol{k})\big] \\
&= -\frac{1}{4}{\sum_{\boldsymbol{k}}}' \big[V_1^-(\boldsymbol{k}) + V_1^-(-\boldsymbol{k}) + V_1^+(\boldsymbol{k}) + V_1^+(-\boldsymbol{k})\big] \\
&= -\frac{1}{4}{\sum_{\boldsymbol{k}}}' \Bigg[2(\Delta\mathcal{E}_{\boldsymbol{k}}^+ + \Delta\mathcal{E}_{\boldsymbol{k}}^-) \\
&\qquad\qquad + \sum_i \frac{n_i}{2}\Big(\tilde{U}_\downarrow(\boldsymbol{k},\boldsymbol{k}^i,\boldsymbol{k}) + \tilde{U}_\downarrow(-\boldsymbol{k},\boldsymbol{k}^i,-\boldsymbol{k}) + \tilde{U}_\uparrow(\boldsymbol{k},\boldsymbol{k}^i,\boldsymbol{k}) \\
&\quad + \tilde{U}_\uparrow(-\boldsymbol{k},\boldsymbol{k}^i,-\boldsymbol{k}) + \tilde{U}_\downarrow(\boldsymbol{k},\boldsymbol{k},\boldsymbol{k}^i) + \tilde{U}_\downarrow(-\boldsymbol{k},-\boldsymbol{k},\boldsymbol{k}^i) + \tilde{U}_\uparrow(\boldsymbol{k},\boldsymbol{k},\boldsymbol{k}^i) \\
&\quad + \tilde{U}_\uparrow(-\boldsymbol{k},-\boldsymbol{k},\boldsymbol{k}^i) + 2\tilde{U}_{\uparrow\downarrow}(\boldsymbol{k}^i,\boldsymbol{k}^i,\boldsymbol{k},\boldsymbol{k}) + 2\tilde{U}_{\uparrow\downarrow}(\boldsymbol{k}^i,\boldsymbol{k}^i,-\boldsymbol{k},-\boldsymbol{k})\Big)\Bigg].
\end{aligned} \tag{4.57}$$

The constant term H_0 will be further considered in the ensuing limiting case.

4.2 Nearest neighbor hopping, on-site interactions

In the remainder of our use of the Bose-Hubbard model we will consider the limiting case of hopping only occurring to the nearest neighbor, and particles only interacting when situated at the same lattice point. In a tight-binding situation these first order kinetics and interactions provide a reasonable approximation of the more general case.

Only considering nearest-neighbor hopping means that there remains only one hopping parameter t:

$$t(\boldsymbol{\delta}) \to t. \tag{4.58}$$

Having only on-site interactions changes the Fourier transformed potentials into $\boldsymbol{k}$-independent constants U_α and $U_{\uparrow\downarrow}$:

$$\begin{aligned}
\tilde{U}_\alpha(\boldsymbol{k}_2,\boldsymbol{k}_3,\boldsymbol{k}_4) =& U_\alpha(0,0,0) + \sum_{\{\boldsymbol{\delta}_i\}} U_\alpha(\boldsymbol{\delta}_1,\boldsymbol{\delta}_2,\boldsymbol{\delta}_3) e^{i(\boldsymbol{k}_2\cdot\boldsymbol{\delta}_1 - \boldsymbol{k}_3\cdot\boldsymbol{\delta}_2 - \boldsymbol{k}_4\cdot\boldsymbol{\delta}_3)}, \\
&\to U_\alpha(0,0,0) \equiv U_\alpha, \\
\tilde{U}_{\uparrow\downarrow}(\boldsymbol{k}_1,\boldsymbol{k}_2,\boldsymbol{k}_3,\boldsymbol{k}_4) =& U_{\uparrow\downarrow}(0,0,0) + \frac{1}{2}\sum_{\{\boldsymbol{\delta}_i\}} U_{\uparrow\downarrow}(\boldsymbol{\delta}_1,\boldsymbol{\delta}_2,\boldsymbol{\delta}_3) \\
&\cdot \left(e^{i(\boldsymbol{k}_1\cdot\boldsymbol{\delta}_1 - \boldsymbol{k}_2\cdot\boldsymbol{\delta}_2 - \boldsymbol{k}_4\cdot\boldsymbol{\delta}_3)} + e^{i(\boldsymbol{k}_3\cdot\boldsymbol{\delta}_1 - \boldsymbol{k}_4\cdot\boldsymbol{\delta}_2 - \boldsymbol{k}_2\cdot\boldsymbol{\delta}_3)}\right) \\
&\to U_{\uparrow\downarrow}(0,0,0) \equiv U_{\uparrow\downarrow}.
\end{aligned} \tag{4.59}$$

We observe that in this regime the requirements (4.38) are vacuously fulfilled.

4.2.1 Energy spectrum

The matrix elements (4.47) can now be simplified. For the elastic terms we have

$$\begin{aligned}
E^\pm(\boldsymbol{k}) \to& \Delta\mathcal{E}^\pm_{\boldsymbol{k}} + \sum_i \frac{n_i}{2}\left[U_\downarrow + U_\uparrow + U_{\uparrow\downarrow}\left(1 \mp \cos(\gamma_{\boldsymbol{k}} - \gamma_{\boldsymbol{k}^i})\right)\right] \\
=& \Delta\mathcal{E}^\pm_{\boldsymbol{k}} + \frac{n_0}{2}\left[U_\downarrow + U_\uparrow + U_{\uparrow\downarrow}\right] \mp U_{\uparrow\downarrow}\sum_i \frac{n_i}{2}\cos(\gamma_{\boldsymbol{k}} - \gamma_{\boldsymbol{k}^i}) \\
\equiv& E^\pm_{\boldsymbol{k}}, \\
V_1(\boldsymbol{k}) \to& \sum_i \frac{n_i}{2}\left[U_\downarrow - U_\uparrow + iU_{\uparrow\downarrow}\sin(\gamma_{\boldsymbol{k}} - \gamma_{\boldsymbol{k}^i})\right] \\
=& \frac{n_0}{2}(U_\downarrow - U_\uparrow) + iU_{\uparrow\downarrow}\sum_i \frac{n_i}{2}\sin(\gamma_{\boldsymbol{k}} - \gamma_{\boldsymbol{k}^i}) \\
\equiv& F_{\boldsymbol{k}},
\end{aligned} \tag{4.60}$$

where

$$n_0 \equiv \sum_i n_i = \frac{N_0}{N_s}. \tag{4.61}$$

The unknown parameter n_0 can be eliminated from the expression as follows. If the ratio of the total number of bosons to number of lattice sites is given by $\frac{N}{N_s} = \kappa$, and since

$$N_0 = N - {\sum_{\boldsymbol{k}\alpha}}' a^\dagger_{\boldsymbol{k}\alpha} a_{\boldsymbol{k}\alpha}, \tag{4.62}$$

then

$$n_0 = \frac{\kappa N_0}{N} = \kappa - \frac{\kappa}{N} \sum_{\boldsymbol{k}\alpha}{}' a^\dagger_{\boldsymbol{k}\alpha} a_{\boldsymbol{k}\alpha}. \tag{4.63}$$

When (4.63) is inserted into a matrix element, the latter term leads to a term biquadratic in non-ground state boson operators, and is thus ignored in the mean-field approach, i.e.

$$\begin{aligned} E^\pm_{\boldsymbol{k}} =& \Delta\mathcal{E}^\pm_{\boldsymbol{k}} + \frac{\kappa}{2}\left[U_\downarrow + U_\uparrow + U_{\uparrow\downarrow}\right] \mp U_{\uparrow\downarrow} \sum_i \frac{n_i}{2} \cos(\gamma_{\boldsymbol{k}} - \gamma_{\boldsymbol{k}^i}), \\ F(\boldsymbol{k}) =& \frac{\kappa}{2}(U_\downarrow - U_\uparrow) + iU_{\uparrow\downarrow} \sum_i \frac{n_i}{2} \sin(\gamma_{\boldsymbol{k}} - \gamma_{\boldsymbol{k}^i}). \end{aligned} \tag{4.64}$$

The antisymmetry of $e^{i\gamma_{\boldsymbol{k}}}$ from (3.47) implies that $\cos(\gamma_{\boldsymbol{k}} - \gamma_{\boldsymbol{k}^i})$ and $\sin(\gamma_{\boldsymbol{k}} - \gamma_{\boldsymbol{k}^i})$ is also antisymmetric in $\boldsymbol{k}$. This leads to $F(-\boldsymbol{k}) = F^*(\boldsymbol{k})$, and accordingly we suppress the argument for this matrix element. $E^\pm_{\boldsymbol{k}}$ do not possess any symmetry in $\boldsymbol{k}$.

The inelastic matrix terms can be further simplified by realizing that $\sqrt{n_i n_{-i}} e^{i\gamma_{\boldsymbol{k}^i}}$ is antisymmetric in $\boldsymbol{k}^i$[1]:

$$\begin{aligned} \sum_i \sqrt{n_i n_{-i}} e^{-i(\gamma_{\boldsymbol{k}} - \gamma_{\boldsymbol{k}^i})} &= e^{-i\gamma_{\boldsymbol{k}}} \sum_j \sqrt{n_j n_{-j}} (e^{i\gamma_{\boldsymbol{k}^j}} + e^{i\gamma_{-\boldsymbol{k}^j}}) \\ &= e^{-i\gamma_{\boldsymbol{k}}} \sum_j \sqrt{n_j n_{-j}} (e^{i\gamma_{\boldsymbol{k}^j}} - e^{i\gamma_{\boldsymbol{k}^j}}) \\ &= 0, \end{aligned} \tag{4.65}$$

where the sum over j is over $\boldsymbol{k}^i$'s from only one half plane. This produces

$$\begin{aligned} V^\pm(\boldsymbol{k}) = \sum_i \frac{\sqrt{n_i n_{-i}}}{4} \Big[& \tilde{U}_\downarrow(-\boldsymbol{k}, \boldsymbol{k}^i, -\boldsymbol{k}^i) + \tilde{U}_\uparrow(-\boldsymbol{k}, \boldsymbol{k}^i, -\boldsymbol{k}^i) e^{-2i(\gamma_{\boldsymbol{k}} - \gamma_{\boldsymbol{k}^i})} \\ & \pm 2\tilde{U}_{\uparrow\downarrow}(\boldsymbol{k}, \boldsymbol{k}^i, -\boldsymbol{k}, -\boldsymbol{k}^i) e^{-i(\gamma_{\boldsymbol{k}} - \gamma_{\boldsymbol{k}^i})} \Big] \\ \to \sum_i \frac{\sqrt{n_i n_{-i}}}{4} & \left[U_\downarrow + U_\uparrow e^{-2i(\gamma_{\boldsymbol{k}} - \gamma_{\boldsymbol{k}^i})}\right] \\ \equiv G_1(\boldsymbol{k}), & \end{aligned} \tag{4.66}$$

[1]The factor n_i destroys this antisymmetry in the elastic terms.

$$
\begin{aligned}
V_2(\boldsymbol{k}) &= \sum_i \frac{\sqrt{n_i n_{-i}}}{4}\left[\tilde{U}_\downarrow(-\boldsymbol{k},\boldsymbol{k}^i,-\boldsymbol{k}^i) - \tilde{U}_\uparrow(-\boldsymbol{k},\boldsymbol{k}^i,-\boldsymbol{k}^i)e^{-2i(\gamma_{\boldsymbol{k}}-\gamma_{\boldsymbol{k}^i})}\right] \\
&\to \sum_i \frac{\sqrt{n_i n_{-i}}}{4}\left[U_\downarrow - U_\uparrow e^{-2i(\gamma_{\boldsymbol{k}}-\gamma_{\boldsymbol{k}^i})}\right] \\
&\equiv G_2(\boldsymbol{k}).
\end{aligned}
$$

The inelastic terms G_1 and G_2 are seen to be symmetric in $\boldsymbol{k}$, and we suppress the argument for these matrix elements as well.

Since $E^{\pm}_{\boldsymbol{k}}$ do not have any symmetry in $\boldsymbol{k}$, they should appear in the form of both $E^{\pm}_{\boldsymbol{k}}$ and $E^{\pm}_{-\boldsymbol{k}}$. This leads to four distinct matrix elements on the diagonal, producing impossibly large eigenvalues. However, since the sum over $\boldsymbol{k}$ in the Hamiltonian includes both $\boldsymbol{k}$ and $-\boldsymbol{k}$, we may consider both terms as a single matrix element. This procedure on the diagonal and antidiagonal, leaving the matrix Hermitian, produces the following limiting case matrix:

$$
\widetilde{\mathcal{M}}_{\boldsymbol{k}} = \begin{pmatrix} N_1 & N_2 \\ N_2^* & N_1^* \end{pmatrix}, \tag{4.67}
$$

where

$$
N_1 = \begin{pmatrix} 2E^+_{\boldsymbol{k}} & 0 & F & 0 \\ 0 & 0 & 0 & F^* \\ F & 0 & 0 & 0 \\ 0 & F^* & 0 & 2E^-_{-\boldsymbol{k}} \end{pmatrix}, \tag{4.68}
$$

$$
N_2 = \begin{pmatrix} 0 & G_1 & 0 & 2G_2 \\ G_1 & 0 & 0 & 0 \\ 0 & 0 & 0 & G_1 \\ 2G_2 & 0 & G_1 & 0 \end{pmatrix}. \tag{4.69}
$$

The four-branched excitation spectrum is thus

$$
\mathscr{E}^+_{\boldsymbol{k}\sigma} = \left[K + \sqrt{R} + \sigma\sqrt{2}\sqrt{H + K\sqrt{R}}\right]^{\frac{1}{2}}, \tag{4.70}
$$

$$
\mathscr{E}^-_{\boldsymbol{k}\sigma} = \left[K - \sqrt{R} + \sigma\sqrt{2}\sqrt{H - K\sqrt{R}}\right]^{\frac{1}{2}}, \tag{4.71}
$$

for $\sigma = +, -$, and where

$$K = (E^+_{\boldsymbol{k}})^2 + (E^-_{-\boldsymbol{k}})^2 + |F|^2 - |G_1|^2 - 2|G_2|^2, \tag{4.72}$$

$$R = ((E^+_{\boldsymbol{k}} + E^-_{-\boldsymbol{k}})^2 - 4|G_2|^2)(E^+_{\boldsymbol{k}} - E^-_{-\boldsymbol{k}})^2, \tag{4.73}$$

$$\begin{aligned} H = &\left[(E^+_{\boldsymbol{k}})^2 + (E^-_{-\boldsymbol{k}})^2 - 2|G_2|^2\right] \cdot \left[|F|^2 - |G_1|^2 - 4|G_2|^2\right] \\ &+ (E^+_{\boldsymbol{k}})^4 + (E^-_{-\boldsymbol{k}})^4 + 2|G_2|^2 \left[2E^+_{\boldsymbol{k}} E^-_{-\boldsymbol{k}} - 3|G_2|^2\right], \end{aligned} \tag{4.74}$$

$$\begin{aligned} E^\pm_{\boldsymbol{k}} =& \Delta\mathcal{E}^\pm_{\boldsymbol{k}} + \frac{\kappa}{2}\left[U_\downarrow + U_\uparrow + U_{\uparrow\downarrow}\right] \mp U_{\uparrow\downarrow} \sum_i \frac{n_i}{2} \cos(\gamma_{\boldsymbol{k}} - \gamma_{\boldsymbol{k}^i}), \\ F =& \frac{\kappa}{2}(U_\downarrow - U_\uparrow) + iU_{\uparrow\downarrow} \sum_i \frac{n_i}{2} \sin(\gamma_{\boldsymbol{k}} - \gamma_{\boldsymbol{k}^i}), \\ G_1 =& \sum_i \frac{\sqrt{n_i n_{-i}}}{4} \left[U_\downarrow + U_\uparrow e^{-2i(\gamma_{\boldsymbol{k}} - \gamma_{\boldsymbol{k}^i})}\right], \\ G_2 =& \sum_i \frac{\sqrt{n_i n_{-i}}}{4} \left[U_\downarrow - U_\uparrow e^{-2i(\gamma_{\boldsymbol{k}} - \gamma_{\boldsymbol{k}^i})}\right], \end{aligned} \tag{4.75}$$

and where κ is the number of bosons per lattice site. These are the eigenvalues of the matrix $\widetilde{\mathcal{M}}_{\boldsymbol{k}}\check{\boldsymbol{\sigma}}$, as described at the end of Section 4.1.3, found by the use of the symbolic computing environment *Maple*.

We see that in the limit of $U_{\uparrow\downarrow} = U_\uparrow = U_\downarrow = 0$, i.e. reducing the system to non-interacting spin-orbit coupled bosons, we obtain $\mathscr{E}^\pm_{\boldsymbol{k}+} = 2\Delta\mathcal{E}^\pm_{\boldsymbol{k}}$, $\mathscr{E}^\pm_{\boldsymbol{k}-} = 0$.

Verification of matrix simplifications

The procedure of moving diagonal and anti-diagonal matrix elements in order to obtain (4.68) and (4.69) will now be discussed briefly. The new matrix clearly has a new set of eigenvalues, since the two matrices are not similar. This means that the diagonalized Hamiltonian expresses the energy in terms of different quasiparticles than without the procedure. However, since the sum over $\boldsymbol{k}$ remains unchanged, so should the total free energy. We will investigate this by considering the free energy $\mathcal{F}$ at temperature $T = 0$ of the known non-SOC case from Ref. [14], part B, expressed in terms of these distinct sets of quasiparticles.

The corresponding real block matrices read

$$N_1 = \begin{pmatrix} E^A_{\boldsymbol{k}} & 0 & F_{AB} & 0 \\ 0 & E^A_{\boldsymbol{k}} & 0 & F_{AB} \\ F_{AB} & 0 & E^B_{\boldsymbol{k}} & 0 \\ 0 & F_{AB} & 0 & E^B_{\boldsymbol{k}} \end{pmatrix}, N_2 = \begin{pmatrix} 0 & F & 0 & F_{AB} \\ F & 0 & F_{AB} & 0 \\ 0 & F_{AB} & 0 & F \\ F_{AB} & 0 & F & 0 \end{pmatrix}. \tag{4.76}$$

Diagonalization of $\breve{\mathcal{M}}_{\boldsymbol{k}} \cdot \breve{\boldsymbol{\sigma}}$ gives $D = \mathrm{diag}(\mathscr{E}_{\boldsymbol{k},+}, \mathscr{E}_{-\boldsymbol{k}+}, \mathscr{E}_{\boldsymbol{k},-}, \mathscr{E}_{\boldsymbol{k},-})$. The four eigenvalues are identified as two distinct branches each represented with $\boldsymbol{k}$ and $-\boldsymbol{k}$. Renaming the basis $(\boldsymbol{k}, 2) \to (-\boldsymbol{k}, 1)$, $(\boldsymbol{k}, 4) \to (-\boldsymbol{k}, 3)$, $1, 3 \to +, -$ in (4.51), inserting into (4.53) and performing $-\boldsymbol{k} \to \boldsymbol{k}$ in the summation produces

$$H = H_0 + \sum_{\sigma} {\sum_{\boldsymbol{k}}}' \mathscr{E}_{\boldsymbol{k}\sigma} \left(n_{\boldsymbol{k}\sigma} + \frac{1}{2} \right). \tag{4.77}$$

In the limit of zero temperature, $T = 0$, an argument similar to the one in Appendix B leads to the following expression for the Helmholtz free energy:

$$\mathcal{F} = H_0 + \frac{1}{2} \sum_{\sigma} {\sum_{\boldsymbol{k}}}' \mathscr{E}_{\boldsymbol{k}\sigma}, \tag{4.78}$$

where $\sigma = +, -$.

By instead defining

$$N_1 = \begin{pmatrix} 2E^A_{\boldsymbol{k}} & 0 & F_{AB} & 0 \\ 0 & 0 & 0 & F_{AB} \\ F_{AB} & 0 & 0 & 0 \\ 0 & F_{AB} & 0 & 2E^B_{-\boldsymbol{k}} \end{pmatrix}, N_2 = \begin{pmatrix} 0 & F & 0 & 2F_{AB} \\ F & 0 & 0 & 0 \\ 0 & 0 & 0 & F \\ 2F_{AB} & 0 & F & 0 \end{pmatrix}, \tag{4.79}$$

we end up with the four distinct branches $D = \mathrm{diag}(\mathscr{E}^+_{\boldsymbol{k},+}, \mathscr{E}^+_{\boldsymbol{k}-}, \mathscr{E}^-_{\boldsymbol{k},+}, \mathscr{E}^-_{\boldsymbol{k},-})$, as in (4.70) and (4.71). Assigning each basis member in (4.51) to these branches we retain the unchanged expression (B.6):

$$\mathcal{F} = H_0 + \frac{1}{4} \sum_{\sigma} {\sum_{\boldsymbol{k}}}' \mathscr{E}_{\boldsymbol{k}\sigma}, \tag{4.80}$$

where $\sigma = 1, 2, 3, 4$.

As a validation of the equality of the total free energy in the two bases, the second terms in (4.78) and (4.80) are investigated numerically by using the explicit expressions given in Ref. [14]. We set $F_A = F_B \equiv F$ in order to make the matrix more comparable to (4.69). In addition we set $U_A = U_B = U_{AB} \equiv U$, and calculate the dimensionless quantity $\frac{\mathcal{F} - H_0}{U}$ on a two-dimensional square lattice. Using 40^2 lattice points we find that the two cases differ by only 0.0014%. This supports the claim that the changes that resulted in (4.68) and (4.69), thereby producing manageable eigenvalues, do

not change the total free energy. This allows for the use of the obtained eigenvalues in the process of minimizing free energy.

In our expression for the energy spectrum (4.70) and (4.71) the unknown densities of particles n_i in the four degenerate single-particle ground states remain to be found. We will find this distribution of densities self-consistently by minimization of free energy, in the one-dimensional and two-dimensional cases in Sections 4.2.3 and 4.2.4, respectively. The result from this final part of the mean field procedure can also serve as a form of validation of our model by comparing the distribution to known results.

4.2.2 Constant term

The limiting case of nearest-neighbor hopping and on-site interactions reduces the constant term (4.54) to

$$\begin{aligned}
H_0 &= H_0^1 + H_0^{MFT} + H_0^{SYM} \\
&= \mathcal{E}^0 N + \frac{N_s}{8} \sum_i n_i^2 \left[U_\downarrow + U_\uparrow + 2U_{\uparrow\downarrow} \right] \\
&\quad + \frac{N_s}{8} \sum_{i \neq j} n_i n_j \left[2(U_\downarrow + U_\uparrow) + 2U_{\uparrow\downarrow} + 2U_{\uparrow\downarrow} e^{i(\gamma_{\boldsymbol{k}^j} - \gamma_{\boldsymbol{k}^i})} \right] \\
&\quad - \frac{1}{4} {\sum_{\boldsymbol{k}}}' \left[2(\Delta\mathcal{E}_{\boldsymbol{k}}^+ + \Delta\mathcal{E}_{\boldsymbol{k}}^-) + \sum_i n_i \left(2(U_\downarrow + U_\uparrow) + 2U_{\uparrow\downarrow} \right) \right] \\
&= \mathcal{E}^0 N + \frac{N_s}{8} \left[U_\downarrow + U_\uparrow + U_{\uparrow\downarrow} \right] n_0^2 + \frac{N_s}{8} \sum_{i \neq j} n_i n_j \left[U_\downarrow + U_\uparrow + 2U_{\uparrow\downarrow} e^{i(\gamma_{\boldsymbol{k}^j} - \gamma_{\boldsymbol{k}^i})} \right] \\
&\quad - \frac{1}{2} {\sum_{\boldsymbol{k}}}' \left[\Delta\mathcal{E}_{\boldsymbol{k}}^+ + \Delta\mathcal{E}_{\boldsymbol{k}}^- + n_0 \left(U_\downarrow + U_\uparrow + U_{\uparrow\downarrow} \right) \right] \\
&= C + \frac{N_s}{8} \sum_{i \neq j} n_i n_j \left[U_\downarrow + U_\uparrow + 2U_{\uparrow\downarrow} e^{i(\gamma_{\boldsymbol{k}^j} - \gamma_{\boldsymbol{k}^i})} \right].
\end{aligned} \tag{4.81}$$

The terms proportional to n_0 will contribute with terms quadratic in boson operators from (4.63) that enter into the matrix elements. Reminding that $\kappa = \frac{N}{N_s}$ and $n_0 = \frac{N_0}{N_s}$, the first of these quadratic terms is

$$-\frac{N_s}{8}\left[U_\downarrow + U_\uparrow + 2U_{\uparrow\downarrow}\right]\cdot\frac{2\kappa^2}{N}\sum_{\boldsymbol{k}\alpha}{}' a^\dagger_{\boldsymbol{k}\alpha}a_{\boldsymbol{k}\alpha} = -\frac{\kappa}{4}\left[U_\downarrow + U_\uparrow + 2U_{\uparrow\downarrow}\right]\sum_{\boldsymbol{k}\alpha}{}' a^\dagger_{\boldsymbol{k}\alpha}a_{\boldsymbol{k}\alpha}, \tag{4.82}$$

while the second one is

$$\frac{1}{2}\sum_{\boldsymbol{k}'}{}'\left[U_\downarrow + U_\uparrow + U_{\uparrow\downarrow}\right]\cdot\frac{\kappa}{N}\sum_{\boldsymbol{k}\alpha}{}' a^\dagger_{\boldsymbol{k}\alpha}a_{\boldsymbol{k}\alpha} = \frac{1}{2}\left[U_\downarrow + U_\uparrow + U_{\uparrow\downarrow}\right]\sum_{\boldsymbol{k}\alpha}{}' a^\dagger_{\boldsymbol{k}\alpha}a_{\boldsymbol{k}\alpha}, \tag{4.83}$$

where we used that there are N_s terms in the sum over $\boldsymbol{k}'$.

The contribution from the n_in_j sum in (4.81) cannot be considered until the distribution of n_i is found. The terms in C do not depend on this distribution, and so it will not influence minimization of free energy carried out in its derivation. Therefore we do not include the terms in (4.82) and (4.83) until the distribution is determined.

4.2.3 One-dimensional chain

Single-particle ground state

We consider the special case of a one-dimensional lattice in the x-direction with lattice parameter a.

$$\begin{aligned}\mathcal{E}^\pm_{\boldsymbol{k}} &= \varepsilon_{\boldsymbol{k}} \pm |s_{\boldsymbol{k}}| = -\sum_{\boldsymbol{\delta}} t_\alpha(\boldsymbol{\delta})e^{-i\boldsymbol{k}\cdot\boldsymbol{\delta}} \pm 2\lambda_R\Big|\sum_j e^{-i\theta_j}\sin(\boldsymbol{k}\cdot\boldsymbol{a}_j)\Big| \\ &= -2t\cos(k_xa) \pm 2\lambda_R|\sin(k_xa)|.\end{aligned} \tag{4.84}$$

The phase factor $e^{i\gamma_{k_x}}$ is now real, i.e.

$$\begin{aligned}e^{i\gamma_{k_x}} &= \frac{s_{k_x}}{|s_{k_x}|} \\ &= \frac{\sin k_xa}{|\sin(k_xa)|} \\ &= \begin{cases}1, & \text{if } 0 < k_x < \frac{\pi}{a} \\ -1, & \text{if } -\frac{\pi}{a} \le k_x < 0,\end{cases}\end{aligned} \tag{4.85}$$

and by consequence the phase γ_{k_x} is given by

$$\gamma_{k_x} = \begin{cases} 0, & \text{if } 0 < k_x < \frac{\pi}{a} \\ \pi, & \text{if } -\frac{\pi}{a} \leq k_x < 0, \end{cases} \tag{4.86}$$

which describes mathematically the obvious fact that any k vector is either parallel or anti-parallel to the positive direction of the only axis available, the x-axis. From now on we drop the subscript on k_x.

The ground state vectors are now $k^1 = -k^2 = \frac{\arctan(\lambda/t)}{a} \equiv k_0$ by minimization of (4.84). The ground state energy is

$$\begin{aligned} \mathcal{E}^0 &= -2t\frac{t}{\sqrt{t^2+\lambda_R^2}} - 2\lambda_R\frac{\lambda_R}{\sqrt{t^2+\lambda_R^2}} \\ &= -2\sqrt{t^2+\lambda_R^2}. \end{aligned} \tag{4.87}$$

Several simplifications can now be made to the matrix elements of (4.44). The sum over k^i reduces to

$$\begin{aligned} \sum_i \frac{n_i}{4}\cos(\gamma_k - \gamma_{k^i}) &= \frac{1}{4}\left[n_1\cos(\gamma_k) + n_2\cos(\gamma_k - \pi)\right] \\ &= \frac{1}{4}\cos(\gamma_k)\left[n_1 - n_2\right], \end{aligned} \tag{4.88}$$

producing

$$E_k^+ = \Delta\mathcal{E}_k^+ + \frac{\kappa}{2}\left[U_\downarrow + U_\uparrow + U_{\uparrow\downarrow}\right] - \frac{1}{2}U_{\uparrow\downarrow}\cos(\gamma_k)\left[n_1 - n_2\right], \tag{4.89}$$

$$E_{-k}^- = \Delta\mathcal{E}_k^- + \frac{\kappa}{2}\left[U_\downarrow + U_\uparrow + U_{\uparrow\downarrow}\right] - \frac{1}{2}U_{\uparrow\downarrow}\cos(\gamma_k)\left[n_1 - n_2\right]. \tag{4.90}$$

E_{-k}^- has been written in this form by using the antisymmetry of $\cos(\gamma_k)$ with respect to k.

The sum over k^i in F produces $\sin(\gamma_k)$ which is zero, since $e^{i\gamma_k}$ is real, consequently

$$F = \frac{\kappa}{2}(U_\downarrow - U_\uparrow). \tag{4.91}$$

The remaining sums over k^i gives

$$\begin{aligned}\sum_i \frac{\sqrt{n_i n_{-i}}}{4} e^{-2i(\gamma_k - \gamma_{k^i})} &= \frac{\sqrt{n_1 n_2}}{4}\left[e^{-2i\gamma_k} + e^{-2i(\gamma_k - \pi)}\right] \\ &= \frac{\sqrt{n_1 n_2}}{2} e^{-2i\gamma_k} \\ &= \frac{\sqrt{n_1 n_2}}{2},\end{aligned} \tag{4.92}$$

where we used that $e^{i\gamma_k} = \pm 1$, and thus

$$G_1 = \frac{\sqrt{n_1 n_2}}{2}\left[U_\downarrow + U_\uparrow\right], \tag{4.93}$$

$$G_2 = \frac{\sqrt{n_1 n_2}}{2}\left[U_\downarrow - U_\uparrow\right]. \tag{4.94}$$

In what follows we set $U_\downarrow = U_\uparrow = U$, meaning that $F = G_2 = 0$. We obtain the four excitation branches

$$\mathscr{E}^+_{k\sigma} = \left[2(E^+_k)^2 - G_1^2 + 2\sigma E^+_k \sqrt{(E^+_k)^2 - G_1^2}\right]^{\frac{1}{2}}, \tag{4.95}$$

$$\mathscr{E}^-_{k\sigma} = \left[2(E^-_{-k})^2 - G_1^2 + 2\sigma E^-_{-k} \sqrt{(E^-_{-k})^2 - G_1^2}\right]^{\frac{1}{2}}. \tag{4.96}$$

Determination of ground state density distribution

The excitation energies (4.95) and (4.96) are used to calculate $\mathcal{F}/U$, where we have introduced the parameter α such that $U_{\uparrow\downarrow} = \alpha U$. The occupation numbers n_1 and n_2 are found numerically by minimization of $\mathcal{F}/U$ using 10^5 lattice points. In addition to computing the sum over k for the excitation branches, we must also include the constant term (4.81). However, the term C is independent of the distribution and may be omitted.

For $\alpha \leq 1$ it is found that condensation occurs to the ground state n_1, i.e. the ground state with positive k vector. Since the choice of positive k-direction is arbitrary, it is evident that condensation to both ground states is equally likely. To put it differently, the direction to which the condensation

spontaneously occurs is defining the positive direction of the k axis in our system. This single-k valued phase is called the plane wave phase.

For $\alpha > 1$ it is found that condensation occurs equally to both ground states. The condensate consists of an equal number of particles with two equal but opposite directed momenta. This leads to a stripy distribution of spin particles in real space, giving rise to the name stripe phase.

Final excitation energy: Plane wave phase

First we consider the plane wave phase:

$$\begin{aligned} n_1 &= n_0 = \kappa - \frac{\kappa}{N} {\sum_{k\alpha}}' a^\dagger_{k\alpha} a_{k\alpha}, \\ n_2 &= 0. \end{aligned} \tag{4.97}$$

The last term in the constant (4.81) vanishes:

$$\frac{N_s}{8} \sum_{i \neq j} n_i n_j \left[2U + 2U_{\uparrow\downarrow} e^{i(\gamma_{kj} - \gamma_{ki})} \right] = 0. \tag{4.98}$$

Using (4.82) and (4.83), the total renormalization of the chemical potential from H_0 s then

$$\begin{aligned} \mu &= \frac{1}{2} \left[2U + U_{\uparrow\downarrow} \right] - \frac{\kappa}{2} \left[U + U_{\uparrow\downarrow} \right] \\ &= U \left(1 - \frac{\kappa}{2} \right) + \frac{1}{2} U_{\uparrow\downarrow} \left(1 - \kappa \right). \end{aligned} \tag{4.99}$$

When inserted into the matrix elements the approximation $n_1 \approx \kappa$ holds, since these terms are already part of expressions quadratic in boson operators. Only $E^{\pm}_{\pm k}$ is now non-zero:

$$E^{\pm}_{\pm k} = \Delta \mathcal{E}^{\pm}_k + \kappa U + \frac{\kappa}{2} U_{\uparrow\downarrow} \left[1 - \cos(\gamma_k) \right], \tag{4.100}$$

$$\begin{aligned} G_1 &= U \sqrt{n_1 n_2} \\ &= 0. \end{aligned} \tag{4.101}$$

We end up with the final result for the energy spectrum on the one-dimensional chain. From (4.95) and (4.96) it is clear that $\mathscr{E}^{+}_{k-}$ and $\mathscr{E}^{-}_{k-}$ vanish, and we are left with the two branches

$$\mathscr{E}^{\pm}_{k+} = 2E^{\pm}_{k} = 2\Delta\mathcal{E}^{\pm}_{k} + 2\kappa U + \kappa U_{\uparrow\downarrow}\left[1 - \cos(\gamma_k)\right]. \tag{4.102}$$

which are plotted in Figure 4.2. $\cos(\gamma_k)$ causes a discontinuity for both branches at $k = 0$, illustrated in Figure 4.3. See Section 5 for a discussion of this suspicious finding.

Final excitation energy: Stripe phase

The stripe phase is characterized by

$$n_1 = n_2 = \frac{\kappa}{2} - \frac{\kappa}{2N}{\sum_{k\alpha}}' a^{\dagger}_{k\alpha}a_{k\alpha}. \tag{4.103}$$

The last term in the constant (4.81) gives rise to the quadratic term:

$$\begin{aligned}\frac{N_s}{8}\sum_{i\neq j} n_i n_j \left[2U + 2U_{\uparrow\downarrow}e^{i(\gamma_{kj}-\gamma_{ki})}\right] &= \frac{N_s}{2}n_1 n_2\left[U - U_{\uparrow\downarrow}\right] \\ &\approx \frac{N_s}{2}\left[U - U_{\uparrow\downarrow}\right]\cdot\left[\frac{\kappa}{2} - \frac{\kappa}{2N}{\sum_{k\alpha}}' a^{\dagger}_{k\alpha}a_{k\alpha}\right] \\ &\to -\frac{1}{4}\left[U - U_{\uparrow\downarrow}\right]{\sum_{k\alpha}}' a^{\dagger}_{k\alpha}a_{k\alpha},\end{aligned} \tag{4.104}$$

where we have used that

$$\sum_{i\neq j} e^{i(\gamma_{kj}-\gamma_{ki})} = e^{i(\pi-0)} + e^{i(0-\pi)} = -2. \tag{4.105}$$

Combined with (4.82) and (4.83), the total renormalization of the chemical potential from H_0 is then

$$\mu = \frac{1}{2}U\left(\frac{3}{2} - \kappa\right) + \frac{1}{2}U_{\uparrow\downarrow}\left(\frac{1}{2} - \kappa\right). \tag{4.106}$$

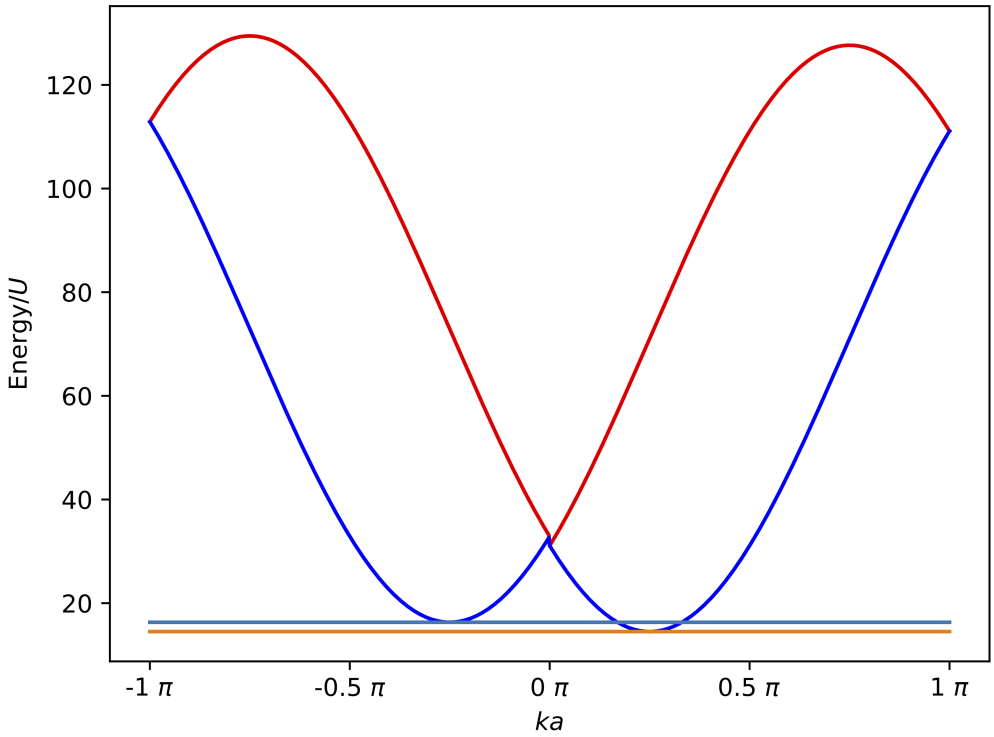

Figure 4.2: Energy divided by interaction strength U in the first Brillouin zone for the plane wave phase $\alpha \leq 1$. Upper energy band $\mathscr{E}^{+}_{k+}$ in red; lower energy band $\mathscr{E}^{\pm}_{k-}$ in blue. The spectrum is almost identical to the single-particle spectrum, except for a lowering of energy by the amount of $2\kappa U_{\uparrow\downarrow}$ for positive k compared with negative k, illustrated by the two horizontal bars. In this plot $\alpha = 1$, and $t/U = \lambda_R/U = 10$.

Keeping in mind that $F = G_2 = 0$ from $U_\downarrow = U_\uparrow = U$, and using $n_0 \approx \kappa$ where terms are already quadratic in boson operators, the remaining matrix elements read

$$\begin{aligned} E^{\pm}_{\pm k} =& \Delta\mathcal{E}^{\pm}_k + \kappa U + \frac{\kappa}{2}U_{\uparrow\downarrow}, \\ G_1 =& \frac{\kappa}{2}U. \end{aligned} \tag{4.107}$$

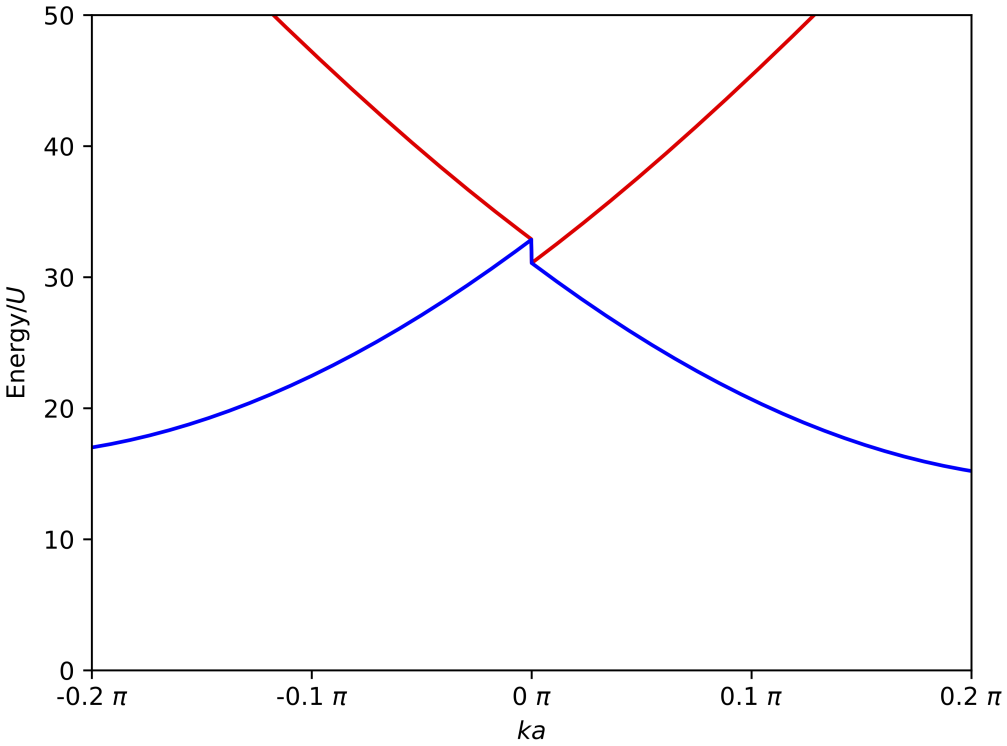

Figure 4.3: The same plot as in Figure 4.2, where the region around $k = 0$ has been enlarged. We observe a discontinuity of the dispersion caused by $e^{i\gamma_k}$ being ill-defined in the origin.

We obtain the four excitation energies, where again $\sigma = \pm 1$,

$$\mathscr{E}^{+}_{k\sigma} = \left[K + \sqrt{R} + \sigma\sqrt{2}\sqrt{H + K\sqrt{R}}\right]^{\frac{1}{2}}, \tag{4.108}$$

$$= \left[2(E^{+}_{k})^2 - |G_1|^2 + 2\sigma E^{+}_{k}\sqrt{(E^{+}_{k})^2 - |G_1|^2}\right]^{\frac{1}{2}},$$

$$\begin{aligned}\mathscr{E}^{-}_{k\sigma} &= \left[K - \sqrt{R} + \sigma\sqrt{2}\sqrt{H - K\sqrt{R}}\right]^{\frac{1}{2}} \\ &= \left[2(E^{-}_{-k})^2 - |G_1|^2 + 2\sigma E^{-}_{-k}\sqrt{(E^{-}_{-k})^2 - |G_1|^2}\right]^{\frac{1}{2}}.\end{aligned} \tag{4.109}$$

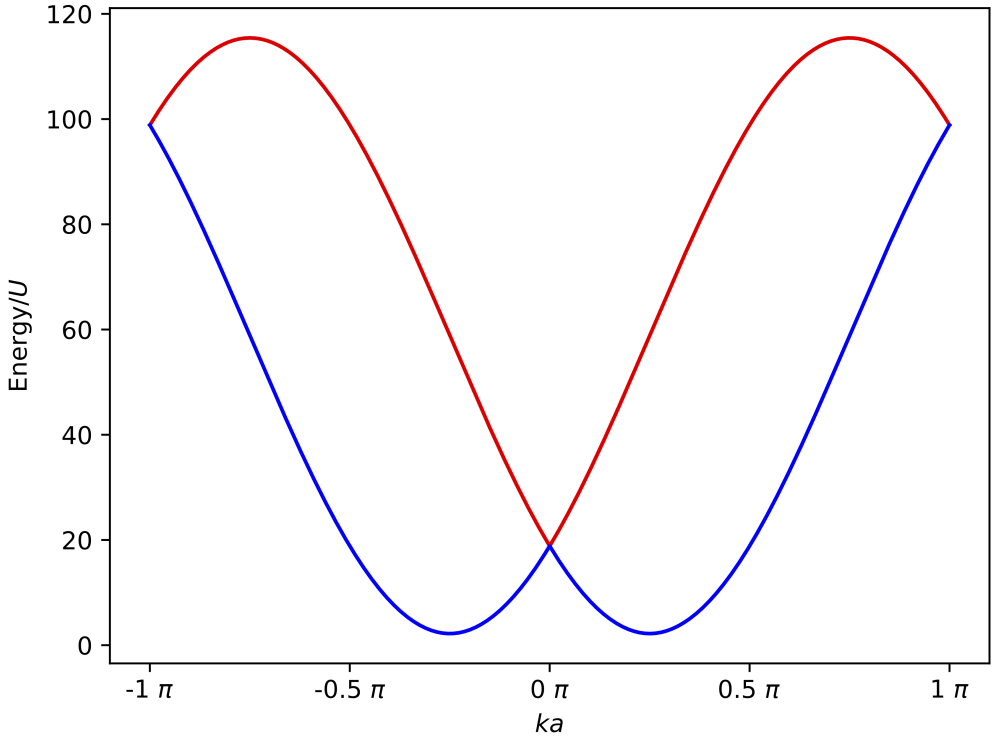

Figure 4.4: Upper excitation branches divided by interaction strength U in the first Brillouin zone for a spin-orbit coupled BEC on a 1D chain in the weak interaction limit, for the stripe phase $\alpha > 1$. $\mathscr{E}^{+}_{k+}$ in red; $\mathscr{E}^{-}_{k+}$ in blue. The spectrum is almost identical to the single-particle spectrum, except for a lowering of energy by a small symmetrically distributed amount. In this plot $\alpha = 1.1$, $\kappa = 1$, and $t/U = \lambda_R/U = 10$.

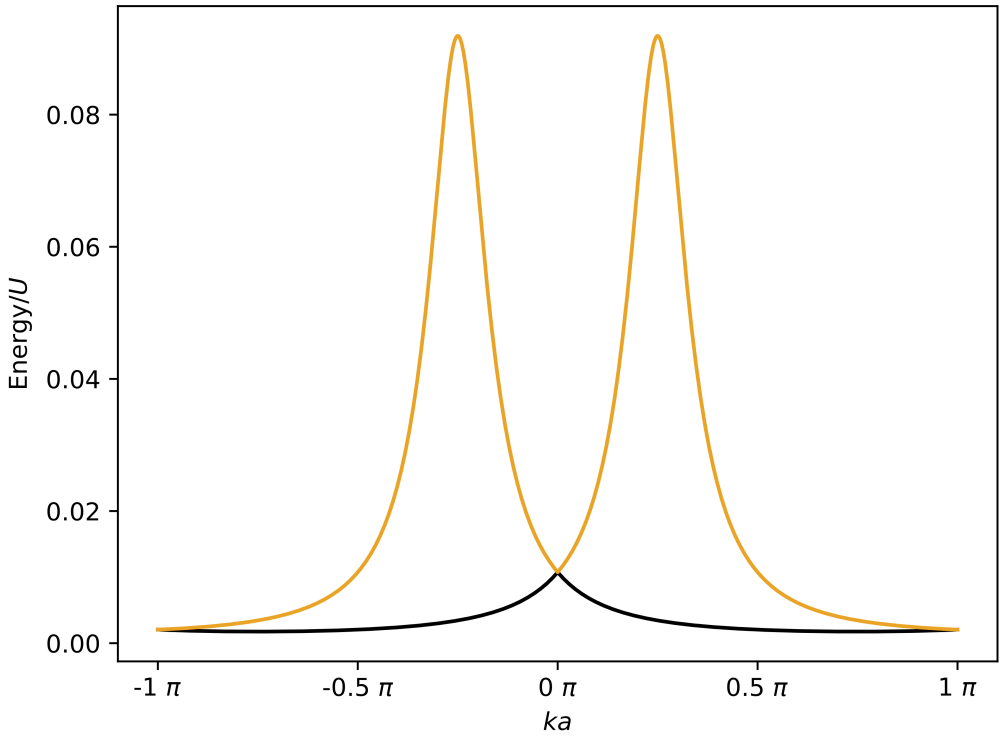

Figure 4.5: Lower excitation branches divided by interaction strength U in the first Brillouin zone for a spin-orbit coupled BEC on a 1D chain in the weak interaction limit, for the stripe phase $\alpha > 1$. $\mathscr{E}^{-}_{k-}$ in orange; $\mathscr{E}^{+}_{k-}$ in black. In this plot $\alpha = 1.1$, $\kappa = 1$, and $t/U = \lambda_R/U = 10$.

The $\sigma = -1$ branches will now be shown to be negligible compared to $\sigma = +1$. The maximum of $\frac{G_1}{E^{\pm}_{\pm k}}$ is

$$\begin{aligned}\max\left(\frac{G_1}{E^{\pm}_{\pm k}}\right) &= \max\left(\frac{\kappa U/2}{\Delta\mathcal{E}^{\pm}_k + \kappa U\left(1+\frac{\alpha}{2}\right)}\right)\\ &= \frac{\kappa U/2}{\min(\Delta\mathcal{E}^{\pm}_k) + \kappa U\left(1+\frac{\alpha}{2}\right)}\\ &= \frac{\kappa U/2}{\kappa U\left(1+\frac{\alpha}{2}\right)}\\ &= \frac{1}{2+\alpha}\\ &< \frac{1}{3},\end{aligned} \tag{4.110}$$

since $\alpha > 1$. Expanding the $\sigma = -1$ branches in $\frac{G_1^2}{(E^{\pm}_{\pm k})^2} < \frac{1}{9}$ to second order yields

$$\begin{aligned}(\mathscr{E}^{\pm}_{k,-1})^2 &= 2(E^{\pm}_{\pm k})^2 - G_1^2 - 2E^{\pm}_{\pm k}\sqrt{(E^{\pm}_{\pm k})^2 - G_1^2}\\ &\approx 2(E^{\pm}_{\pm k})^2 - G_1^2 - 2E^{\pm}_{\pm k}\left(E^{\pm}_{\pm k} - \frac{G_1^2}{2E^{\pm}_{\pm k}} - \frac{G_1^4}{8(E^{\pm}_{\pm k})^3}\right)\\ &= \frac{G_1^4}{4(E^{\pm}_{\pm k})^2}.\end{aligned} \tag{4.111}$$

The $\sigma = -1$ branches are thus maximal when $E^{\pm}_{\pm k}$ are minimal, since G_1 is constant, i.e.

$$\max(\mathscr{E}^{\pm}_{k,-1}) \approx \sqrt{\frac{(\kappa U/4)^4}{4(\kappa U\left(1+\frac{\alpha}{2}\right))^2}} = \frac{\kappa U}{32\left(1+\frac{\alpha}{2}\right)}. \tag{4.112}$$

Expanding the $\sigma = +1$ branches in $\frac{|G_1|^2}{(E^{\pm}_{\pm k})^2} < \frac{1}{9}$ to second order yields

$$\begin{aligned}(\mathscr{E}^{\pm}_{k,+1})^2 &= 2(E^{\pm}_{\pm k})^2 - G_1^2 + 2E^{\pm}_{\pm k}\sqrt{(E^{\pm}_{\pm k})^2 - G_1^2}\\ &\approx 2(E^{\pm}_{\pm k})^2 - G_1^2 + 2E^{\pm}_{\pm k}\left(E^{\pm}_{\pm k} - \frac{G_1^2}{2E^{\pm}_{\pm k}} - \frac{G_1^4}{8(E^{\pm}_{\pm k})^3}\right)\\ &= 4(E^{\pm}_{\pm k})^2 - 2G_1^2 - \frac{G_1^4}{4(E^{\pm}_{\pm k})^2},\end{aligned} \tag{4.113}$$

so that

$$\begin{aligned}\min\left((\mathscr{E}^{\pm}_{k,+1})^2\right) &\approx 4\kappa^2U^2\left(1+\frac{\alpha}{2}\right)^2-2\left(\frac{\kappa}{2}U\right)^2-\left(\frac{\kappa U}{32\left(1+\frac{\alpha}{2}\right)}\right)^2\\ &=\kappa^2U^2\left[4\left(1+\frac{\alpha}{2}\right)^2-\frac{1}{2}-\left(\frac{1}{32\left(1+\frac{\alpha}{2}\right)}\right)^2\right]\\ &=\frac{\kappa^2U^2}{32^2\left(1+\frac{\alpha}{2}\right)^2}\left[64^2\left(1+\frac{\alpha}{2}\right)^4-512\left(1+\frac{\alpha}{2}\right)^2-1\right].\end{aligned} \tag{4.114}$$

The maximum of $E^{\pm}_{k,-1}$ and minimum of $E^{\pm}_{k,+1}$ are both located at $k=\pm k_0$. The smallest possible ratio of the $\sigma=+1$ branches to the $\sigma=-1$ branches is then

$$\begin{aligned}\min\left(\frac{\mathscr{E}^{\pm}_{k,+1}}{\mathscr{E}^{\pm}_{k,-1}}\right)&=\frac{\mathscr{E}^{\pm}_{k_0,+1}}{\mathscr{E}^{\pm}_{k_0,-1}}\\ &\approx\sqrt{64^2\left(1+\frac{\alpha}{2}\right)^4-512\left(1+\frac{\alpha}{2}\right)^2-1}\\ &>139,\end{aligned} \tag{4.115}$$

for $\alpha>1$. It is clear that $\mathscr{E}^{\pm}_{k,-1}<\mathscr{E}^{\pm}_{k,+1}/139$ and therefore negligible.

The weak coupling thus creates two quasi-particle modes that are slight perturbations of the single-particle modes, and two quasi-particle modes of comparably negligible energy.

4.2.4 Two-dimensional square lattice

Single-particle ground state

On the two-dimensional square lattice the single-particle energy becomes

$$\begin{aligned}\mathcal{E}^{\pm}_{\boldsymbol{k}}=\varepsilon_{\boldsymbol{k}}\pm|s_{\boldsymbol{k}}|&=-\sum_{\boldsymbol{\delta}}t(\boldsymbol{\delta})e^{-i\boldsymbol{k}\cdot\boldsymbol{\delta}}\pm2\lambda_R\Big|\sum_j e^{-i\theta_j}\sin(\boldsymbol{k}\cdot\boldsymbol{a}_j)\Big|\\ &=-2t\left[\cos(k_xa)+\cos(k_ya)\right]\pm2\lambda_R\sqrt{\sin^2(k_xa)+\sin^2(k_ya)}.\end{aligned} \tag{4.116}$$

Defining $\tau=\lambda_R/t$ we obtain the following expression for the ground state:

$$\sin(k_x a) = \pm\frac{\tau}{\sqrt{2+\tau^2}} \equiv \pm\beta, \tag{4.117}$$

where we have assumed that $a \neq 0$, $\sin(k_x a) \neq 0$, and $\cos(k_x a) \geq 0$. The last requirement is true in the first Brillouin zone, where we obtain the solutions

$$k_x = \pm\frac{\arcsin(\beta)}{a}. \tag{4.118}$$

The same arguments also yield

$$k_y = \pm\frac{\arcsin(\beta)}{a}. \tag{4.119}$$

The ground state energy is

$$\begin{aligned} \mathcal{E}_0 &= -4t\sqrt{1-\beta^2} - 2\sqrt{2}\lambda_R\beta \\ &= -2\sqrt{2t^2+\lambda_R^2}. \end{aligned} \tag{4.120}$$

We define the ground state $\boldsymbol{k}$-vectors:

$$\begin{aligned} \boldsymbol{k}^1 &= \frac{\arcsin(\beta)}{a}(\hat{\boldsymbol{x}} + \hat{\boldsymbol{y}}), \\ \boldsymbol{k}^2 &= -\frac{\arcsin(\beta)}{a}(\hat{\boldsymbol{x}} - \hat{\boldsymbol{y}}), \\ \boldsymbol{k}^3 &= -\frac{\arcsin(\beta)}{a}(\hat{\boldsymbol{x}} + \hat{\boldsymbol{y}}), \\ \boldsymbol{k}^4 &= \frac{\arcsin(\beta)}{a}(\hat{\boldsymbol{x}} - \hat{\boldsymbol{y}}). \end{aligned} \tag{4.121}$$

On the square lattice the factor $e^{i\gamma_{\boldsymbol{k}}}$ becomes

$$\begin{aligned} e^{i\gamma_{\boldsymbol{k}}} &= \frac{s_{\boldsymbol{k}}}{|s_{\boldsymbol{k}}|} \\ &= \frac{\sum_j e^{-i\theta_j}\sin(\boldsymbol{k}\cdot\boldsymbol{a}_j)}{|\sum_l e^{-i\theta_l}\sin(\boldsymbol{k}\cdot\boldsymbol{a}_l)|} \\ &= \frac{\sin(k_x a) - i\sin(k_y a)}{\sqrt{\sin^2(k_x a)+\sin^2(k_y a)}}, \end{aligned} \tag{4.122}$$

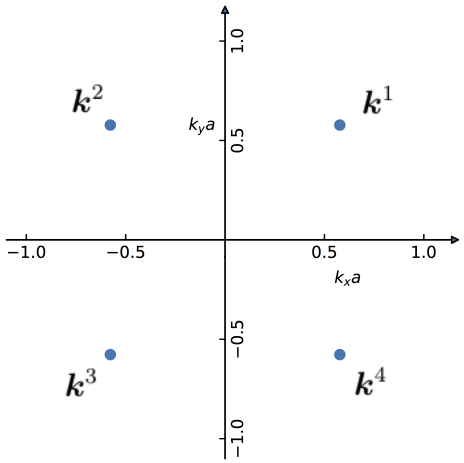

Figure 4.6: The four single-particle ground state $\boldsymbol{k}$ vectors for spin-orbit coupled bosons on a quadratic lattice, with $\tau = \lambda_R/t = 1$.

giving rise to the corresponding ground state phase factors[2]

$$\gamma_{\boldsymbol{k}^1} = -\frac{\pi}{4}, \gamma_{\boldsymbol{k}^2} = -\frac{3\pi}{4}, \gamma_{\boldsymbol{k}^3} = \frac{3\pi}{4}, \gamma_{\boldsymbol{k}^4} = \frac{\pi}{4}. \tag{4.123}$$

We can now consider the sums over $\boldsymbol{k}^i$ in (4.75):

$$\begin{aligned}\sum_i n_i \cos(\gamma_{\boldsymbol{k}} - \gamma_{\boldsymbol{k}^i}) &= n_1 \cos(\gamma_{\boldsymbol{k}} + \frac{\pi}{4}) + n_2 \cos(\gamma_{\boldsymbol{k}} + \frac{3\pi}{4}) \\ &\quad + n_3 \cos(\gamma_{\boldsymbol{k}} - \frac{3\pi}{4}) + n_4 \cos(\gamma_{\boldsymbol{k}} - \frac{\pi}{4}) \\ &= \frac{1}{\sqrt{2}}(n_1 - n_2 - n_3 + n_4)\cos(\gamma_{\boldsymbol{k}}) \\ &\quad - \frac{1}{\sqrt{2}}(n_1 + n_2 - n_3 - n_4)\sin(\gamma_{\boldsymbol{k}}),\end{aligned} \tag{4.124}$$

[2]By defining the factor $s_{\boldsymbol{k}}/|s_{\boldsymbol{k}}|$ differently in Section 3.2.3, e.g. $-ie^{i\gamma_{\boldsymbol{k}}}$, the phase factors would have corresponded to the polar angle of the ground state $\boldsymbol{k}$ vectors, as is done in Ref. [28]. Obviously, this does not affect the physics.

$$\begin{aligned}\sum_i n_i \sin(\gamma_{\boldsymbol{k}} - \gamma_{\boldsymbol{k}^i}) &= n_1 \sin(\gamma_{\boldsymbol{k}} + \frac{\pi}{4}) + n_2 \sin(\gamma_{\boldsymbol{k}} + \frac{3\pi}{4}) \\ &\quad + n_3 \sin(\gamma_{\boldsymbol{k}} - \frac{3\pi}{4}) + n_4 \sin(\gamma_{\boldsymbol{k}} - \frac{\pi}{4}) \\ &= \frac{1}{\sqrt{2}}(n_1 + n_2 - n_3 - n_4)\cos(\gamma_{\boldsymbol{k}}) \\ &\quad + \frac{1}{\sqrt{2}}(n_1 - n_2 - n_3 + n_4)\sin(\gamma_{\boldsymbol{k}}).\end{aligned} \tag{4.125}$$

$$\begin{aligned}\sum_i \sqrt{n_i n_{-i}} e^{2i\gamma_{\boldsymbol{k}^i}} &= \sqrt{n_1 n_3}(-i) + \sqrt{n_2 n_4} i + \sqrt{n_1 n_3}(-i) + \sqrt{n_2 n_4} i \\ &= -2i(\sqrt{n_1 n_3} - \sqrt{n_2 n_4}).\end{aligned} \tag{4.126}$$

We thus obtain the following matrix elements:

$$\begin{aligned}E^{\pm}_{\pm\boldsymbol{k}} = \Delta\mathcal{E}^{\pm}_{\boldsymbol{k}} + \frac{\kappa}{2}\left[U_\downarrow + U_\uparrow + U_{\uparrow\downarrow}\right] - \frac{1}{2\sqrt{2}} U_{\uparrow\downarrow} \left[(n_1 - n_2 - n_3 + n_4)\cos(\gamma_{\boldsymbol{k}})\right. \\ \left. - (n_1 + n_2 - n_3 - n_4)\sin(\gamma_{\boldsymbol{k}})\right],\end{aligned} \tag{4.127}$$

$$\begin{aligned}F = \frac{\kappa}{2}(U_\downarrow - U_\uparrow) + \frac{i}{2\sqrt{2}} U_{\uparrow\downarrow} \left[(n_1 + n_2 - n_3 - n_4)\cos(\gamma_{\boldsymbol{k}})\right. \\ \left. + (n_1 - n_2 - n_3 + n_4)\sin(\gamma_{\boldsymbol{k}})\right],\end{aligned} \tag{4.128}$$

$$G_1 = \frac{1}{2} U_\downarrow (\sqrt{n_1 n_3} + \sqrt{n_2 n_4}) - \frac{1}{2} i U_\uparrow e^{-2i\gamma_{\boldsymbol{k}}} (\sqrt{n_1 n_3} - \sqrt{n_2 n_4}), \tag{4.129}$$

$$G_2 = \frac{1}{2} U_\downarrow (\sqrt{n_1 n_3} + \sqrt{n_2 n_4}) + \frac{1}{2} i U_\uparrow e^{-2i\gamma_{\boldsymbol{k}}} (\sqrt{n_1 n_3} - \sqrt{n_2 n_4}). \tag{4.130}$$

Determination of ground state density distribution

For the numerical determination of the density parameters $n_1, ..., n_4$ we again set $U_\downarrow = U_\uparrow = U$, and define α such that $U_{\uparrow\downarrow} = \alpha U$. By the using the matrix elements (4.127) – (4.130) and 10^{12} lattice points, $\mathcal{F}/U$ is calculated and minimized with respect to the density parameters. As in the 1D case the

term $H_0 - C$ is included in this calculation. The result is similar to that of the one-dimensional case.

For $\alpha < 1$ condensation occurs to n_3. However, by renaming the x and y axes any of the ground state vectors could be represented by n_3, so that condensation to any one of the four ground state vectors is equally likely. This phase is referred to as the plane wave phase.

For $\alpha \geq 1$ condensation occurs to n_2 and n_4. This is the plane wave phase where condensation occurs to two opposite momenta. Again, condensation to the ground state vectors represented by n_1 and n_3 is equally likely by a redefinition of the x and y axes conserving right-handedness.

Final excitation energy: Plane wave phase

The plane wave phase is characterized by

$$\begin{aligned} n_1 = n_2 = n_4 = 0, \\ n_3 = n_0 = \kappa - \frac{\kappa}{N} {\sum_{\boldsymbol{k}\alpha}}' a^\dagger_{\boldsymbol{k}\alpha} a_{\boldsymbol{k}\alpha}. \end{aligned} \tag{4.131}$$

The last term in the constant (4.81) vanishes:

$$\frac{N_s}{8} \sum_{i \neq j} n_i n_j \left[2U + 2U_{\uparrow\downarrow} e^{i(\gamma_{\boldsymbol{k}^j} - \gamma_{\boldsymbol{k}^i})} \right] = 0. \tag{4.132}$$

Using (4.82) and (4.83), the total renormalization of the chemical potential from H_0 is then

$$\mu = U \left(1 - \frac{\kappa}{2} \right) + \frac{1}{2} U_{\uparrow\downarrow} (1 - \kappa) . \tag{4.133}$$

The resulting matrix elements, with $U_\downarrow = U_\uparrow = U$, again using the approximation $n_0 \approx \kappa$, are

$$E^{\pm}_{\pm \boldsymbol{k}} = \Delta \mathcal{E}^{\pm}_{\boldsymbol{k}} + \kappa U + \frac{\kappa}{2} U_{\uparrow\downarrow} + \frac{\kappa}{2\sqrt{2}} U_{\uparrow\downarrow} \left[\cos(\gamma_{\boldsymbol{k}}) - \sin(\gamma_{\boldsymbol{k}}) \right] , \tag{4.134}$$

$$F = -\frac{i\kappa}{2\sqrt{2}} U_{\uparrow\downarrow} \left[\cos(\gamma_{\boldsymbol{k}}) + \sin(\gamma_{\boldsymbol{k}}) \right] , \tag{4.135}$$

$$G_1 = G_2 = 0. \tag{4.136}$$

The four excitation branches for the plane wave phase are thus

$$\mathscr{E}^{+}_{\boldsymbol{k}\sigma} = \left[2(E^{+}_{\boldsymbol{k}})^2 + |F|^2 + 2\sigma E^{+}_{\boldsymbol{k}}\sqrt{(E^{+}_{\boldsymbol{k}})^2 + |F|^2}\right]^{\frac{1}{2}}, \tag{4.137}$$

$$\mathscr{E}^{-}_{\boldsymbol{k}\sigma} = \left[2(E^{-}_{-\boldsymbol{k}})^2 + |F|^2 + 2\sigma E^{-}_{-\boldsymbol{k}}\sqrt{(E^{-}_{-\boldsymbol{k}})^2 + |F|^2}\right]^{\frac{1}{2}}, \tag{4.138}$$

for $\sigma = +, -$. It is seen numerically that the minima of $\mathscr{E}^{-}_{\boldsymbol{k}+}$ corresponding to $\boldsymbol{k}^1$ and $\boldsymbol{k}^3$ are found at the same $\boldsymbol{k}$ values while the minima corresponding to $\boldsymbol{k}^2$ and $\boldsymbol{k}^4$ are displaced slightly in negative x- and y-direction.

The weak coupling thus creates two quasi-particle modes that are slight perturbations of the single-particle modes, and two quasi-particle modes of comparably negligible energy, none being symmetric in $\boldsymbol{k}$.

Final excitation energy: Stripe phase

In the stripe phase we have that

$$\begin{aligned} &n_1 = n_3 = 0, \\ &n_2 = n_4 = \frac{n_0}{2} = \frac{\kappa}{2} - \frac{\kappa}{2N}{\sum_{\boldsymbol{k}\alpha}}' a^{\dagger}_{\boldsymbol{k}\alpha} a_{\boldsymbol{k}\alpha}. \end{aligned} \tag{4.139}$$

The last term in the constant (4.81) contributes with a term quadratic in boson operators:

$$\begin{aligned} &\frac{N_s}{8}\sum_{i\neq j} n_i n_j \left[2U + 2U_{\uparrow\downarrow} e^{i(\gamma_{\boldsymbol{k}^j} - \gamma_{\boldsymbol{k}^i})}\right] \\ &= \frac{N_s}{8} n_2 n_4 \left[4U + 2U_{\uparrow\downarrow}\left(e^{i(\gamma_{\boldsymbol{k}^2} - \gamma_{\boldsymbol{k}^4})} + e^{i(\gamma_{\boldsymbol{k}^4} - \gamma_{\boldsymbol{k}^2})}\right)\right] \\ &= \frac{N_s}{8} n_2 n_4 \left[4U + 4U_{\uparrow\downarrow}\cos\left(\frac{\pi}{4} + \frac{3\pi}{4}\right)\right] \\ &= \frac{N_s}{2} n_0^2 \left[U - U_{\uparrow\downarrow}\right] \\ &\to -\frac{N_s}{2}\left[U - U_{\uparrow\downarrow}\right] \cdot \frac{\kappa^2}{2N}{\sum_{\boldsymbol{k}\alpha}}' a^{\dagger}_{\boldsymbol{k}\alpha} a_{\boldsymbol{k}\alpha} \\ &= -\frac{1}{4}\left[U - U_{\uparrow\downarrow}\right]{\sum_{\boldsymbol{k}\alpha}}' a^{\dagger}_{\boldsymbol{k}\alpha} a_{\boldsymbol{k}\alpha}. \end{aligned} \tag{4.140}$$

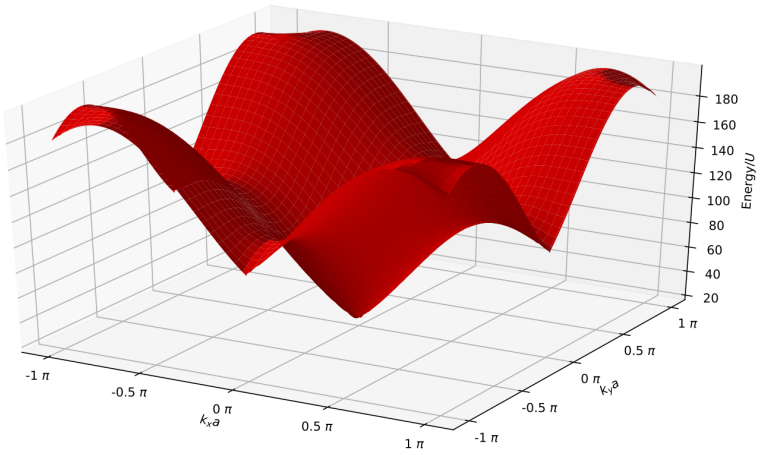

(a) $\mathscr{E}^{+}_{\boldsymbol{k}+}$ branch.

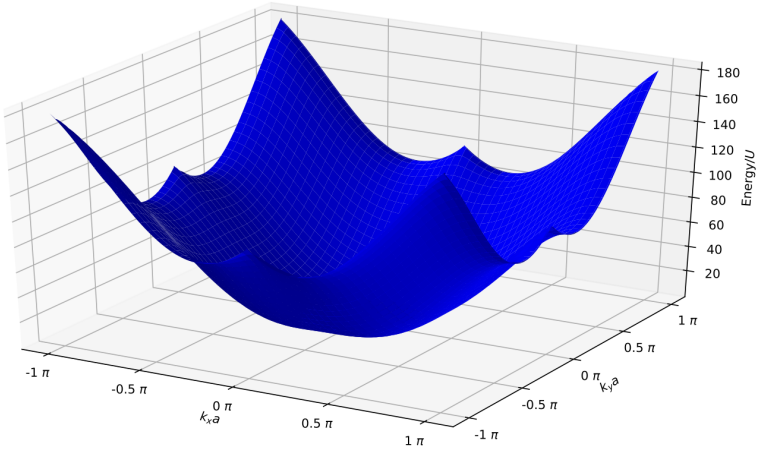

(b) $\mathscr{E}^{-}_{\boldsymbol{k}+}$ branch.

Figure 4.7: Upper branches of the excitation spectrum divided by interaction strength U in the first Brillouin zone for the plane wave phase $\alpha < 1$. In this plot $\alpha = 0.9$, $t/U = \lambda_R/U = 10$, $\kappa = 1$, and $9 \cdot 10^6$ lattice points.

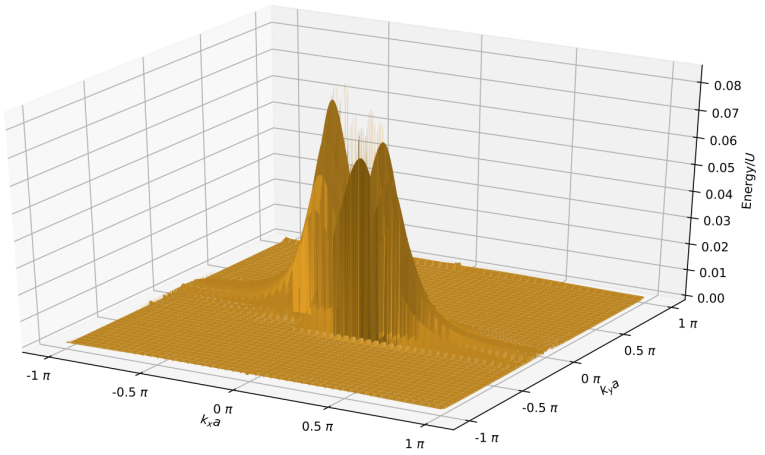

(a) $\mathscr{E}^{-}_{\boldsymbol{k}_-}$ branch.

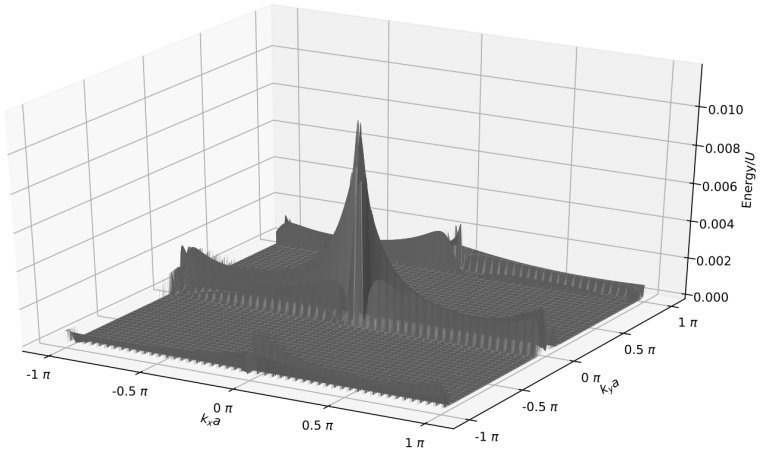

(b) $\mathscr{E}^{+}_{\boldsymbol{k}_-}$ branch.

Figure 4.8: Lower branches of the excitation spectrum divided by interaction strength U in the first Brillouin zone for the plane wave phase $\alpha < 1$. In this plot $\alpha = 0.9$, $t/U = \lambda_R/U = 10$, $\kappa = 1$, and $9 \cdot 10^6$ lattice points.

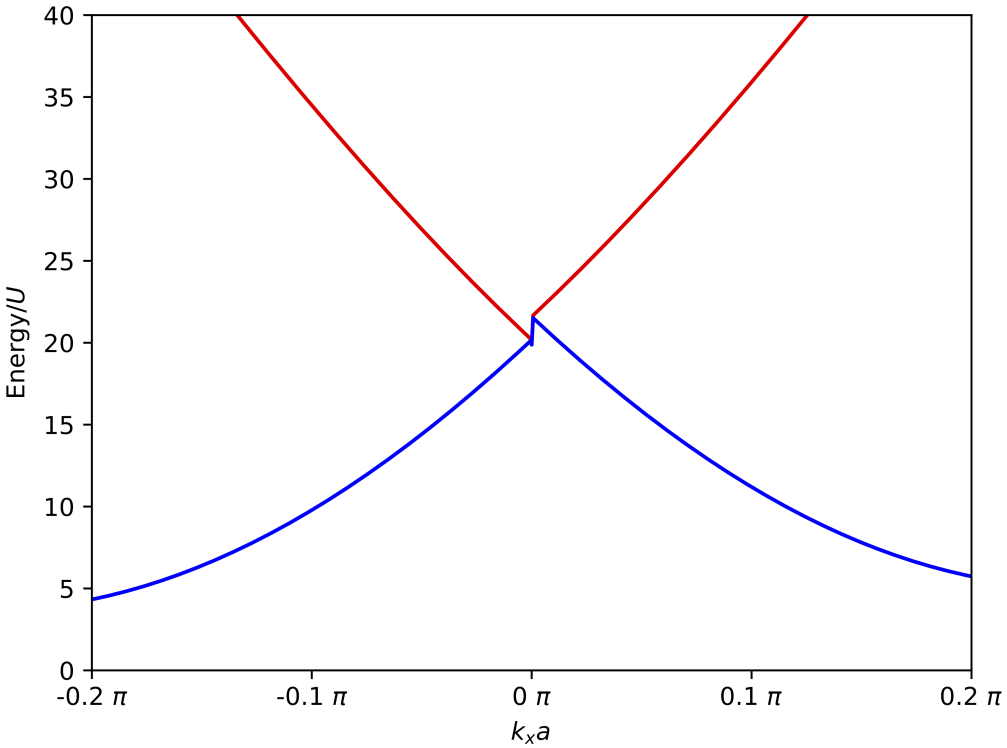

Figure 4.9: The same plot as in Figure 4.7, for $k_y = 0$ and where the region around $k_x = 0$ has been enlarged. $\mathscr{E}^{+}_{\boldsymbol{k}+}$ branch in red; $\mathscr{E}^{-}_{\boldsymbol{k}+}$ branch in blue. As in the 1D plane wave phase, we observe a discontinuity of the dispersion caused by $e^{i\gamma_{\boldsymbol{k}}}$ being ill-defined in the origin.

Combined with (4.82) and (4.83), the total renormalization of the chemical potential from H_0 is then

$$\mu = \frac{1}{2}U\left(\frac{3}{2} - \kappa\right) + \frac{1}{2}U_{\uparrow\downarrow}\left(\frac{1}{2} - \kappa\right). \tag{4.141}$$

The matrix elements are now

$$E^{\pm}_{\pm\boldsymbol{k}} = \Delta\mathcal{E}^{\pm}_{\boldsymbol{k}} + \kappa\left[U + \frac{U_{\uparrow\downarrow}}{2}\right], \tag{4.142}$$

$$F = 0, \tag{4.143}$$

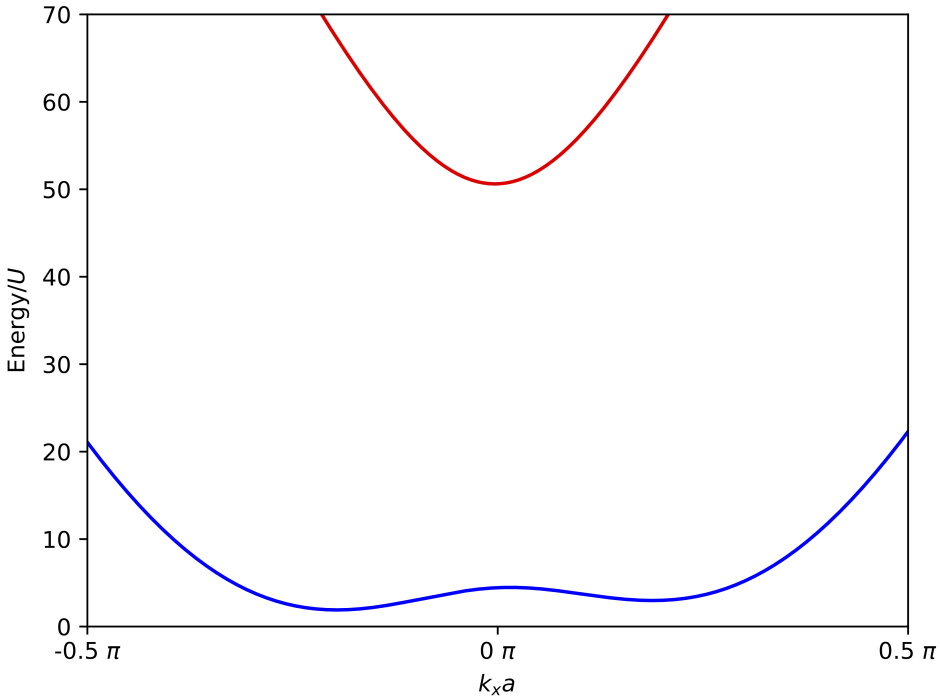

Figure 4.10: $\mathscr{E}^{+}_{\boldsymbol{k}+}$ branch and $\mathscr{E}^{-}_{\boldsymbol{k}+}$ branch in red and blue, respectively, with constant $k_y = (\boldsymbol{k}^3)_y$ in the asymmetric plane wave phase. In this plot $\alpha = 0.9$, and $t/U = \lambda_R/U = 10$.

$$G_1 = \frac{\kappa U}{4}\left(1 + ie^{-2i\gamma_{\boldsymbol{k}}}\right), \tag{4.144}$$

$$G_2 = \frac{\kappa U}{4}\left(1 - ie^{-2i\gamma_{\boldsymbol{k}}}\right). \tag{4.145}$$

The resulting expressions for the excitation branches cannot be readily simplified, so we keep the form of (4.70) and (4.71) with the following quantities:

$$K = (E^{+}_{\boldsymbol{k}})^2 + (E^{-}_{-\boldsymbol{k}})^2 - |G_1|^2 - 2|G_2|^2, \tag{4.146}$$

$$R = ((E^{+}_{\boldsymbol{k}} + E^{-}_{-\boldsymbol{k}})^2 - 4|G_2|^2)(E^{+}_{\boldsymbol{k}} - E^{-}_{-\boldsymbol{k}})^2, \tag{4.147}$$

$$\begin{aligned} H = (E^+_{\boldsymbol{k}})^4 + (E^-_{-\boldsymbol{k}})^4 + 2|G_2|^2 \left[2E^+_{\boldsymbol{k}} E^-_{-\boldsymbol{k}} - 3|G_2|^2\right] \\ - \left[(E^+_{\boldsymbol{k}})^2 + (E^-_{-\boldsymbol{k}})^2 - 2|G_2|^2\right] \cdot \left[|G_1|^2 + 4|G_2|^2\right] . \end{aligned} \tag{4.148}$$

As in the plane wave phase, the $\mathscr{E}^+_{\boldsymbol{k}+}$ and $\mathscr{E}^-_{\boldsymbol{k}+}$ modes are seen to be almost identical to the single-particle spectrum, the latter having four degenerate global minima at the same values of $\boldsymbol{k}$. The stripe phase thus contains two quasi-particle modes that are slight perturbations of the single-particle modes, and two quasi-particle modes of comparably negligible energy that are all symmetric in $\boldsymbol{k}$.

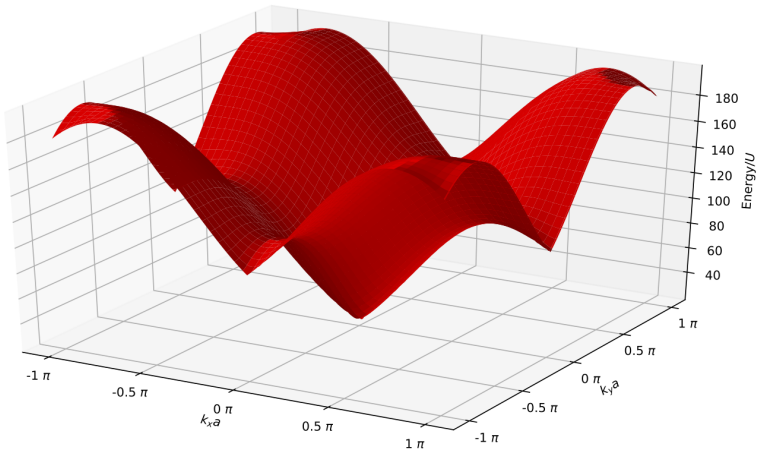

(a) $\mathscr{E}^{+}_{\boldsymbol{k}+}$ branch.

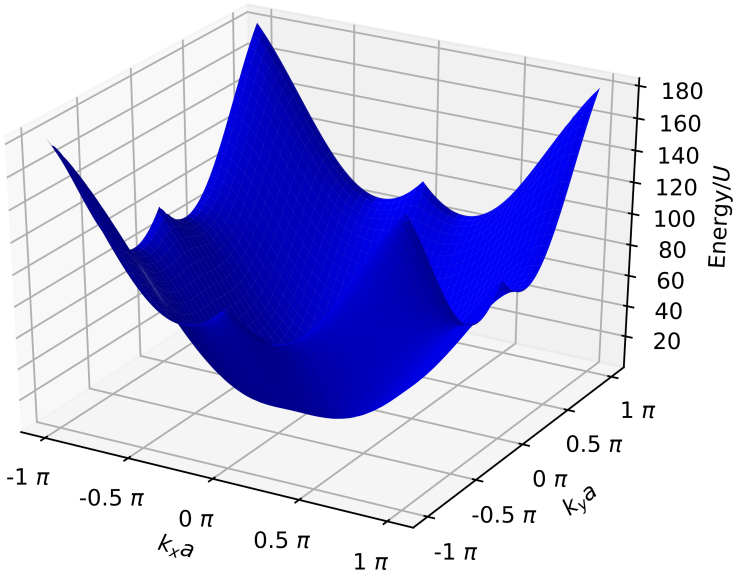

(b) $\mathscr{E}^{-}_{\boldsymbol{k}+}$ branch.

Figure 4.11: Upper branches of the excitation spectrum divided by interaction strength U in the first Brillouin zone for the stripe phase $\alpha \geq 1$. In this plot $\alpha = 1$, $t/U = \lambda_R/U = 10$, $\kappa = 1$, and $9 \cdot 10^6$ lattice points.

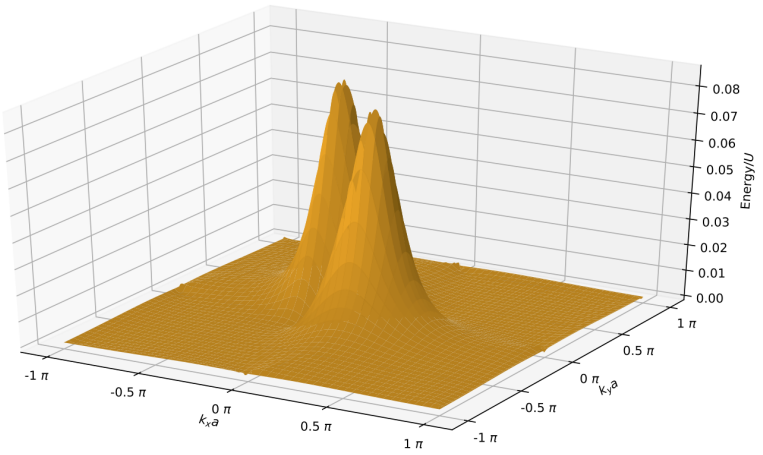

(a) $\mathscr{E}^{-}_{\boldsymbol{k}_-}$ branch.

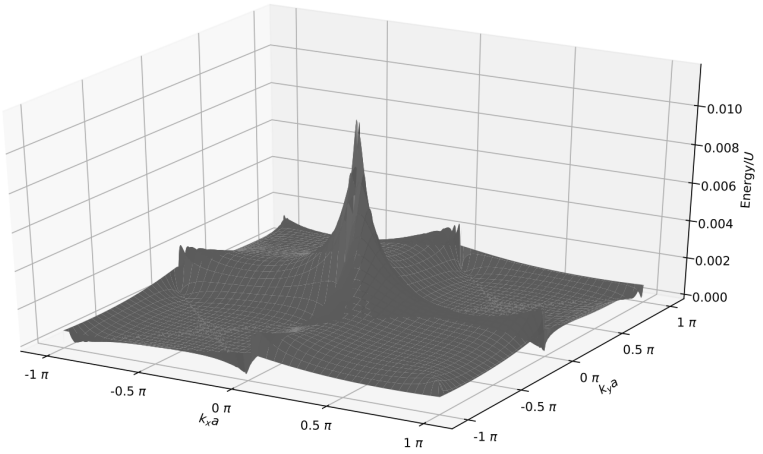

(b) $\mathscr{E}^{+}_{\boldsymbol{k}_-}$ branch.

Figure 4.12: Lower branches of the excitation spectrum divided by interaction strength U in the first Brillouin zone for the stripe phase $\alpha \geq 1$. In this plot $\alpha = 1$, $t/U = \lambda_R/U = 10$, $\kappa = 1$, and $9 \cdot 10^6$ lattice points.

5. Discussion

α dependency

Most of the verifiable content is found in Sections 4.2.3 and 4.2.4 where the model is applied to a one-dimensional chain and a two-dimensional quadratic lattice. In both of these cases the minimization of free energy showed that the phases to which the system condensed, namely the plane wave and stripe phases, had a dependency on the $\alpha = U_{\uparrow\downarrow}/U$ parameter that agreed with literature. This was described for a one-dimensional chain in Ref. [29] and for the a two-dimensional quadratic lattice in Refs. [13] and [30]. Both situations, and many other topical subjects are described in the extensive review on spin-orbit coupling in optical lattices in Ref. [28].

In the process of numerically investigating the α dependency of the ground state distribution, it was observed that the term $H_0 - C$ itself was responsible for the $\alpha = 1$ watershed between the two phases. This term written out explicitly for the two-dimensional square lattice is

$$\begin{aligned} \frac{UN_s}{4} \sum_{i \neq j} n_i n_j \left[1 + \alpha e^{i(\gamma_{\boldsymbol{k}^j} - \gamma_{\boldsymbol{k}^i})}\right] &= \frac{UN_s}{2} \sum_{i<j} n_i n_j \left[1 + \alpha \cos(\gamma_{\boldsymbol{k}^j} - \gamma_{\boldsymbol{k}^i})\right] \\ &= \frac{UN_s}{2} \left(n_1 n_3 + n_2 n_4\right) \left[1 - \alpha\right]. \end{aligned} \tag{5.1}$$

Upon minimizing free energy it is clear that for $\alpha > 1$ the term $(n_1 n_3 + n_2 n_4)$ must be maximized subject to constraint $\sum_i n_i = n_0$. This leads to the stripe phase $n_1 = n_3 = n_0/2$, $n_2 = n_4 = 0$, or $n_2 = n_4 = n_0/2$, $n_1 = n_3 = 0$. For $\alpha < 1$ the term $(n_1 n_3 + n_2 n_4)$ must be minimized which leads to $n_i = n_0$ for one of the ground states while the other densities vanish. The sum over the excitations lead to one of the equivalent cases being chosen, but this choice is arbitrary since it merely depends on the definition of axes. Thus the constant term resulting from pure ground state interactions seem to be responsible for

the widely accepted result while the validation of excitation branches is more obscure, and more research is needed to confirm or repudiate the excitation spectrum.

Discontinuous dispersion relations

In the one- and two-dimensional cases of the plane wave phase there was a distinct discontinuity in the two highest excitation branches at the origin, illustrated in Figures 4.3 and 4.9. In both cases they are caused by the discontinuous functions $\cos(\gamma_{\boldsymbol{k}})$ and $\sin(\gamma_{\boldsymbol{k}})$ in $E^{\pm}_{\pm\boldsymbol{k}}$, see (4.100) and (4.134), causing a broken Dirac point at $\boldsymbol{k} = 0$. These problematic parts do not cause a discontinuity in the stripe phases, since in the equivalent expressions they vanish. We also observe that in both instances the discontinuous terms are proportional to $U_{\uparrow\downarrow}$. Essentially, the discontinuity indicate that our model is unable to describe $\boldsymbol{k} = 0$ modes, since both their energy and group velocity $\boldsymbol{v}_g = \partial\mathscr{E}/\partial\boldsymbol{k}$ are ill-defined.

The mathematical root of the problem is that the phase factor $e^{i\gamma_{\boldsymbol{k}}} = s_{\boldsymbol{k}}/|s_{\boldsymbol{k}}|$ is not defined for $\boldsymbol{k} = 0$. Moreover, this only causes problems in terms proportional to $U_{\uparrow\downarrow}$, and when the condensate is in the asymmetric plane wave phase. What this tells us physically is that there is a significant pathology present when our model is applied on a spin-orbit coupled BEC of finite inter-spin interactions $U_{\uparrow\downarrow}$ in the plane wave phase, where the helicity basis contains a phase factor $e^{i\gamma_{\boldsymbol{k}}}$ which is not defined for $\boldsymbol{k} = 0$.

A second possibility is that there is something fundamentally wrong with the mean-field approach used in this thesis. The assumption that the number of particles in a given ground state i, N_i, is much greater that one (4.8) is the basis for the subsequent treatment. We later obtain that $n_i = 0$ for some i, which might seem contradictory. However, it was assessed that since $n_i = N_i/N_s$, where the number of lattice sites N_s is macroscopic, the physical situation of $n_i = 0$ does not necessarily exclude $N_i >> 1$. If e.g. $N_i = 20$, $n_i = 0$ still holds physically.

The no-SOC limit

An ideal way of verifying our results would be to consider the excitation spectrum in the no-SOC limit and compare with known results. These results could be the excitation spectrum of an interacting two-component BEC as in Ref. [14], or further simplifying to a one-component BEC and the standard

result in e.g. Ref. [26]. The latter result reads

$$\mathscr{E}_{\boldsymbol{k}} = \sqrt{\varepsilon_{\boldsymbol{k}}\left(\varepsilon_{\boldsymbol{k}} + 2Un_0\right)}, \tag{5.2}$$

for both spin states. In order to obtain a comparable result we set $\mathcal{E}_0 = 0$, $U_\downarrow = U_\uparrow$, energy offset $T = 0$, and $U_{\uparrow\downarrow} = 0$. Using (4.70) and (4.71) without using (4.63), i.e. keeping n_0 instead of κ, we obtain in the limit of on-site interactions and nearest-neighbor hopping the four excitation energies

$$\mathscr{E}^{\pm}_{\boldsymbol{k}\sigma} = \Bigg[2(\varepsilon_{\boldsymbol{k}} \pm |s_{\boldsymbol{k}}| + n_0U)^2 - |U\sum_i \frac{\sqrt{n_i n_{-i}}}{2}\left[1 + e^{-2i(\gamma_{\boldsymbol{k}} - \gamma_{\boldsymbol{k}^i})}\right]|^2 + 2\sigma(\varepsilon_{\boldsymbol{k}} \pm |s_{\boldsymbol{k}}| + n_0U)\sqrt{(\varepsilon_{\boldsymbol{k}} \pm |s_{\boldsymbol{k}}| + n_0U)^2 - |U\sum_i \frac{\sqrt{n_i n_{-i}}}{2}\left[1 + e^{-2i(\gamma_{\boldsymbol{k}} - \gamma_{\boldsymbol{k}^i})}\right]|^2}\Bigg]^{\frac{1}{2}}, \tag{5.3}$$

where $\sigma = \pm 1$. An attempt at a no-SOC limit would be to set $\lambda_R = 0$ leading to $s_{\boldsymbol{k}} = 0$, and setting $\sum_i \sqrt{n_i n_{-i}} = n_0$. However, the limiting value of the phase factor $e^{i\gamma_{\boldsymbol{k}}} = s_{\boldsymbol{k}}/|s_{\boldsymbol{k}}|$ does not exist. $s_{\boldsymbol{k}}$ was in fact assumed to be non-zero upon defining the single-particle eigenvectors in (3.42).

The limit of $\lambda_R = 0$ must hence be considered in the spin basis, before applying the mean-field procedure using the non-degenerate $\boldsymbol{k} = 0$ ground state. This treatment is the same as in Ref. [14] with components A and B representing spin up and spin down. In order to make the SOC and no-SOC matrices comparable, we must set the matrix elements $F_A = F_B \equiv F$ in Ref. [14]. The equality of the inter-spin potential means that the inter-component also must be equal, and hence that the densities of particles must be equal, $n_A = n_B = \kappa/2$, using the notation for the total density of particles κ from our thesis. With $t_A = t_B$, and considering the one-dimensional chain with lattice parameter a, we obtain $\epsilon^A_k = \epsilon^B_k = 4t\sin(ka/2)$.

The excitation spectrum in the $\lambda_R = 0$ limit is then found in two separate cases: using the unchanged matrix (4.76), and the changed matrix (4.79). In the situation under consideration, both spectra contain two distinct branches. In fact, upon plotting these it is clear that the upper branch of the changed matrix equals the sum of both branches of the unchanged matrix. The role of the lower branch of the changed matrix is more uncertain to the author. It does not seem to equal the difference between the two branches. See figure 5.1.

This finding in the no-SOC case might suggest that the upper branches found in Sections 4.2.3 and 4.2.4 are in fact the sums of pairs of branches in

the corresponding unchanged matrix, the spectrum of which was too complicated to study.

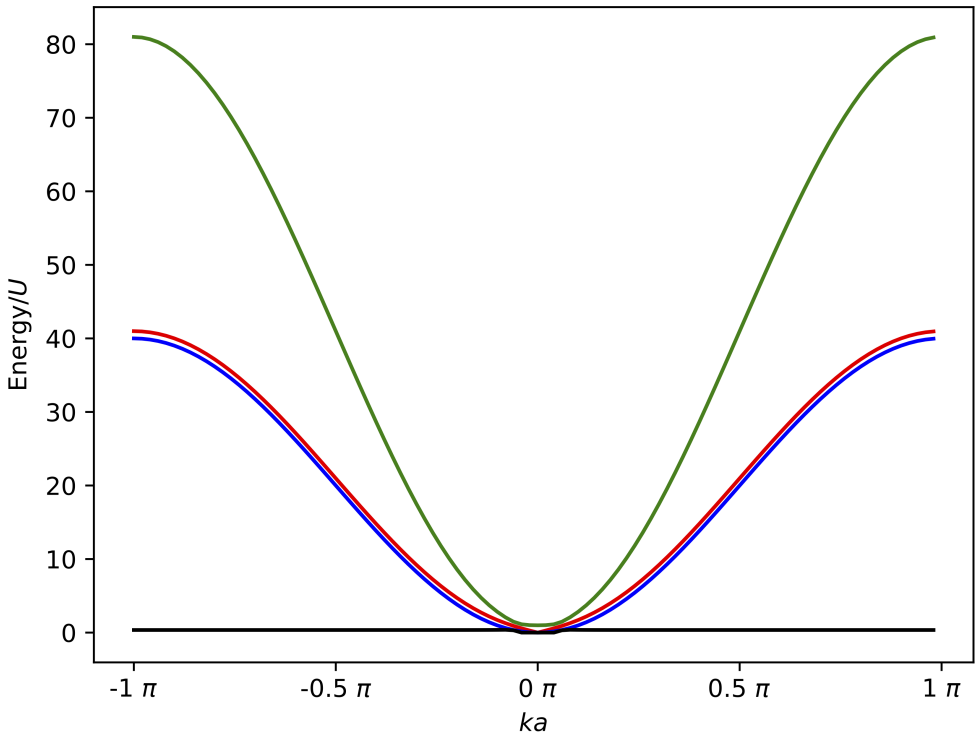

Figure 5.1: Energy divided by interaction strength U in the first Brillouin zone in the $\lambda_R = 0$ case. The upper and lower branch of the spectrum from the unchanged matrix are represented in red and blue, respectively. The upper branch and lower branch of the spectrum from the changed matrix are represented in green and black, respectively. We have set $\alpha = \kappa = 1$, and $t/U = 10$.

Absence of Zeeman fields

Zeeman fields perpendicular to the lattice are not included in this treatment. In the two-dimensional case these are terms in the Hamiltonian proportional to σ_z. These terms are commonly included in literature on synthetic SOC.

Zeeman fields causes Zeeman splitting, i.e. a gap between the two excitation branches. One of the synthetic spin states is energetically favored over the other, making the Zeeman fields play the role of a synthetic magnetic field in the synthetic spin system. This is achieved experimentally by having the SOC lasers pumping more particles into one of the spin states than the other [31]. The SOC Hamiltonian that accounts for the complete interaction with lasers that create SOC is called Raman coupling, and is equivalent to having equal amounts of Dresselhaus og Rashba coupling [32]. The standard long-wavelength limit result from Raman coupling is thus that SOC creates phonon and gap branches in a spectrum that is either symmetric or asymmetric in $\boldsymbol{k}$, depending on α [32]. Ignoring the Zeeman field in this treatment leads to a conservation of the ungapped Dirac points at the origin as seen in the one-dimensional case in plots 4.2 and 4.4. Consequently, there are relatively few analytical results in literature that are directly comparable to our excitation spectra.

Low-energy modes

The unorthodox manipulations performed to obtain the matrix (4.67) led to manageable eigenvalues. It was subsequently demonstrated that this procedure did not change the total free energy of the system. It did, however, lead to strange low energy modes that even vanished in the one-dimensional plane wave phase. The physical implications of these modes remain puzzling to the author. In a matrix of diagonal elements symmetric in $\boldsymbol{k}$ pairs of eigenvalues would merge into one by a change of variable $-\boldsymbol{k} \to \boldsymbol{k}$, as in [14]. This would arguably not transpire in our situation had the manipulations not been performed, since the diagonal matrix elements are not symmetric in $\boldsymbol{k}$.

By using (4.111) we see that in the long-wavelength limit the lower modes in the one-dimensional stripe phase go as

$$\mathscr{E}^{\pm}_{k,-1} \sim \frac{1}{D \pm |k|a}, \tag{5.4}$$

where $D = \kappa\,(U + U_{\uparrow\downarrow}/2) - \mathcal{E}_0$.

Exclusion of terms in mean field approximation

Certain terms that would fulfill the delta function requirements in the mean field approach could not be included. These are terms where the ground state

particle that interacts with the non-ground-state particle change $\boldsymbol{k}^i$ vector, e.g. for the intra-spin interaction

$$\boldsymbol{k}_1 = \boldsymbol{k}^j, \quad \boldsymbol{k}_3 = \boldsymbol{k}^i, \quad \boldsymbol{k}_2 = \boldsymbol{k}', \quad \boldsymbol{k}_4 = \boldsymbol{k}, \tag{5.5}$$

where $\boldsymbol{k}^i \neq \boldsymbol{k}^j$ and $\boldsymbol{k}' = \boldsymbol{k} + \boldsymbol{k}^i - \boldsymbol{k}^j$. These terms are not included since there are no boson operators of type $\boldsymbol{k} + \boldsymbol{k}^i - \boldsymbol{k}^j$, only $\pm\boldsymbol{k}$.

6. Conclusion and outlook

A spin-orbit coupled Bose-Einstein condensate was treated as a two-component BEC where the single-particle spin basis was exchanged for the helicity basis of a spin-orbit coupled single-particle Hamiltonian. A general form for the undiagonalized Hamiltonian on a Bravais lattice is presented in (4.44). The excitation energy for the limiting case of on-site interactions and nearest-neighbor hopping is then found on a one-dimensional chain and a two-dimensional square lattice. The densities of particles in the ground states is found self-consistently by minimizing the free energy of the system. These mean field parameters define two distinct phases depending on the relative strength of the intra-spin couplings U to the inter-spin coupling $U_{\uparrow\downarrow}$. These two phases are the plane wave phase for $U > U_{\uparrow\downarrow}$ and the stripe phase for $U < U_{\uparrow\downarrow}$. This dependency agrees with literature. Inserting these densities into the excitation spectrum yields the final expressions for the excitation spectra for the two phases in one and two dimensions, shown in Sections 4.2.3 and 4.2.4.

The undiagonalized Hamiltonian could be used to further investigate other limiting cases. The discontinuous nature of the excitation spectrum, in addition to the lack of comparable standard results, imply that further research into the validity of the results is needed.

An interesting application of the results of this thesis would be an investigation into the drag coefficient of a spin-orbit coupled BEC. Ref. [33] is a thorough treatment of drag. Drag in a two-component interacting BEC was found in Ref. [14]. In this treatment, the Galilean transformation $\boldsymbol{k} \to \boldsymbol{k} - m_\tau \boldsymbol{v}_\tau$ simply led to Doppler-shifted single-particle energies $\epsilon^\tau_{\boldsymbol{k}} \to \epsilon^\tau_{\boldsymbol{k}} - m_\tau \boldsymbol{v}_\tau \cdot \nabla_{\boldsymbol{k}} \epsilon^\tau_{\boldsymbol{k}}$, for components $\tau = A, B$, that could then be substituted in the energy spectrum. An idea would be to do the same in a BEC with SOC, where helicity states are used as components. In our case, however, there is $\boldsymbol{k}$ dependence in non-diagonal matrix elements as well, not only in the single-particle energy, making it more complicated to assign a given $\boldsymbol{k}$

to a specific helicity state.

Another complicating factor is the influence of spin-orbit coupling on Galilean invariance. The implications of SOC breaking Galilean invariance must be investigated. As an example, the critical velocity depends on the frame of reference. We thus have different physics in different frames of reference. For literature on Galilean invariance, see Refs. [34, 35, 36, 37]. Finding drag from an expansion in velocities is explained in Ref. [38].

An alternative approach for investigating the drag coefficient is described in Ref. [39]. Wave functions subjected to periodic boundary conditions have phases ϕ that minimize the free energy of the system. $\Delta\phi_i$ describe a deviation from ϕ_i, for components $i = 1, 2$. $\frac{d^2F}{d(\Delta\phi_1)d(\Delta\phi_2)}|_{\Delta\phi_1=\Delta\phi_2=0}$ is then interpreted as the drag coefficient between these two components 1 and 2.

A. Commutation relations*

The helicity band operators in terms of spin operators are, by inversion of (3.45):

$$\begin{aligned} a_{\boldsymbol{k}+} &= \frac{1}{\sqrt{2}}\left(e^{-i\gamma_{\boldsymbol{k}}}b_{\boldsymbol{k}\uparrow} + b_{\boldsymbol{k}\downarrow}\right), \\ a_{\boldsymbol{k}-} &= \frac{1}{\sqrt{2}}\left(-e^{-i\gamma_{\boldsymbol{k}}}b_{\boldsymbol{k}\uparrow} + b_{\boldsymbol{k}\downarrow}\right), \\ a^\dagger_{\boldsymbol{k}+} &= \frac{1}{\sqrt{2}}\left(e^{i\gamma_{\boldsymbol{k}}}b^\dagger_{\boldsymbol{k}\uparrow} + b^\dagger_{\boldsymbol{k}\downarrow}\right), \\ a^\dagger_{\boldsymbol{k}-} &= \frac{1}{\sqrt{2}}\left(-e^{i\gamma_{\boldsymbol{k}}}b^\dagger_{\boldsymbol{k}\uparrow} + b^\dagger_{\boldsymbol{k}\downarrow})\right). \end{aligned} \tag{A.1}$$

The boson operators $b_{\boldsymbol{k}\alpha}$, $\alpha = \uparrow, \downarrow$, obey the commutation relations

$$[b_{\boldsymbol{k}\alpha}, b_{\boldsymbol{k}'\beta}] = 0, \tag{A.2a}$$

$$\left[b^\dagger_{\boldsymbol{k}\alpha}, b^\dagger_{\boldsymbol{k}'\beta}\right] = 0, \tag{A.2b}$$

$$\left[b_{\boldsymbol{k}\alpha}, b^\dagger_{\boldsymbol{k}'\beta}\right] = \delta_{\boldsymbol{k},\boldsymbol{k}'}\delta_{\alpha,\beta}. \tag{A.2c}$$

by assumption upon their introduction into the Bose-Hubbard model. We now show that they are valid for $a_{\boldsymbol{k}\pm}$ as well. (A.2a) and (A.2b) are valid for $a_{\boldsymbol{k}\pm}$ and $a^\dagger_{\boldsymbol{k}\pm}$ as well by inspection since they both only contain $b_{\boldsymbol{k}\alpha}$ and $b^\dagger_{\boldsymbol{k}\alpha}$ terms, respectively. For the last commutation relation we check the different cases separately, excluding terms that are zero by (A.2a) and (A.2b), and using (A.2c):

$$\begin{aligned}\left[a_{\boldsymbol{k}+}, a^\dagger_{\boldsymbol{k}'+}\right] &= \frac{1}{2}\left[e^{-i\gamma_{\boldsymbol{k}}} b_{\boldsymbol{k}\uparrow} + b_{\boldsymbol{k}\downarrow}, e^{i\gamma_{\boldsymbol{k}'}} b^\dagger_{\boldsymbol{k}'\uparrow} + b^\dagger_{\boldsymbol{k}'\downarrow}\right] \\ &= \frac{1}{2}\left(e^{i(\gamma_{\boldsymbol{k}'}-\gamma_{\boldsymbol{k}})}\left[b_{\boldsymbol{k}\uparrow}, b^\dagger_{\boldsymbol{k}'\uparrow}\right] + \left[b_{\boldsymbol{k}\downarrow}, b^\dagger_{\boldsymbol{k}'\downarrow}\right]\right) \\ &= \frac{1}{2}\left(e^{i(\gamma_{\boldsymbol{k}'}-\gamma_{\boldsymbol{k}})}\delta_{\boldsymbol{k},\boldsymbol{k}'} + \delta_{\boldsymbol{k},\boldsymbol{k}'}\right) \\ &= \delta_{\boldsymbol{k},\boldsymbol{k}'},\end{aligned} \tag{A.3}$$

$$\begin{aligned}\left[a_{\boldsymbol{k}+}, a^\dagger_{\boldsymbol{k}'-}\right] &= \frac{1}{2}\left[e^{-i\gamma_{\boldsymbol{k}}} b_{\boldsymbol{k}\uparrow} + b_{\boldsymbol{k}\downarrow}, -e^{i\gamma_{\boldsymbol{k}'}} b^\dagger_{\boldsymbol{k}'\uparrow} + b^\dagger_{\boldsymbol{k}'\downarrow}\right] \\ &= \frac{1}{2}\left(-e^{i(\gamma_{\boldsymbol{k}'}-\gamma_{\boldsymbol{k}})}\left[b_{\boldsymbol{k}\uparrow}, b^\dagger_{\boldsymbol{k}'\uparrow}\right] + \left[b_{\boldsymbol{k}\downarrow}, b^\dagger_{\boldsymbol{k}'\downarrow}\right]\right) \\ &= \frac{1}{2}\left(-e^{i(\gamma_{\boldsymbol{k}'}-\gamma_{\boldsymbol{k}})}\delta_{\boldsymbol{k},\boldsymbol{k}'} + \delta_{\boldsymbol{k},\boldsymbol{k}'}\right) \\ &= 0,\end{aligned} \tag{A.4}$$

$$\begin{aligned}\left[a_{\boldsymbol{k}-}, a^\dagger_{\boldsymbol{k}'+}\right] &= \frac{1}{2}\left[-e^{-i\gamma_{\boldsymbol{k}}} b_{\boldsymbol{k}\uparrow} + b_{\boldsymbol{k}\downarrow}, e^{i\gamma_{\boldsymbol{k}'}} b^\dagger_{\boldsymbol{k}'\uparrow} + b^\dagger_{\boldsymbol{k}'\downarrow}\right] \\ &= \frac{1}{2}\left(-e^{i(\gamma_{\boldsymbol{k}'}-\gamma_{\boldsymbol{k}})}\left[b_{\boldsymbol{k}\uparrow}, b^\dagger_{\boldsymbol{k}'\uparrow}\right] + \left[b_{\boldsymbol{k}\downarrow}, b^\dagger_{\boldsymbol{k}'\downarrow}\right]\right) \\ &= \frac{1}{2}\left(-e^{i(\gamma_{\boldsymbol{k}'}-\gamma_{\boldsymbol{k}})}\delta_{\boldsymbol{k},\boldsymbol{k}'} + \delta_{\boldsymbol{k},\boldsymbol{k}'}\right) \\ &= 0,\end{aligned} \tag{A.5}$$

$$\begin{aligned}\left[a_{\boldsymbol{k}-}, a^\dagger_{\boldsymbol{k}'-}\right] &= \frac{1}{2}\left[-e^{-i\gamma_{\boldsymbol{k}}} b_{\boldsymbol{k}\uparrow} + b_{\boldsymbol{k}\downarrow}, -e^{i\gamma_{\boldsymbol{k}'}} b^\dagger_{\boldsymbol{k}'\uparrow} + b^\dagger_{\boldsymbol{k}'\downarrow}\right] \\ &= \frac{1}{2}\left(e^{i(\gamma_{\boldsymbol{k}'}-\gamma_{\boldsymbol{k}})}\left[b_{\boldsymbol{k}\uparrow}, b^\dagger_{\boldsymbol{k}'\uparrow}\right] + \left[b_{\boldsymbol{k}\downarrow}, b^\dagger_{\boldsymbol{k}'\downarrow}\right]\right) \\ &= \frac{1}{2}\left(e^{i(\gamma_{\boldsymbol{k}'}-\gamma_{\boldsymbol{k}})}\delta_{\boldsymbol{k},\boldsymbol{k}'} + \delta_{\boldsymbol{k},\boldsymbol{k}'}\right) \\ &= \delta_{\boldsymbol{k},\boldsymbol{k}'}.\end{aligned} \tag{A.6}$$

We thus obtain the commutation relations

$$\left[a_{\boldsymbol{k}\alpha}, a_{\boldsymbol{k}'\beta}\right] = 0, \tag{A.7a}$$

$$\left[a^\dagger_{\boldsymbol{k}\alpha}, a^\dagger_{\boldsymbol{k}'\beta}\right] = 0, \tag{A.7b}$$

$$\left[a_{\boldsymbol{k}\alpha}, a^\dagger_{\boldsymbol{k}'\beta}\right] = \delta_{\boldsymbol{k},\boldsymbol{k}'}\delta_{\alpha,\beta}, \tag{A.7c}$$

where in this case, $\alpha, \beta = +, -$.

B. Helmholtz free energy

In order to find the Helmholtz free energy of the system we need to find the partition function $\mathcal{Z}$ of the system. Using (4.53) we find

$$\begin{aligned}\mathcal{Z} &= \mathrm{Tr}(e^{-\beta H}) \\ &= \sum_m \langle N_m| \, e^{-\beta H} \, |N_m\rangle \\ &= \sum_m \langle N_m| \, e^{-\beta H_0} \exp\{-\frac{\beta}{2} \sum_\sigma {\sum_{\boldsymbol{k}}}' \mathscr{E}_{\boldsymbol{k}\sigma} \left(n_{\boldsymbol{k}\sigma} + \frac{1}{2} \right) \} \, |N_m\rangle \\ &= e^{-\beta H_0} \exp\{-\frac{\beta}{4} \sum_\sigma {\sum_{\boldsymbol{k}}}' \mathscr{E}_{\boldsymbol{k}\sigma} \} \sum_m \langle N_m| \exp\{-\frac{\beta}{2} \sum_\sigma {\sum_{\boldsymbol{k}}}' \mathscr{E}_{\boldsymbol{k}\sigma} n_{\boldsymbol{k}\sigma} \} \, |N_m\rangle \, ,\end{aligned} \tag{B.1}$$

where $\beta = \frac{1}{k_B T}$. The $|N_m\rangle$ states constitute a many-particle Fock basis, i.e. the product of one-particle number states for each quantum number μ_i represented in $|N_m\rangle$:

$$|N_m\rangle = |n_{\mu_1}\rangle \, |n_{\mu_2}\rangle \cdots |n_{\mu_{N_m}}\rangle \, . \tag{B.2}$$

Each $|N_m\rangle$ thus picks out the eigenvalues n_{μ_i} represented in each term:

$$\begin{aligned}&\sum_m \langle N_m| \exp\{-\frac{\beta}{2} \sum_\sigma {\sum_{\boldsymbol{k}}}' \mathscr{E}_{\boldsymbol{k}\sigma} n_{\boldsymbol{k}\sigma} \} \, |N_m\rangle \\ &\qquad = \prod_{\boldsymbol{k}\sigma} \sum_m \langle N_m| \exp\{-\frac{1}{2} \beta \mathscr{E}_{\boldsymbol{k}\sigma} n_{\boldsymbol{k}\sigma} \} \, |N_m\rangle \\ &\qquad = \prod_{\boldsymbol{k}\sigma} \sum_{n_{\boldsymbol{k}}} \exp\{-\frac{1}{2} \beta \mathscr{E}_{\boldsymbol{k}\sigma} n_{\boldsymbol{k}\sigma} \}.\end{aligned} \tag{B.3}$$

This expression is a geometric sum, thus

$$\mathcal{Z} = e^{-\beta H_0} \exp\{-\frac{\beta}{4} \sum_{\sigma} {\sum_{\boldsymbol{k}}}' \mathscr{E}_{\boldsymbol{k}\sigma}\} \prod_{\boldsymbol{k}\sigma} \frac{1}{1 - \exp\{-\frac{1}{2}\beta \mathscr{E}_{\boldsymbol{k}\sigma}\}}. \tag{B.4}$$

The free energy $\mathcal{F}$ can now be found:

$$\begin{aligned} \mathcal{F} &= -\frac{1}{\beta} \ln \mathcal{Z} \\ &= H_0 + \frac{1}{2} \sum_{\sigma} {\sum_{\boldsymbol{k}}}' \mathscr{E}_{\boldsymbol{k}\sigma} + k_B T \sum_{\sigma} {\sum_{\boldsymbol{k}}}' \ln\left(1 - \exp\{-\mathscr{E}_{\boldsymbol{k}\sigma}/2k_B T\}\right). \end{aligned} \tag{B.5}$$

Since we are considering the case $T = 0$ the last term vanishes, so

$$\mathcal{F} = H_0 + \frac{1}{4} \sum_{\sigma} {\sum_{\boldsymbol{k}}}' \mathscr{E}_{\boldsymbol{k}\sigma}, \tag{B.6}$$

where the sum is over σ is over four branches. In many cases, as in (4.77), there are only two unique branches. In these cases the sum is usually only taken over these two branches, increasing the factor 1/4 to a factor 1/2.

C. Python files

Python files used are handed in together with the thesis. These files and their descriptions are listed in the following table.

Filename	Description
totalfreeenergy.py	Comparison of free energy calculated from (4.78) and (4.80).
minimizefreeenergy1D.py	Minimizing free energy with respect to the ground state densities in one dimension.
minimizefreeenergy2D.py	Minimizing free energy with respect to the ground state densities in two dimensions.

Bibliography

[1] P. Kapitza, "Viscosity of Liquid Helium below the λ-Point," 1938.

[2] J. F. Allen and A. D. Misener, "Flow of Liquid Helium II," *Nature*, vol. 141, no. 3558, pp. 75–75, 1938.

[3] M. H. Anderson, J. R. Ensher, M. R. Matthews, C. E. Wieman, and E. a. Cornell, "Evidence for Bose-Einstein Condensation in a Dilute Atomic Vapor," *Science*, vol. 269, p. 3, jul 1995.

[4] K. B. Davis, M. O. Mewes, M. R. Andrews, N. J. van Druten, D. S. Durfee, D. M. Kurn, and W. Ketterle, "Bose-Einstein Condensation in a Gas of Sodium Atoms," *Phys. Rev. Lett.*, vol. 75, pp. 3969–3973, nov 1995.

[5] C. Myatt, E. Burt, R. Ghrist, E. Cornell, and C. Wieman, "Production of Two Overlapping Bose-Einstein Condensates by Sympathetic Cooling," *Physical Review Letters*, vol. 78, no. 4, pp. 586–589, 1997.

[6] J. J. Sakurai, *Modern Quantum Mechanics*, vol. 54. 1986.

[7] V. Galitski and I. B. Spielman, "Spin-orbit coupling in quantum gases," *Nature*, vol. 494, no. 7435, pp. 49–54, 2013.

[8] Y.-J. Lin, K. Jiménez-García, and I. B. Spielman, "Spin–orbit-coupled Bose–Einstein condensates," *Nature*, vol. 471, no. 7336, pp. 83–86, 2011.

[9] T.-L. Ho and V. Shenoy, "Binary Mixtures of Bose Condensates of Alkali Atoms," *Physical Review Letters*, vol. 77, no. 16, pp. 3276–3279, 1996.

[10] J. Dalibard, F. Gerbier, G. Juzeliunas, and P. Öhberg, "Colloquium: Artificial gauge potentials for neutral atoms," *Reviews of Modern Physics*, vol. 83, no. 4, pp. 1523–1543, 2011.

[11] M. A. Khamehchi, K. Hossain, M. E. Mossman, Y. Zhang, T. Busch, M. M. N. Forbes, and P. Engels, "Negative-Mass Hydrodynamics in a Spin-Orbit-Coupled Bose-Einstein Condensate," *Physical Review Letters*, vol. 118, no. 15, pp. 1–6, 2017.

[12] Phys.org, "Physicists create 'negative mass'."

[13] W. S. Cole, S. Zhang, A. Paramekanti, and N. Trivedi, "Bose-Hubbard models with synthetic spin-orbit coupling: Mott insulators, spin textures, and superfluidity," *Physical Review Letters*, vol. 109, no. 8, pp. 1–5, 2012.

[14] J. Linder and A. Sudbø, "Calculation of drag and superfluid velocity from the microscopic parameters and excitation energies of a two-component Bose-Einstein condensate in an optical lattice," *Physical Review A - Atomic, Molecular, and Optical Physics*, vol. 79, no. 6, pp. 1–11, 2009.

[15] S. Solli, "Spin-orbit coupled Bose-Einstein condensates," specialization project, 2016.

[16] H. Bruus and K. Flensberg, *Many-Body Quantum Theory in Condensed Matter Physics: An Introduction*. Oxford University Press, USA, 2004.

[17] J. O. Fjærestad, "Second quantization (lecture notes)," 2016.

[18] J. O. Fjærestad, "Tight-binding model for electrons in a crystal (lecture notes)," 2016.

[19] Pethick and Smith, *Bose Einstein Condensation in Dilute Gases*, vol. 25. 2014.

[20] M. Krämer, C. Menotti, L. Pitaevskii, and S. Stringari, "Bose-Einstein condensates in 1D optical lattices," *The European Physical Journal D - Atomic, Molecular and Optical Physics*, vol. 27, no. 3, pp. 247–261, 2003.

[21] A. Altland and B. Simons, *Condensed Matter Field Theory*, vol. 115. 2006.

[22] D. J. Griffiths, *Introduction to Quantum Mechanics*, vol. 1. 2005.

[23] B. H. Bransden and C. J. Joachain, *Quantum Mechanics*. Pearson, second ed., 2000.

[24] S. Sjømark, "Superconductivity in Dirac Materials," master's thesis, 2016.

[25] J. Higbie and D. M. Stamper-Kurn, "Periodically dressed Bose-Einstein condensate: a superfluid with an anisotropic and variable critical velocity.," *Physical review letters*, vol. 88, no. 9, p. 090401, 2002.

[26] D. V. Oosten, P. V. D. Straten, H. T. C. Stoof, D. van Oosten, and P. van der Straten, "Quantum phases in an optical lattice," *Physical Review A*, vol. 63, no. 5, p. 053601, 2001.

[27] C. Tsallis, "Diagonalization methods for the general bilinear Hamiltonian of an assembly of bosons," *Journal of Mathematical Physics*, vol. 19, no. 1, p. 277, 1978.

[28] S. Zhang, W. S. Cole, A. Paramekanti, and N. Trivedi, "Spin-orbit Coupling in Optical lattices," *1411.2297*, pp. 1–30, 2014.

[29] S.-C. Ji, J.-Y. Zhang, L. Zhang, Z.-D. Du, W. Zheng, Y.-J. Deng, H. Zhai, S. Chen, and J.-W. Pan, "Experimental determination of the finite-temperature phase diagram of a spin-orbit coupled Bose gas," *Nature Physics*, vol. 10, no. 4, pp. 314–320, 2014.

[30] C. Wang, C. Gao, C. M. Jian, and H. Zhai, "Spin-orbit coupled spinor Bose-Einstein condensates," *Physical Review Letters*, vol. 105, no. 16, pp. 1–4, 2010.

[31] Y. Li, G. I. Martone, L. P. Pitaevskii, and S. Stringari, "Superstripes and the excitation spectrum of a spin-orbit-coupled bose-einstein condensate," *Physical Review Letters*, vol. 110, no. 23, pp. 1–5, 2013.

[32] G. I. Martone, Y. Li, L. P. Pitaevskii, and S. Stringari, "Anisotropic dynamics of a spin-orbit-coupled Bose-Einstein condensate," *Physical Review A - Atomic, Molecular, and Optical Physics*, vol. 86, no. 6, 2012.

[33] A. F. Andreev and E. P. Bashkin, "Three-velocity hydrodynamics of superfluid solutions," *Zh. Eksp. Teor. Fiz*, vol. 69, no. 1, pp. 319–326, 1975.

[34] Y. C. Zhang, Z. Q. Yu, T. K. Ng, S. Zhang, L. Pitaevskii, and S. Stringari, "Superfluid density of a spin-orbit-coupled Bose gas," *Physical Review A - Atomic, Molecular, and Optical Physics*, vol. 94, no. 3, pp. 1–5, 2016.

[35] H. Zhai, "Degenerate Quantum Gases with Spin-Orbit Coupling," p. 23, 2014.

[36] W. Zheng, Z.-Q. Yu, X. Cui, and H. Zhai, "Properties of Bose gases with the Raman-induced spin–orbit coupling," *Journal of Physics B: Atomic, Molecular and Optical Physics*, vol. 46, no. 13, p. 134007, 2013.

[37] Q. Zhu, C. Zhang, and B. Wu, "Exotic superfluidity in spin-orbit coupled Bose-Einstein condensates," *EPL (Europhysics Letters)*, vol. 100, no. 5, p. 50003, 2012.

[38] D. V. Fil and S. I. Shevchenko, "Nondissipative drag of superflow in a two-component Bose gas," *Physical Review A - Atomic, Molecular, and Optical Physics*, vol. 72, no. 1, pp. 1–13, 2005.

[39] P. B. Weichman, "Crossover scaling in a dilute bose superfluid near zero temperature," *Physical Review B*, vol. 38, no. 13, pp. 8739–8759, 1988.